Ptpn22 silencing in the NOD model of type 1 diabetes indicates the human susceptibility allele of *PTPN22* is a gain-of-function variant

Ptpn22 knockdown im NOD Modell für Diabetes Typ 1 belegt einen Aktivitätsgewinn der humanen Krankheitsvariante

Doctoral thesis for a doctoral degree at the Graduate School of Life Science
Julius-Maximilians University of Würzburg
Section Biomedicine

submitted by

Peilin Zheng

From
Hunan, China
Würzburg, 2012

Submitted on: ……..

(Office stamp)

Members of the Promotionskomitee:

Chairperson: Prof. Dr. rer. nat. Thomas Hünig

Primary Supervisor: Dr. Stephan Kissler

Supervisor (Second): Prof. Dr. rer. nat. Antje Gohla

Supervisor (Third): Prof. Dr. med. Heinz Wiendl

Date of Public Defence: ……

Date of receipt of Certificates: …….

Acknowledgements

First and foremost, I am very grateful to my supervisor Dr. Stephan Kissler, who inspired, encouraged, and supported me throughout my PhD study. I owe a lot to my supervisory committee, Prof. Dr. Antje Gohla and Prof. Dr. Heinz Wiendl for kind support and valuable suggestions.

I would like to express my sincere gratitude to the Graduate School of Life Sciences, University of Würzburg for offering me the "*Excellence Initiative*" scholarship and giving me the chance to achieve a Doctoral degree in Germany. I would like to extend my gratitude to the Rudolf Virchow Center for Experimental Biomedicine for financial support in my 4th year of study.

I would like to thank all the lab members: Nicole Hain, Heike Rudolf, Julie Joseph, Kay Gerold, Katharina Herrmann and Fabian Kaiser for the indispensable help in and out of lab. I also thank members of the Zernecke lab, Nieswandt lab and Hermanns lab for the technical help. I am grateful to Prof. Dr. Thomas Hünig, Prof. Dr. Thomas Herrmann, Prof. Dr. Manfred Lutz and Dr. Niklas Beyersdorf from the Institute of Virology and Immunobiology for helpful discussion and valuable suggestions.

This thesis is dedicated to my wife Mrs. Mingming Li and my parents for their understanding and endless support.

Table of content

Summary

PTPN22 encodes the lymphoid tyrosine phosphatase Lyp that can dephosphorylate Lck, ZAP-70 and Fyn to attenuate TCR signaling. A single-nucleotide polymorphism (C1858T) causes a substitution from arginine (R) to tryptophan (W) at 620 residue (R620W). Lyp-620W has been confirmed as a susceptible allele in multiple autoimmune diseases, including type 1 diabetes (T1D). Several independent studies proposed that the disease-associated allele is a gain-of-function variant. However, a recent report found that in human cells and a knockin mouse containing the R620W homolog that Ptpn22 protein degradation is accelerated, indicating Lyp-620W is a loss-of-function variant. Whether Lyp R620W is a gain- or loss-of-function variant remains controversial. To resolve this issue, we generated two lines (P2 and P4) of nonobese diabetic (NOD) mice in which *Ptpn22* can be inducibly silenced by RNAi. We found long term silencing of *Ptpn22* increased spleen cellularity and regulatory T (Treg) cell numbers, replicating the effect of gene deletion reported in the knockout (KO) B6 mice. Notably, *Ptpn22* silencing also increased the reactivity and apoptotic behavior of B lymphocytes, which is consistent with the reduced reactivity and apoptosis of human B cells carrying the alleged gain-of-function *PTPN22* allele. Furthermore, loss of *Ptpn22* protected P2 KD mice from spontaneous and Cyclophosphamide (CY) induced diabetes. Our data support the notion that Lyp-620W is a gain-of-function variant. Moreover, Lyp may be a valuable target for the treatment of autoimmune diseases.

Zusammenfassung

PTPN22 kodiert die *lymphoid tyrosine phosphatase* Lyp, die Lck, ZAP-70 und Fyn dephosphorilieren kann, um T Zell Rezeptor Signale zu vermindern. Ein Polymorphismus (C1858T) verursacht einen Aminosäurenaustausch auf Position 620 von Arginin zu Tryptophan (R620W). Lyp-620W erhöht das Risiko einer Vielfalt von Autoimmunerkrankungen, darunter auch Diabetes Typ 1 (T1D). Mehrere Studien haben belegt, dass dieses Krankheitsallel die Funktion von Lyp verstärkt. Eine neuere Studie hat andererseits gezeigt, dass die R620W Variante schneller degradiert wird, was bedeuten würde, dass das C1858T Allel einen Funktionsverlust verursachen könnte. Ob Lyp R620W die Funktion dieser Phosphatase erhöht oder mindert bleibt demnach bis jetzt ungewiss. Um diese Frage zu klären haben wir zwei transgene Mauslinien (P2 und P4) im diabetischen Hintergrund der NOD Maus generiert, in denen *Ptpn22* auf induzierbare Weise durch RNAi gehemmt werden kann. Unsere Ergebnisse zeigen, dass die langfristige Hemmung von *Ptpn22* zu einer Zunahme der Milzzellularität und der Anzahl regulatorischer T Zellen führt, was dem Phänotyp des *Ptpn22* knockout im B6 Hintergrund entspricht. Bemerkenswert ist, dass die Hemmung von *Ptpn22* auch zu einer Zunahme der Reaktivität und des apoptotischen Verhaltens von B Lymphozyten führt, also dem entgegengesetzten Phänotypen, der in menschlichen B Zellen beobachtet wurde, die das Krankheitsallel exprimierten. Zusätzlich konnte die *Ptpn22* Inhibierung NOD Mäuse vor spontanem und Cyclophosphamid-induziertem Diabetes schützen. Unsere Daten unterstützen also die Hypothese, dass Lyp-620W eine stärkere Aktivität vorweist. Dies würde auch bedeuten, dass *Ptpn22* möglicherweise zu therapeutischen Zwecken inhibiert werden könnte, um Autoimmunerkrankungen zu bekämpfen.

Abbreviations

APS	- Ammonium persulfate
BCR	- B cell receptor
bp	- Base pair
CFA	- Complete Freund's adjuvant
cppt	- Central poly purine tract sequence
CSK	- C-terminal Src kinase
CSR	- Class switch recombination
CY	- Cyclophosphamide
DC	- Dendritic cells
DMSO	- Dimethyl sulfoxid
Dox	- Doxycycline
dsRNA	- double strand RNA
EAE	- Experimental autoimmune encephalomyelitis
ES cell	- Embryonic stem cell
FCS	- Fetal calf serum
flCTLA-4	- Full length CTLA-4
FO	- Follicular
GAD65	- Glutamic acid decarboxylase 65
GWAS	- Genome-wide association study
HCG	- Human chorionic gonadotropin
HLA	- Human leukocyte antigen
IA-2	- Tyrosine phsphatase like protein
Idd	- Insulin-dependent diabetes
IDDM	- Insulin-dependent diabetes mellitus
INS	- Insulin
IP-10	- IFN-inducible protein-10
IPD	- Invasive pneumococcal disease
ITAM	- Immunoreceptor tyrosine-based activation motif
iTreg	- Induced regulatory T cells
JIA	- Juvenile idiopathic arthritis
LCMV	- Lymphocytic choriomeningitis virus
liCTLA-4	- Ligand independent CTLA-4

MAR/SAR	- Matrix/scaffold attachment region
MCP-1	- Monocyte chemoattractant protein-1
MDC	- Macrophage-derived chemokine
MZ	- Marginal zone
NOD	- Non-obese diabetic
nTreg	- Natural regulatory T cells
P/S	- Penicillin/ streptomycin
PEC	- Peritoneal exduate cells
Pep	- PEST domain-enriched tyrosine phosphatase
PKR	- Interferon-induced protein kinase
PMA	- Phorbol myristate acetate
PNA	- Peanut agglutinin
PS	- Phosphatidylserine
RA	- Rheumatoid arthritis
RIP	- Rat insulin promoter
RNAi	- RNA interference
RRE	- Rev responsive element
sCTLA4	- Soluble CTLA-4
SHM	- Somatic hypermutation
SIN	- Self-inactivation
SLE	- Systemic lupus erythematosus
SNP	- Single-nucleotide polymorphism
T1D	- Type 1 diabetes
Tconv	- Conventional T cells
TCR	- T cell receptor
Teff	- Effector T cell
TetO	- Tetracycline operator
TetR	- Tetracycline repressor
TGF-β	- Transforming Growth Factor β
Treg	- Regulatory T cell
VCP	- Valosin containing protein
VNTR	- Variable number tandem repeat
VSV-G	- Vesicular Stomatitis Virus protein G
WPRE	- Woodchuck postregulatory element

CHAPTER 1
INTRODUCTION

1.1 Type 1 diabetes

Type 1 diabetes (T1D; also called insulin-dependent diabetes mellitus, IDDM) is an autoimmune disease, resulting from the infiltration of immune cells into the pancreas that cause the permanent destruction of insulin producing β cells. Multiple factors influence the susceptibility to T1D, including genetic and environmental factors. Although gender is a very important factor in many autoimmune diseases (women are generally more susceptible than men), males and females are almost equally prone to T1D (Beeson et al., 1994; Amur et al., 2011).

Many studies have demonstrated that environmental factors, like virus infection, bacteria and diet, can accelerate or protect from T1D. In 1987, Foulis and colleagues reported that a large amount of IFN-α and HLA class I could be found in the islets of newly diabetic children, indicating that virus infection may be involved in T1D. Follow-up studies found that viruses, particularly enteroviruses and rotaviruses, may accelerate T1D by 1) molecular mimicry of autoantigens which are found in the islets (Kaufman et al., 1992); 2) directly infecting β cells to induce insulitis (Yoon et al., 1978). In the case of bacteria, many studies have been done to clarify their role, especially that of commensal bacteria in T1D. Commensal bacteria are abundant in the gut and intestine. In 2002, Bach and colleagues demonstrated that commensal bacteria interfered with T1D in the NOD mouse (Bach et al., 2002). Li and colleagues further reported that commensal bacteria could protect the NOD mouse from T1D in a MyD88-independent manner (Li et al., 2008). Another environmental factor, diet, also affects the susceptibility to T1D. Vitamin D was found to decrease the risk of T1D in the NOD mouse (Mathieu et al., 1994). Interestingly, some proteins in common food items can mimick autoantigens in the islets, which may accelerate the pathogenesis of T1D. For example, albumin in cow's milk is a molecular mimick of ICA-1, which is a surface protein on β cells (Karjalainen et al., 1992). Moreover, there is elevated T cell reactivity to wheat gluten in the blood of T1D patients, although the cause of this is not clear (Klemetti et al., 1998).

In the case of genetic factors, so far, multiple single-nucleotide polymorphisms (SNPs) have been identified in association with human T1D by genome-wide

association studies (GWAS) (Table1, modified from www.t1dbase.org).

Table 1. T1D risk loci in humans (modified from www.t1dbase.org)

	Chrom	SNP	Gene of Interest	OR Minor Allele (95% CI)	Publication
1	1p13.2	rs2476601	PTPN22	2.05 [1.90-2.20]	Bottini et al., 2006
2	1q31.2	rs2816316		0.89 [0.84-0.95]	Smyth et al., 2008
3	1q32.1	rs3024505	IL10, CD55	0.84 [0.77-0.91]	Barrett et al., 2009
4	2q11.2	rs1160542			
		rs9653442		1.11 [1.07-1.16]	
5	2q12.1	rs917997	IL18RAP	0.83 [0.72-0.96]	Smyth et al., 2008
6	2q24.2	rs1990760	IFIH1	0.86 [0.82-0.90]	Smyth et al., 2006
7	2q32.2	rs6752770	STAT4	1.11 []	Fung et al., 2009
		rs7574865		1.10 [1.04-1.15]	
8	2q33.2	rs3087243	CTLA4	0.88 [0.83-0.93]	Ueda et al., 2003 Nisticò et al., 1998 Smyth et al., 2008
9	3p21.31	rs11711054			Smyth et al., 2008
		rs333		0.85 [0.80-0.92]	
10	4p15.2	rs10517086		1.09 [1.02-1.17]	Barrett et al., 2009
11	4q27	rs2069762	IL2	0.89 [0.85-0.93]	Todd et al., 2007
		rs4505848			Cooper et al., 2008
12	5p13.2	rs6897932	IL7R	0.89 [0.84-0.94]	Todd et al., 2007
13	6p21.33, 6p21.31	rs9268645	HLA II		Nejentsev et al., 2007
14	6q15	rs11755527	BACH2	1.13 [1.09-1.18]	Cooper et al., 2008
15	6q22.32	rs9388489		1.17 [1.10-1.24]	Barrett et al., 2009
16	6q23.3	rs6920220		1.09 [1.04-1.15]	Fung et al., 2009
17	6q25.3	rs1738074	TAGAP	0.92 [0.88-0.96]	Smyth et al., 2008
18	7p15.2	rs7804356		0.88 [0.82-0.94]	Barrett et al., 2009
19	7p12.1	rs4948088		0.77 [0.67-0.90]	Barrett et al., 2009
20	9p24.2	rs7020673	GLIS3	0.88 [0.83-0.93]	Barrett et al., 2009
21	10p15.1	rs11594656	IL2RA	0.87 [0.82-0.92]	Lowe et al., 2007
		rs12722495		0.62 [0.57-0.68]	
22	10p15.1	rs11258747			Cooper et al., 2008
		rs947474			
23	10q22.3	rs1250550			
		rs1250558			
24	10q23.31	rs10509540	RNLS	0.75 [0.70-0.80]	Barrett et al., 2009
25	11p15.5	rs689	INS	0.95 [0.89-1.03]	Bell et al., 1984
		rs7111341			

26	12p13.31	rs4763879		1.09 [1.02-1.16]	Barrett et al., 2009
27	12q13.2	rs2292239	IKZF4	1.31 [1.22-1.34]	Todd et al., 2007 Hakonarson et al., 2008
28	12q13.3	rs1678536		0.89 [0.82-0.97]	Cooper et al., 2008
		rs1678542		0.92 [0.88-0.96]	Fung et al., 2009
29	12q24.12	rs3184504	SH2B3	1.28 [1.22-1.35]	Todd et al., 2007
30	14q24.1	rs1465788		0.86 [0.80-0.91]	Barrett et al., 2009
31	14q32.2	rs4900384		1.09 [1.02-1.16]	Barrett et al., 2009
32	14q32.2	rs941576		0.90 [0.86-0.94]	Wallace et al., 2010
33	15q14	rs17574546			Qu et al., 2009
		rs7171171			
34	15q25.1	rs3825932		0.86 [0.82-0.90]	Cooper et al., 2008
35	16p13.13	rs12708716		0.81 [0.77-0.86]	Todd et al., 2007 Hakonarson et al., 2008
36	16p11.2	rs4788084	IL27	0.86 [0.81-0.91]	Barrett et al., 2009
37	16q23.1	rs7202877		1.28 [1.17-1.41]	Barrett et al., 2009
38	17q12	rs2290400	ORMDL3, GSDMB	0.87 [0.82-0.93]	Barrett et al., 2009
39	17q21.2	rs7221109		0.95 [0.89-1.01]	Barrett et al., 2009
40	18p11.21	rs1893217	PTPN2		Todd et al., 2007
		rs478582		0.83 [0.79-0.88]	
41	18q22.2	rs763361	CD226	1.16 [1.10-1.22]	Todd et al., 2007
42	19p13.2	rs2304256		0.86 [0.82-0.90]	Wallace et al., 2010
43	19q13.32	rs425105		0.86 [0.79-0.93]	Barrett et al., 2009
44	20p13	rs2281808		0.90 [0.84-0.95]	Barrett et al., 2009
45	21q22.3	rs3788013	UBASH3A	1.13 [1.08-1.18]	Concannon et al., 2008
46	22q12.2	rs5753037		1.10 [1.04-1.17]	Barrett et al., 2009
47	22q12.3	rs3218253			
48	22q13.1	rs229541		1.12 [1.07-1.17]	Cooper et al., 2008
49	Xp22.2	rs5979785	TLR8	0.84 [0.73-0.96]	Cooper et al., 2008
50	Xq28	rs2664170		1.16 [1.07-1.24]	Barrett et al., 2009

Among so many identified genes, not every gene contributes to disease susceptibility equally. A small number of them confer substantial effects. The risk factor HLA class II gene was discovered over 20 years ago. In familial T1D, it contributes to 40-50% of the risk of developing disease. The insulin (INS) gene can also confer susceptibility or resistance to T1D. In humans, in the 5' regulatory region of the insulin gene there is a unique variable number tandem repeat (VNTR), which comes from tandem repetition of a 14-15 base pair (bp) oligonucleotide sequence. Based on

the different sizes, VNTR is divided into three types: type 1 (26-63 repeats), type 2 (about 80 repeats), and type 3 (141-209 repeats) (Bell et al., 1982; Rotwein P., 1986; Bennett et al., 1995). The type 1 allele increases disease risk 2-5 fold, whereas the type 3 allele is T1D protective. (Bell et al., 1984; Julier et al., 1991; Lucassen et al., 1993; Owerbach et al., 1993; Julie et al., 1994; Undlien et al., 1995). Further study found that compared to type 1 VNTR, type 3 VNTR correlated with higher INS mRNA in thymus and lower mRNA in the pancreas, which benefited negative selection of T lymphocytes in the thymus and reduced self-antigen exposure in the pancreas. (Lucassen et al., 1995; Kennedy et al., 1995; Pugliese et al., 1997; Vafiadis et al., 1997; Vafiadis et al., 2001).

CTLA-4 and *PTPN22* are general risk factors in many human autoimmune diseases. *PTPN22* will be discussed in a later section. CTLA-4 has been confirmed in association with many autoimmune diseases, including Multiple Sclerosis (Sawcer et al., 1996), T1D (Copeman et al., 1995), Graves' disease (Kouki et al., 2002), Hashimoto's thyroiditis (Nithiyananthan et al., 2002), Addison's disease and Rheumatoid Arthritis (Becker et al., 1998). CTLA-4 is a potent negative regulator of T cell activation. CTLA-4 knockout mice quickly died due to the massive lymphoproliferation and multiorgan destruction (Waterhouse et al., 1995; Tivol et al., 1995). Specific loss of CTLA-4 in regulatory T cells (Treg cells) leads to the same symptom, but with delayed onset (Wing et al., 2008). CTLA-4 has been proposed to transmit negative signals by distinct mechanisms: 1) it could outcompete CD28 by virtue of a higher affinity for CD80/86, which provide costimulatory signal for T cell activation (Ostrov et al., 2000); 2) it may directly block immunoreceptor tyrosine-based activation motif (ITAM) (Lee et al., 1998); 3) it could diminish CD80/86 expression on antigen presenting cells (APCs) to ablate T cell costimulatory signal (Wing et al., 2008; Cedebom et al., 2000).

In humans, *CTLA-4* is located at chromosome 2q33. In the NOD mouse, *Ctla-4* resides in chromosome 1. In both human and mouse, CTLA-4 undergoes alternative splicing. Full length CTLA-4 (flCTLA-4) and soluble CTLA-4 (sCTLA-4) exist in both human and mouse. FlCTLA-4 contains all the four domains (leader peptide, ligand binding domain, transmembrane domain and cytosolic tail), while sCTLA-4 lacks the transmembrane domain. It is believed sCTLA4 is translated, secreted and

circulates in human serum (Magistrelli et al 1999, Oaks et al 2000). In humans, a SNPin the 3′ UTR (CT60, A/G) results in a reduced ratio of sCTLA-4/fl CTLA-4, which is associated with T1D susceptibility (Ueda, et al., 2003). Ligand independent CTLA-4 (liCTLA-4), which is unique in the mouse, lacks the ligand-binding domain. Vijayakrishnan and colleagues found that although liCTLA-4 lacks exon2 including the MYPPPY motif that is essential for CD80/86 binding, liCTLA-4 still could dephosphorylate the TcRζ chain and ZAP-70 *in vitro* (Vijayakrishnan et al., 2004).

Besides the genes mentioned above, many other genes confer susceptibility to T1D. *PTPN2* encodes a tyrosine phosphatase. A recent study found that *PTPN2* is highly expressed in human islet cells and rat β cells. A decrease in *PTPN2* could amplify IFN-γ induced STAT1 phosphorylation and β Cell apoptosis. PRKCQ, another candidate gene, acts in the downstream signaling cascade of the TCR, which plays an important role in T cell differentiation. In PRKCQ deficient mice, the number of Treg cells and $CD4^+$ T cells are greatly decreased (Gupta et al., 2008). Yet another candidate, KIAA0350 (also known as Clec16a) belongs to calcium-dependent lectin (C-type lectin) superfamily, containing an ITAM in the cytosol. *Ema*, which is KIAA0350 homologue in drosophila, is involved in the endosomal maturation (Kim et al., 2010). The exact function of KIAA0350 in mouse and humans is still unknown. IFIH1 (also known as MDA5) selectively recognize the viral double strand RNA (dsRNA). Hence, IFIH1 plays important roles in antiviral responses. BACH2 encodes a leucine zipper transcription factor, which is very important for B cell class switch recombination (CSR) and somatic hypermutation (SHM). So BACH2 is a key regulator in antibody response and humoral immunity (Muto et al., 2004).

So far dozens of SNPs have been implicated in T1D by GWAS. However, the functional consequences of most SNPs are largely unknown. It is also unknown how these SNPs accelerate or exacerbate T1D. To characterize the role of risk alleles in the pathogenesis of T1D, a mouse model for this disease, like the NOD mouse, provides a valuable resource.

1.2 The non-obese diabetic (NOD) mouse model

The NOD mouse strain was developed in Japan in 1970s by Makino and his

colleagues (Makino et al., 1980). This mouse strain harbors some inherent defects in central and peripheral tolerance, leading to immune cell infiltration into the pancreas, β cells destruction and spontaneous T1D (Anderson et al., 2005). In female NOD mice, the frequency of spontaneous diabetes is 60-80% at the age of 4-6 months, compared to 20-30% incidence in the male mice (Kikutani et al., 1992; Bach et al., 1994). This incidence difference between male and female NOD mice may be related to sex hormones, illustrated by the decreased incidence in androgen treated female mice and increased incidence in castrated males (Fitzpatrick et al., 1991; Fox., 1992; Makino et al., 1981). However, this gender-related difference in T1D incidence is not significant in humans (Beeson et al., 1994; Amur et al., 2011). Besides T1D, in some conditions NOD mice are susceptible to other spontaneous or inducible autoimmune diseases, such as autoimmune sialitis (Hu et al., 1992), autoimmune thyroiditis (Many et al., 1996), experimental autoimmune encephalomyelitis (EAE) (Ichikawa et al., 1999), autoimmune peripheral polyneuropathy (Salomon et al., 2001) and systemic lupus erythematosus–like disease (Silveira et al., 2001).

The NOD mouse is a widely used mouse model for human T1D. NOD mice share many similarities with human T1D patients, including the presence of autoreactive T cells, autoreactive B cells, and similar risk loci in the genome. So far, more than 20 potential *Idd* loci have been identified in the NOD mouse (Todd et al., 2001). As in humans, the disease susceptible MHC allele confers the largest risk. The NOD mouse has a unique MHC haplotype, termed H-2^{g7} (Wicker et al., 1995; Tisch et al., 1996). A nonaspartic acid replacement in H-2^{g7} alters T cell receptor (TCR) affinity and then changes the repertoire of MHC binding peptides (Acha-Orbea et al., 1987; Kanagawa et al., 1998). However, the $H2^{g7}$alone is not sufficient for disease development. Other *Idd* loci, which contribute immune tolerance deficit, are required to induce T1D in the NOD mouse (Serreze et al., 2001).

1.2.1 Defective tolerance in the NOD mouse

Immune tolerance comprises two aspects: central tolerance and peripheral tolerance. In the NOD mouse, both central and peripheral tolerance is defective, leading to the disease development.

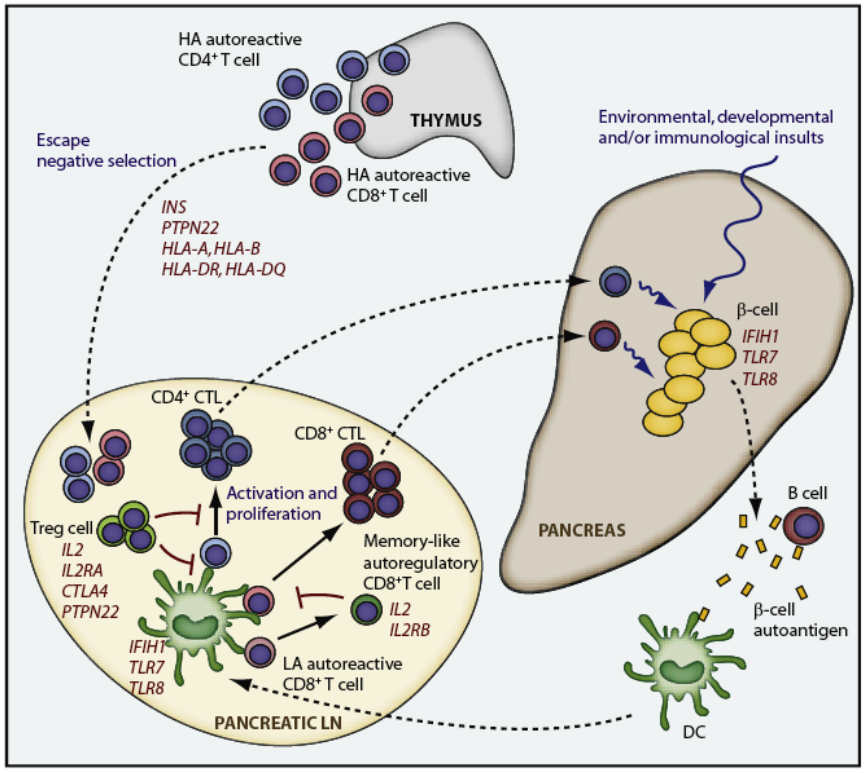

Fig 1.1: Relevant genes involved in the defective immune tolerance in T1D (Santamaria et al., 2010)

1.2.1.1 Central tolerance in the NOD mouse

Central tolerance happens during the process of T cell development in the thymus. During T cell maturation, positive and negative selections occur to optimize our immune system: to protect the body from harmful bacteria and viruses as well as to avoid self-tissue destruction. During positive selection, immature thymocytes reactive to self-antigen obtain a survival signal and proceed to negative selection. During negative selection, thymocytes with high affinity to self-antigen are deleted before they migrate into peripheral tissues. Negative selection, which eliminates most autoreactive T cells, is critical to maintain self tolerance. In the NOD mouse, negative selection is somehow defective, illustrated by the fact that some semi-mature thymocytes, which should be deleted by negative selection, escape from apoptosis (Kishimoto et al., 2001). Some of these escaped autoreactive T cells could destroy β cells by recognizing islet antigen, including insulin (Palmer et al., 1987), glutamic acid decarboxylase (GAD65) (Baekkeskov et al., 1989), and a tyrosine phosphatase like protein (IA-2) (Lan et al., 1996).

1.2.1.2 Peripheral tolerance in the NOD mouse

The presence of autoreactive T cells is not exclusive to the NOD mouse. Negative selection is incomplete both in the NOD and in some disease resistant mice (Lohmann et al., 1996; Semana et al., 1999). T1D in the NOD mouse is also contributed to by defective peripheral tolerance dependent on anti-inflammatory cytokines, and several suppressive cell populations, including Treg cells, Tr1 (IL-10 producing cells), Th3 (TGF-β producing T helper cells) and regulatory B cells ($CD1d^{hi}CD5^{+}$ B cells).

Treg cells are pivotal in peripheral tolerance. Treg cells can be distinguished from other cells types by their unique transcription factor-FoxP3 and highly expressed cell surface markers, including CD25, CTLA-4, and GITR. Based on their origin, Treg cells are classified into two populations: natural Treg cells (nTreg cells; derived from thymus, $FoxP3^{+}Helios^{+}$) and induced Treg cells (iTreg; naïve T cells converted in the periphery, $FoxP3^{+}Helios^{-}$) (Thornton et al., 2010).

So far, it is still controversial whether NOD mice harbor defective Treg cells. Two papers reported that in the NOD mouse the percentage of Treg cells was significantly decreased compared to that in disease resistant mouse strains (Wu et al., 2002; Alard et al., 2006). An opposite result was reported in 2007, claiming that NOD mice were superior in generating Treg cells, at least nTreg cells (Feuerer et al., 2007). D'Alise and colleagues reported that Treg cells from NOD and B6 mice were comparable in cell numbers and function. However, conventional T cells (Tconv, $CD4^{+}CD25^{-}$) from NOD mice are more proliferative than those from B6 mice (D'Alise et al., 2008). Nevertheless, there is no doubt that Treg cells are indispensable to control diabetes in the NOD mouse. On one hand, loss of Treg cells can accelerate or exacerbate T1D (Salomon et al., 2000; Mellanby et al., 2007). On the other hand, a boost in Treg cells by IL-2 treatment or by a genetic approach can protect and even reverse T1D (Peng et al., 2004; Grinberg-Bleyer et al., 2010). Adoptive transfer experiments also demonstrated that Treg cells are potent in controlling effector T cell induced autoimmunity in the NOD.*scid* mice (Asano et al., 1996; Stephens et al., 2000; Hutchings et al., 1990; Boitard et al., 1989; Lepault et al., 2000; Szanya et al., 2002).

Since Treg cells are potent suppressors, an interesting question is a whether boost of Treg cells could control or cure autoimmune diseases. Since the frequency of Treg

cells in peripheral blood is quite low (1-5% in $CD4^+$ cells), it is reasonable to isolate and then expand Treg cells *ex vivo* to obtain enough Treg cells. The Bluestone group at UCSF has conducted preclinical trials of transferring expanded Treg cells into diabetic patients. Treg cells are unable to proliferate unless their TCR and CD28 are continuously engaged by MHC/peptide and B7 molecules, respectively. Tang and colleagues succeeded in achieving a 200-fold Treg cell expansion within 2 weeks by utilizing high dose IL-2 and anti-CD3/CD28 coupled beads. The expanded Treg cells maintained their suppressive phenotype and function (Tang et al., 2004). The same group further expanded BDC 2.5 TCR transgenic Treg cells by coculture with autoantigen pulsed dentritic cells and IL-2. The expanded TCR specific Treg cells are more potent than polyclonal Treg cells to prevent/cure T1D in the NOD mouse (Tarbell et al., 2004). Wiegard and colleagues found that kupffer cell, which is a kind of macrophage in the liver, had the ability to expand Treg cells without IL-2. However, these expanded Treg cells were less suppressive compared to freshly isolated Treg cells (Wiegard et al., 2005).

1.2.2 The role of different cell subsets in T1D

It is an interesting question which cell population is vital in the pathogenesis of T1D in the NOD mouse. Immunodeficient mice, such as NOD.*scid* or NOD.$Rag^{-/-}$ mice which lack T and B cells, are protected from T1D (Katz et al., 1993; Prochazka et al., 1992; Serreze et al., 1994; Soderstrom et al., 1996; Wicker et al., 1994). To further separate the role of T and B cells, adoptive transfer and cell depletion experiments have been employed. B cell depletion by rituximab, an anti-CD20 monoclonal antibody, preserves β cell function to some extent in newly diagnosed T1D patients (Pescovitz et al., 2009). In the mouse, loss of B cells protects NOD mice from T1D, and moreover, reverses the diseases in more than one third of diabetic mice (Serreze et al., 1996. Hu et al., 2007). This protection could be due to the disrupted antigen presentation to T cells, and increased number of Treg cells and regulatory B cells. Charlton and colleagues further utilized adoptive transfer experiments to define the time window during which B cells are required for disease pathogenesis. T cells alone from 5wks old mice are sufficient to induce diabetes in the NOD.*scid* mouse (Charlton et al., 2001). So it seems that B cells are critical in the early stage of diabetes (peri-insulitis and insulitis), but dispensable in the effector stage. T cells from young NOD mice are sufficient to kill beta cells independent of B cell

contribution.

Further studies demonstrated that T cells are the primary cells in disease development. $CD4^+$ T cells could transfer disease, and spontaneous diabetes was blocked in NOD mice by treatment with a monoclonal antibody against CD4 (Shizuru et al., 1988; Wang et al., 1991). Meanwhile, $CD8^+$ T cells also promote disease development (Wang et al., 1996; Wong et al., 1996). $CD8^+$ cells also infiltrate into the pancreas. These $CD8^+$ cells express NKG2D, an activating receptor. Treatment with depleting monoclonal antibody against NKG2D in the prediabetic stage prevents $CD8^+$ cell expansion and T1D development in mice (Ogasawara et al., 2004).

1.2.3 The pathogenesis of T1D

At the age of 3-4 weeks, mononuclear infiltration (peri-insulitis) occurs, without overt diabetes (Delovitch and Singh, 1997; Kanazawa et al., 1984). Disease progresses to severe insulitis by 10 weeks of age, and to overt symptoms at 4-6 months, resulting in high level of glucose in the blood and urine and loss of weight. As mentioned above, T cells are the key cell population causing NOD mice to proceed to the overt diabetic symptoms. However, T cells, including autoreactive T cells, reside in the pancreatic lymph node, not directly in the pancreas. The question is how the T cells enter into the pancreas. To answer this question, chemokines and TCR specificity in cell trafficking will be discussed.

1.2.3.1 Chemokines and chemokine receptors in T1D

Chemokines are small proteins that are secreted by many cell types, e.g. osteoblasts, endothelial cells, monocytes and macrophages. Concentration gradients are formed according to the distance to the source cells. Chemokines attract target cells migrating to the source. According to their structural properties, such as the position and number of conserved cysteine residues, chemokines have been classified into four subfamilies: C, CC, CXC, and CX_3C. The X represents any amino acid. So in the CXC subfamily, there is an amino acid between the two cysteine, while there are three amino acids in the CX_3C subfamily.

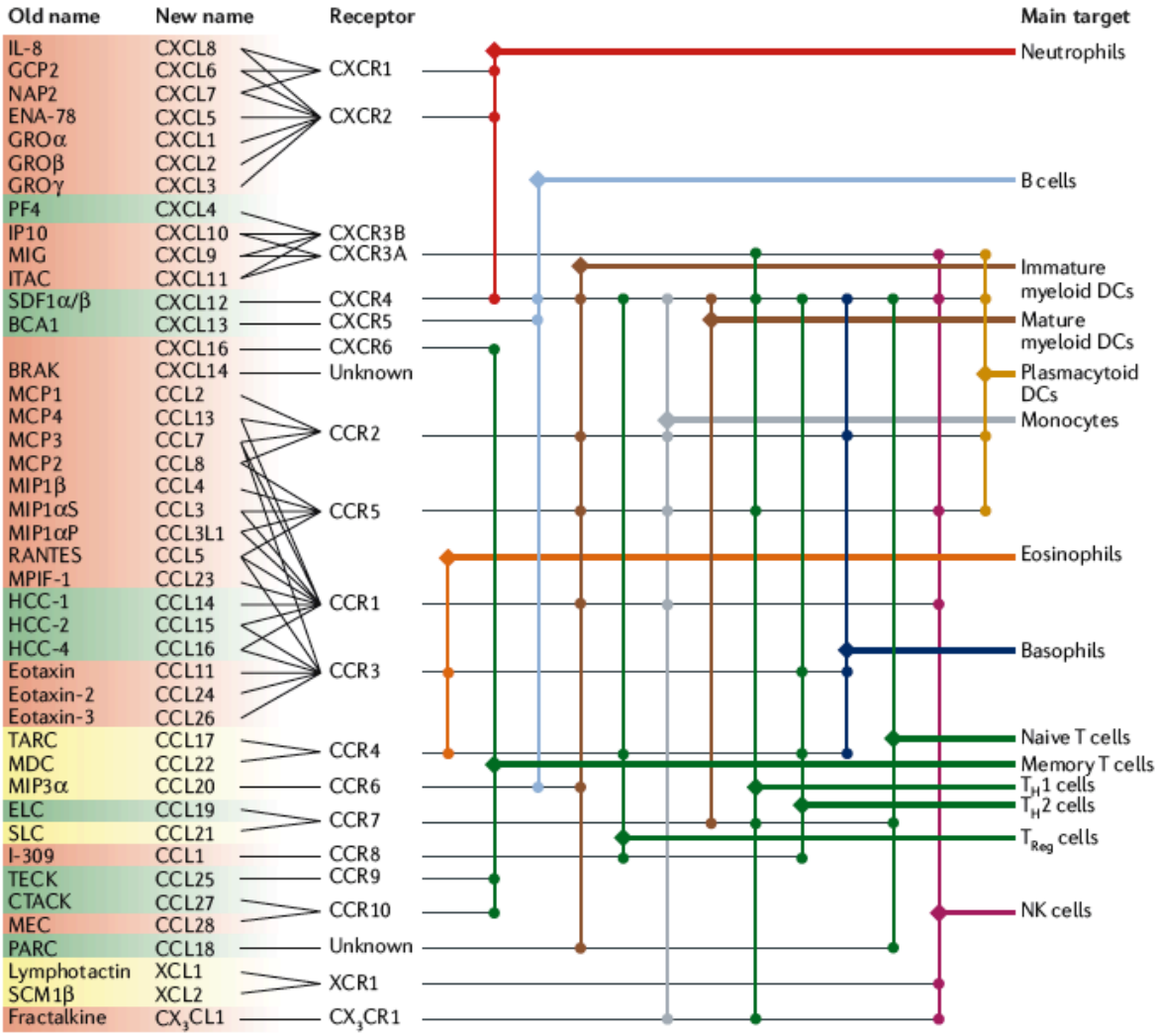

Fig 1.2. Chemokines and chemokine receptors (Mantovani et al., 2006)

Chemokines play important roles in many aspects, such as infection defense, tissue damage repair, atherosclerosis, lymph cell homing and autoimmunity. T cell infiltration into the pancreas is also chemokine dependent. Frigerio and colleagues compared chemokine production in untreated islets and islets exposed to a combination of IL-1β, TNF-α and IFN-γ by real-time PCR. They found the chemokines CXCL10, CXCL9, CCL2, CCL5 are highly elevated in the cytokine-exposed islets (Frigerio et al., 2002). CXCL10 neutralization in the NOD mouse could delay diabetes after cyclophosphamide administration (Morimoto et al., 2004). On the contrary, overexpressing CXCL10 in the pancreas under rat insulin promoter (RIP) accelerated disease after lymphocytic choriomeningitis virus (LCMV) infection by promoting migration of autoreactive T cells into the pancreas (Rhode et al., 2005) CCL2 mainly recruits macrophages and B cells into the pancreas. Overexpression of

CCL2 under the insulin promoter induces insulitis but no diabetes (Grewal et al., 1997). This is consistent with the concept that although B cells, monocytes and macrophages are the first cell types to infiltrate into the pancreas, T cells are the major cells responsible for β cell destruction.

Chemokine receptors belong to the G-protein coupled receptor superfamily, which contain seven transmembrane domains. After recognizing the chemokines, the activated chemokine receptors activate PI(3)K-Dock2-Rac pathway, inducing cell cytoskeleton rearrangement and cell polarization (Weiss-Haljiti C et al., 2004; Viola A et al., 2007). So far, several chemokine receptors have been reported in mediating T cell trafficking and diabetes pathogenesis. CXCR3 is the receptor for CXCL9 and CXCL10. CXCR3 deficient mice are protected from LCMV infection induced diabetes (Frigerio et al., 2002). Similarly, CCR5 neutralization did not inhibit insulitis, but abrogated β cell destruction and diabetes (Carvalho-Pinto et al., 2004). CCR4 is predominantly expressed on Treg and Th2 cells (Lelem et al., 1994; Yagi et al., 2005; Curiel et al., 2004; Ishida et al., 2006; Imai et al., 1999). $CCR4^+$ CD4 T cells are more potent in inducing insulitis than $CCR4^-$ CD4 T cells when transferred into NOD.*scid* mice. Overexpression of macrophage-derived chemokine (MDC, also called CCL22) in the pancreas from birth accelerates diabetes (Kim et al., 2002). A recent paper reported that β cell-specific overexpression of CCL22 from 8 weeks of age prevents disease by recruiting Treg cells into the pancreas (Montane et al., 2011). It is not clear whether the opposite conclusions are due to the timing of CCL22 expression in the pancreas.

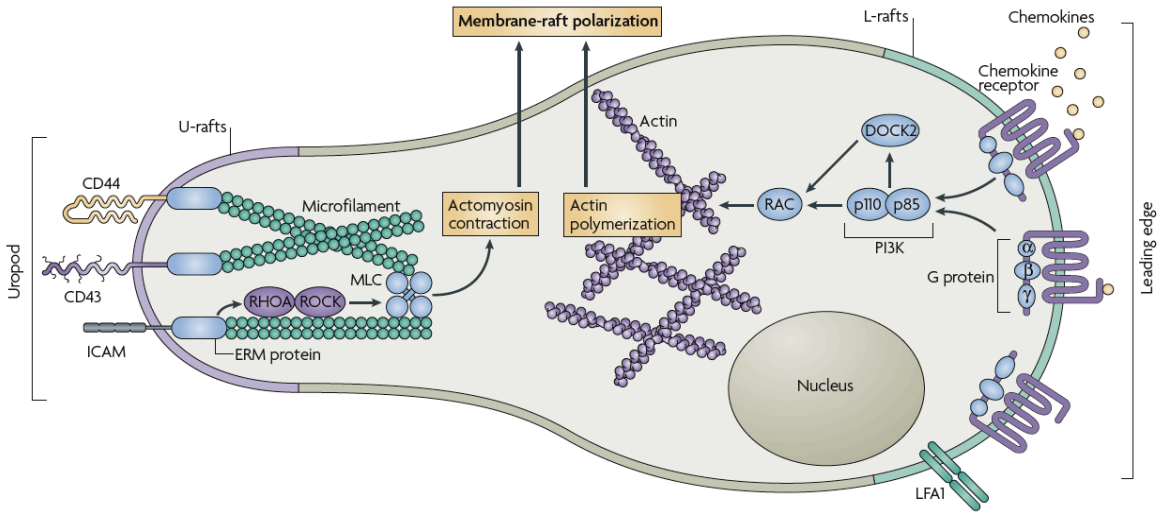

Fig 1.3. Chemokines induced cell cytoskeleton rearrangement (Viola A et al., 2007)

1.2.3.2 T cell specificity in cell trafficking

Another question is whether T cell specificity is required when T cells enter the pancreas. That is, whether autoreactive T cells that recognize the self antigen in the pancreas have priority to enter the pancreas. Fathman and colleagues reported that TCR specificity in $CD4^+$ cells was required for disease transfer, illustrated by the fact that as few as 500 $CD4^{high}$ T cells isolated from islet, but not from spleen, transferred diabetes in $CD8^+$ T cell reconstituted NOD.*scid* mice (Lejon et al., 1999). A recent paper by Lennon and colleagues demonstrated that islet-antigen specificity is required for cell infiltration. According to their model, disease development could be divided into three stages. At the very early stage. monocytes, macrophages, NK cells and B cells enter the pancreas, take up islet antigen and migrate back to the pancreatic lymph node. Only T cells bearing islet specific TCR could efficiently get activated, expanded and trafficked into the pancreas. Bystander T cells play no role at this stage. In the second stage, with increased availability and an array of antigens, T cells that harbor a low affinity to islet antigen are activated and recruited. In the last stage, with the progress of islet destruction, trafficking becomes antigen-independent. (Lennon, et al., 2009)

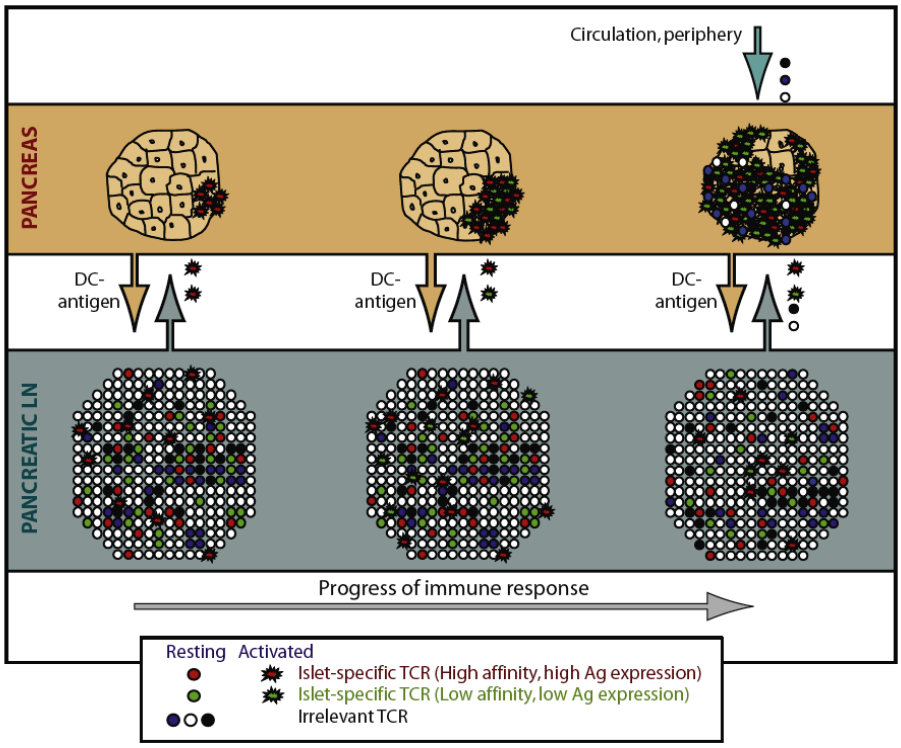

Fig 1.4. Lymph cell infiltration into islet in NOD mouse (Penaranda et al., 2009)

1.3 *PTPN22*

The human gene *PTPN22* is located on chromosome 1p13.3-13.1. *PTPN22* encodes an intracellular tyrosine phosphatase protein, termed Lyp. In mouse, the species homologue gene *Ptpn22* encodes the PEST domain-enriched tyrosine phosphatase (Pep). Lyp/Pep shares a similar structure, bearing 89% sequence homology in the catalytic domain, and 61% homology in the C-terminal domain (Cloutier et al., 1999). The conserved proline-rich motif in C-terminal defines Lyp/Pep belonging to the phosphatase group -PEST (Cloutier et al., 1996; Cloutier et al., 1999; Vang et al., 2008). Other members in this group are PTP-PEST and HSC-PTP (Davidson et al., 1997; Wang et al., 2001). HSC-PTP is exclusively expressed in hematopoietic cells and stem cells. PTP-PEST is widely expressed in many cells (Garton et al., 1996; Shen et al., 2000).

Lyp/Pep is exclusively expressed in hematopoietic cells, including bone marrow, T cells, B cells, as well as myeloid cells (Cloutier et al., 1999; Zikherman et al., 2009). In mouse, only one transcript was detected. In humans, three isoforms of Lyp exist due to alternative splicing. The longest isoform (Lyp1) encodes a 105kDa protein, including N-terminal catalytic PTP domain, and four C-terminal proline-rich motifs. The isoform (Lyp2) encodes a small protein (85kDa), which lacks most of proline-rich motifs (Cloutier et al., 1999). The third isofrom (Lyp3) was reported recently. Lyp3 is almost identical to Lyp1, except the 28bp loss in exon 15 (Wang et al., 2010). The differential roles of these three isoforms remain to be determined.

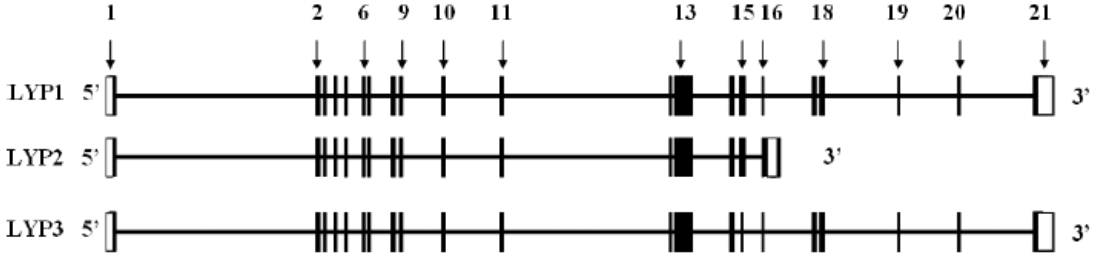

Fig 1.5. Three isoforms of Lyp in humans (Wang et al., 2010)

Overexpression of HA-tagged Lyp, or Myc-tagged Pep followed by imunofluorescent detection revealed that Lyp/Pep is predominantly cytoplasmic (Cohens et al., 1999; Cloutier et al., 1996). 25–50% of Lyp/Pep is constitutively associated with C-terminal Src kinase (Csk) (Cloutier et al., 1996). This association requires SH3 domain of Csk

and the first proline-rich motif of Pep, especially the eight residue stretch (613–621 PPPLPERT) (Cloutier et al., 1996; Gjörloff-Wingren et al., 1999). Substrate trapping identified substrates for Lyp/Pep. The confirmed substrates include Tyr-394 Lck, Tyr-417 Fyn, Tyr-493 Zap70, and TCRξ, which reside in the receptor-proximal point. Potential substrates are Vav, Valosin containing protein (VCP) and CD3ε. Vav is important in cytoskeleton remodeling at the immune synapse, while VCP is involved in cell division/survival (Gjörloff-wingren et al., 1999; Cloutier et al., 1999; Wu et al., 2006).

Lyp/Pep exerts its function in several distinct manners. Lyp/Pep may function alone, or together with its partners, c-Cbl and CSK. Lyp/Pep can be recruited to ZAP-70 through the interactions between SH2 domain of c-Cbl and phospho-Tyr-292 of ZAP-70 (Kawabuchi et al., 2000). Lyp/Pep could also be enriched in the proximity of Src family kinase through the association between SH2 domain of CSK and PAG/Cbp (Brdicka et al., 2000).

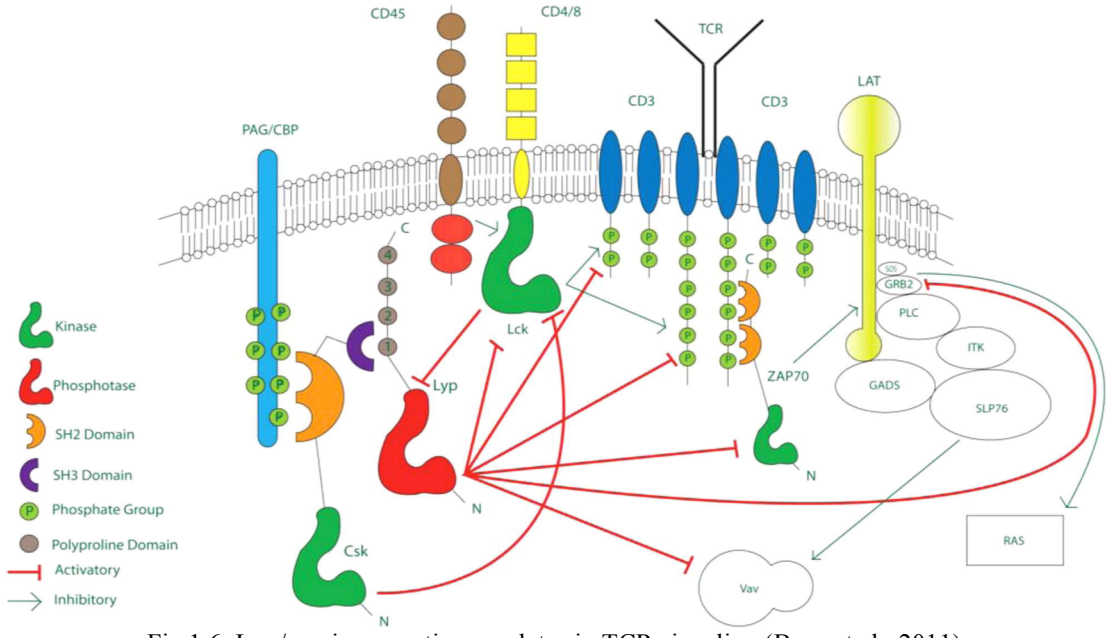

Fig 1.6. Lyp/pep is a negative regulator in TCR signaling (Burn et al., 2011)

1.3.1 The role of *PTPN22* in T cells

Since most of the substrates for Lyp/Pep are involved in TCR signaling, abundant attention has been focused on clarifying the role Lyp/Pep in T cell activation and proliferation. As a tyrosine phophatase, Lyp/Pep can dephosphorylate the positive

regulatory tyrosine residue in Fyn (Y417), Lck (Y394) and ZAP-70, and thereby attenuate T cell activation (Cloutier JF et al., 1999; Gjorloff-Wingren et al., 1999). Interestingly, once T cells are activated, the expression of Lyp/Pep is induced (Cohen et al., 1999). *PTPN22* knockdown by RNAi increases antigen-receptor signaling in Jurkat T-cell line (Begovich et al., 2004), while overexpression suppresses T cell activation (Cloutier et al., 1999).

Although Lyp/Pep acts as a potent negative regulator in TCR signaling, surprisingly, Pep-deficient B6 mice are free from autoimmune disease in spite of some immune disorders: 1) the negative selection in the thymus is unaffected, but positive selection is a little enhanced in the context of TCR transgene; 2) older Pep-deficient mice develop splenomegaly and lymphadenopathy; 3) the effector/memory T cell pool is expanded; 4) naïve T cells are unaffected, while effector /memory T cells are hyperresponsive to TCR stimulation (Hasegawa et al., 2004). 5) Loss of *Ptpn22* increased thymic Treg cell numbers without affecting the function. More surprisingly, although *PTPN22* is not a risk factor in multiple sclerosis, the knockout mice are protected from EAE, possibly due to the increased Treg cells (Maine et al., 2012). In the presence of another risk allele, CD45E613R, Pep-deficient B6 mice develop a lupus-like disease, indicating other risk loci are required for disease development in B6 mice (Zikherman et al., 2009).

1.3.2 The role of *PTPN22* in other cell populations

Besides T cells, *PTPN22* exert important roles in other cells subsets. Increased germinal center formation and elevated serum antibody could be found in the Pep-deficient B6 mice and R619W knockin mice (Hasegawa et al., 2004; Zhang et al., 2011). In the case of dendritic cells (DCs), CD40 expression is upregulated in R619W knockin mice (Zhang et al., 2011). In humans, several reports confirmed that Lyp could alter B cell composition and function. Lyp also participates in the removal of autoreactive B cells (Menard et al., 2011). Heterozygous subjects for *PTPN22* R620W harbor expanded $IgD^{+}CD27^{-}$ B cells (Habib et al., 2012) as well as decreased numbers of memory B cells ($IgD^{+}CD27^{+}$) in peripheral blood (Rieck et al., 2007). BCR signaling is deficient, as illustrated by decreased phosphorylation, calcium flux and impaired proliferation (Arechiga et al., 2009).

1.3.3 *PTPN22* in autoimmune diseases

Like *CTLA-4*, *PTPN22* is also a general risk factor in the human autoimmune disorders. The *PTPN22* susceptibility is contributed by a specific SNP (C1858T). This SNP results in the substitution from arginine 620(620R) to tryptophan(620W) (Bottini et al., 2004). In the mouse, the corresponding replacement is R619W. Lyp-620W has been demonstrated to be a risk factor in many autoimmune diseases, including rheumatoid arthritis (RA) (Orozco et al., 2005; van Oene et al., 2005; Wesoly et al., 2005), juvenile idiopathic arthritis (JIA) (Hinks et al., 2005), systemic lupus erythematosus (SLE) (Kyogoku et al., 2004), Wegener's granulomatosis (Jagiello et al., 2005), Graves' disease (Velaga et al., 2004), generalized vitiligo (Canton et al., 2005), and T1D (Bottini, et al., 2004; Smyth et al., 2004; Onengut-Gumuscu et al., 2004). On the contrary, Lyp-620W is a protective allele in Crohn's disease (Frank et al., 2011; Rivas et al., 2011; Diaz-Gallo et al., 2011). In addition to autoimmune diseases, *PTPN22* is associated with some infectious diseases. Chapman and colleagues reported that Lyp-620W was also a risk allele in invasive pneumococcal disease (IPD) and Gram-positive empyema (Chapman et al., 2006).

R620W substitution in the P1 motif of *PTPN22* disrupts the interaction between Lyp and CSK (Bottini, et al., 2004; Vang et al., 2005). The functional consequence of this mutation is controversial. Several studies demonstrated that R620W is a gain-of-function mutation. When the two variants were transfected into Jurkat T cells, Lyp-620W transfected cells show reduced NF-AT/AP-1 activity. In peripheral blood from heterozygous allele carriers, T cells as well as B cells are less responsive, illustrated by less phosphorylated proteins, reduced IL-2 production, impaired calcium flux and proliferation deficit (Vang et al., 2005; Rieck et al., 2007; Aarnisalo et al., 2008; Habib et al., 2012). Most importantly, the response deficit could be reversed by a Lyp specific inhibitor (Arechiga et al., 2009; Habib et al., 2012). A model was proposed that Lyp and Lck reciprocally inhibit each other. Once TCR is engaged, activated Lck phosphorylates Lyp to attenuate Lyp's function. However, the disease variant Lyp-620W interrupts the interaction between Lyp and Lck, resulting in decreased phosphorylation and elevated Lyp function (Fiorillo et al., 2010).

In contrast, two papers proposed that SNP R620W could be a loss-of-function mutation. Zikherman and colleagues used flow cytometry to strictly control the

expression levels of the two variants in Jurkat T cells. Intracellular staining for phospho-Erk showed Lyp-620W was less potent to dephosphorylate Erk (Zikherman et al. 2009). A paper by Siminovitch and colleagues reported that in the Pep-619W knockin mice, phenotypes of T and B cells are similar to the Pep knockout mice. Further study found that Pep-619W accelerated Pep protein degradation, resulting in lower protein levels (Zhang et al., 2011). However, recent findings indicate that the enhanced Pep degradation in the knockin mice may be due to the interrupted antibody recognition of Pep-619W (Personal communications). Considering the contradictory data, more research is required to clarify these conflicting conclusions about the outcome of R620W mutation in PTPN22. To characterize the role of Pep in T1D within the NOD model, inducible RNA interference (RNAi) was employed in this project.

1.4 Inducible RNAi

Until now, the most conventional method for genetic modification is the knockout technique, which has been widely used in mouse strains for which embryonic stem (ES) cell are available. First, knockout ES cells must be generated, screened and transferred into blastocysts. The surviving blastocysts are then transplanted into the uterus of female mice to deliver chimeric mice. The chimeric mice have to be backcrossed into the original background to derive homozygous knockout Mice. In the case of the NOD mouse, two factors limit the application of this technique. The first is the lack of ES cells for the NOD mouse until 2009 (Nichols et al., 2009). So far, there is no report using NOD ES cells to generate knockout mice. A possible solution is to backcross knockout mice into the NOD genetic background. The second difficulty is the genetic complexity in the NOD mouse. More than 20 risk loci, and dozens of gene variations are implicated in disease onset in the NOD mouse. When backcrossing knockout mice into the NOD background, it is very likely that in addition to the target gene, unexpected genome fragments will also be introduced. For example, in the NOD mouse, *Ptpn22* is located in *Idd* region 18.2 on chromosome 3. On the same chromosome, *Idd*10 and *Idd*18.1 are close to *Ptpn22*. During the backcross, protective B6 gene segments may replace susceptibility genes in *Idd*10, *Idd*18.1 and *Idd*18.2, resulting in the incorrect understanding of *Ptpn22* effect in T1D.

To functionally study the role of Ptpn22 in the pathogenesis of T1D in the NOD mouse, we decided to examine the mouse phenotype when *Ptpn22* is inducibly silenced. Compared to conventional RNAi, inducible RNAi possesses several advantages. First, the knockdown can be initiated at any time, which is valuable when loss of protein is lethal; second, protein expression can be recovered after terminating gene knockdown, which is useful to study phenotype recovery or duration; last, knockdown efficiency can be controlled by different concentrations of inductive material, which is essential to study the effect of gradient TCR/BCR signaling strength on diverse cell populations.

The figure below explains how the inducible knockdown works. The system contains two promoters. shRNA expression is controlled by an RNA polymerase III promoter (H1 promoter) containing a tetracycline operator (TetO). The ubiquitin promoter expresses the tetracycline repressor (TetR) and GFP in all the transfected cells. In the absence of doxycycline (Dox), TetR binds to the tetracycline operator (TetO), blocking shRNA expression. Dox addition in water or food removes TetR from TetO, so that the H1 promoter can transcribe shRNA to induce knockdown (Herold et al., 2008).

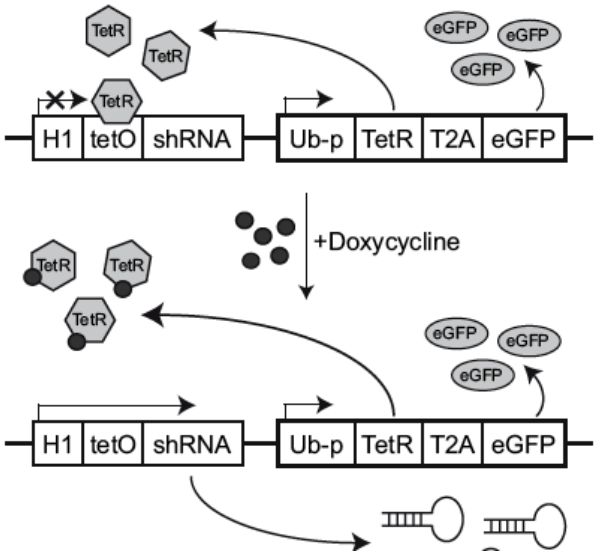

Fig 1.7. Inducible RNAi based on Tetracycline on/off system (Herold et al., 2008)

1.5. Lentiviral transgenesis

Gene knock down can be achieved by siRNA or shRNA. The main disadvantage of using siRNA is the dilution effect (Kim et al., 2007). Once siRNA enters into cells, it cannot be replicated by host cells. During cell division, siRNA concentration will be too low to maintain knockdown. In *in vitro* experiments, siRNA has to be retransfected every 2-3 days. To achieve the sustained knockdown *in vivo*, RNAi based on lentiviral transgenesis was used. Lentiviral vectors provide an alternative tool for transgenesis. Lentiviral vectors derive from immunodeficiency viruses, such as HIV-1. Lentiviral vectors have the capability to incorporate into genomic DNA with high efficiency and long-time duration, in both dividing and non-dividing cells. The preferred integration sites are within intergenic sequences, especially in introns, which means lentiviral integration is unlikely to interrupt endogenous gene function (Yang et al., 2008).

Lentiviral vectors underwent important modifications to improve their safety and gene-transfer efficacy. First, lentiviral vectors were engineered to lose the ability for self-replication. Self-replication components are separated in different vectors. Second, some important DNA elements were added, such as a central poly purine tract sequence (cppt) to enhance the transduction efficacy, woodchuck post regulatory element (WPRE) to stabilize the transcript. Besides, some insulators or matrix/scaffold attachment regions (MAR/SAR) were added to reduce the chance of viral silencing. Last, a 400 bp deletion in the 3'-LTR known as "self-inactivation (SIN)" was performed to prevent transcription from the endogenous LTR internal promoter. Hence, lentiviral vectors have become an appealing method to establish transgenic mice and to manipulate the mammalian genome, especially in ES-deficient mouse strains.

In our study, five plasmids were used to generate lentivirus for gene delivery: transfer vector, Gag-pol, Rev, VSV-G and pAdvantage (Pernod et al., 2004; Singer et al., 2008). Target shRNA was cloned into the transfer vector, which contains Rev responsive element (RRE). Gag-pol encodes reverse transcriptase, integrase and structural proteins. Rev interacts with RRE in the transfer vector to increase virus titers by enhancing nuclear export of viral RNA. VSV-G (Vesicular Stomatitis Virus

protein G) codes for viral envelope proteins, which broaden host cell types. pAdvantage encodes an inhibitor for interferon-induced protein kinase (PKR), that increases lentivirus titers. Five plasmids were cotransfected into 293 F cells to generate lentivirus. Lentivirus carrying inducible shRNA was injected into the perivitelline space of single cell embryo to obtain transgenic NOD mice.

1.6. Aim of study

As mentioned above, Lyp-620W confers susceptibility in many human autoimmune diseases. So far, whether the R620W allele is a gain- or loss- of function remains controversial. Therefore, in this project we aimed to

1) explore if Lyp-620W is a gain- or loss-of-function variant by studying the role of Pep in T1D and colitis in the NOD mouse. Furthermore, by using the inducible knockdown system, *Ptpn22* was silenced in the adult mice when most thymocytes are matured to better mimick the therapy in humans.
2) functionally study the role of Pep in different cell populations (Treg cells, regulatory B cells);
3) examine the role of Pep on chemokine receptors. Chemokine receptors are crucial for lymph cell trafficking into pancreatic islets. So far, a lot of attention was paid on the role of Lyp/Pep in naïve, effector T cells and antigen presenting cells (B cells, DCs). It is totally unknown weather Pep regulates chemokine receptor expression.

CHAPTER 2

MATERIALS AND METHODS

2.1 Materials

2.1.1 Chemicals and reagents

Chemicals/reagents	Source	Application
10X Dreamtaq buffer	Fermentas	PCR
10X T4 ligase buffer	Fermentas	
19G, 27G needles	Neoject	Tissue digest
1ml, 20ml, 30ml syringe	Terumo	Tissue digest
24 well plate	BD	Cell culture
4X laemmli buffer	Roth	Western blot
6 well plate	BD	Cell culture
Absolute Blue SYBR Green ROX mix	Thermo Scientific	RT-PCR
acrylamide solution (30%)	Biorad	
Agarose	Roth	
Ammonium persulfate (APS)	Roth	
Ampicillin	Roth	
BbsI	New England Biolabs	Restriction digest
Beta mercaptoethanol	Roth	
Beta mercaptoethanol	GIBCO	Cell culture
Biotinylated protein ladder	Cell signaling technology	
Brefeldin A	Sigma	Intracellular staining
Bromophenol blue	Roth	
BSA	Sigma	Solution preparation
BSA	New England Biolabs	Pancreas digestion
Buffer 1	New England Biolabs	Restriction digest
Buffer 2	New England Biolabs	Restriction digest
Buffer 4	New England Biolabs	Restriction digest
$CaCl_2$	Roth	
Calf intestinal alkaline phosphtase (CIAP)	Fermentas	
Chloroform	Roth	
Compensation beads	BD	
Complete Freund's adjuvant	Sigma	*In vivo* priming
Cyclophosphamide.H_2O (CY)	Sigma	Diabetes induction

Dimethyl sulfoxid (DMSO)	AppliChem	
DNA ladder (1Kb plus)	Fermentas	
DNA ladder (low range)	Fermentas	
DNase I	Roche	Pancreas digestion
dNTP	Fermentas	
Doxycline hydrate (Dox)	Sigma	RNAi induction
D-PBS	GIBCO	
Dreamtaq polymerase	Fermentas	PCR
Dynabeads mouse T activator CD3/CD28	Invitrogen	
ECL	Perkin Elmer	
EDTA	Roth	
eFluor® 670	eBioscience	Cell proliferation tracer
Elisa 96 well plate (maxi sorp)	Nunc	Elisa assay
Ethanol	Roth	
Ethidium bromide	Roth	
Fetal calf serum (FCS)	GIBCO	
Fugene HD	Roche	Transfection
Genejammer	Agilent (Stratagene)	Transfection
Glutamine	GIBCO	
Glycerol	Roth	
Glycine	Roth	
H2SO4	Roth	
H3-thymidine	Hartmann Analytic	
HEPES	GIBCO	Cell culture
Human chorionic gonadotropin (HCG)	Sigma	
Hybond^{TM}-N^{+} membrane	Amersham GE Healthcare,UK	
Ionomycin	Sigma	
Isofluran	Cp-pharma	
Isopropanol	Roth	
KCl	Roth	
KHCO3	Roth	

LD column	Miltenyi Biotech	Cell isolation
Liberase TL	Roche	Pancreas digestion
LPS	Sigma	
LS column	Miltenyi Biotech	Cell isolation
Methanol	Roth	
MgCl2	Roth	
MgCl2	Fermentas	
MicroAmp clear adhesive film	Applied Biosystems	
MOG peptide	Biotrend	
MS column	Miltenyi Biotech	Cell isolation
Na2-EDTA	Roth	
Na2HPO4 (2H2O)	Roth	
NaCl	Roth	
NaH2PO4 (H2O)	Roth	
NaHCO3	Sigma	
NaOH	Roth	
NH4Cl	Roth	
Nitrocellulose membrane	BioRad	
PacI	Fermentas	Restriction digest
Passive lysis buffer	Sigma-Aldrich	
Penicillin streptomycin solution	Invitrogen	
Pertussis toxin	Sigma	
Phorbol myristate acetate (PMA)	Sigma	
PMS hormone	Sigma	
PNK	Fermentas	
Polybrene	Sigma	Transfection
Polyfect	Qiagen	Transfection
Primer-probe pair	Universal probe library, Roche	
Protein ladder	BioRad	
rhIL-2	R&D	Treg cell expansion
rhTGF-β	R&D	T cell differentiation
RNA later	Qiagen	
RNase A	Qiagen	

RT-PCR plate (384 well clear optical)	Applied Biosystems	
SDS	Roth	
Sodium citrate	Sigma	
Sodium pyruvate	GIBCO	Cell culture
T4 DNA ligase	Fermentas	
TE buffer	Fluka Analytical	
TEMED	BioRad	
Tris	Roth	
Tris-HCl	Roth	
Trizol	Invitrogen	RNA extraction
Trypsin	GIBCO	
Tween20	Roth	
U-100 insulin syringe	Terumo	Mouse injection
U-bottom 96 well plate	BD	Cell culture
Ultra-clear centrifuge tube	Beckman	Virus centrifuge
Universal probe master mix (ROX)	Roche	RT-PCR
V-bottom 96 well plate	Nunc	Cell staining
Whatman paper	VWR	
XhoI	Fermentas	Restriction digest
X-ray film	Fujifilm	

2.1.2 Medium

Medium	Recipe	Application
DMEM	Advanced DMEM (invitrogen, #12491) plus: 10% heat inactivated FCS, Penicillin-Streptomycin	293-F cell culture
RMPI	RMPI 1640 (invitrogen, #51875) plus: 10% heat inactivated FCS, Penicillin-Streptomycin, 1mM Sodium pyruvate 50uM 2- mercaptoethanol 10mM Hepes	T, B and DC culture

2.1.3 Buffer

Buffer	Supplier/recipe	Application
0.4% Trypan blue buffer	Invitrogen	Cell counting
10X PBS	Invitrogen	Buffer/solution preparation
10X SDS running buffer	10g SDS, 30.3g Tris and 144.1g glycine in 1L dd H_2O distilled water.	Western blot
1X PBS	Invitrogen	Cell culutre
ACK buffer	8.29g ammonium chloride, 1.0g potassium bicarbonate and 37.3 mg Na2EDTA in 800ml distilled H_2O. Adjust the pH to 7.2-7.4 and fill up to 1L with distilled H_2O.	Lysis of red blood cells
Annexin V binding buffer	10mM Hepes (2.38g/L), 150mM NaCl (8.766g/L), 5mM KCl (0.372g/L), 1mM MgCl2 (0.203g/L) and 1.8mM CaCl2 (0.199g/L). Adjust pH to 7.4 with NaOH.	Annexin V staining
Blocking solution (5%)	5g nonfat dried milk powder in 100ml 0.2% TBST buffer	Membrane block in western blot
Cell depletion buffer	0.1% FCS (0.5ml) and 2mM EDTA (0.3722 mg) in 1X PBS (500ml, Invitrogen). 50°C for 4-5 hours or RT overnight. Buffer is filtered and stored at 4°C	Cell depletion with invitrogen dynalbeads
FACS buffer	5ml heated inactivated FCS in 500ml PBS. Stored at 4°C	FACS staining
LB medium with Ampr	10g Trypton, 10g yeast extract and 5g sodium chloride in 1L distilled water. Adjust pH to 7.0 with sodium hydroxide. After autoclaved and cooling down 50-55°C , add 50µg/ml Ampicillin (50ml/ml in 50% EtOH)	Bacteria culture

LB plate	Add 8g agar into LB medium (without antibiotics). After autoclaved and cooling down 50-55°C , add 100µg/ml Ampicillin, or 50µg/ml Kanamycin (50ml/ml in 50% EtOH)	Cloning
MACS buffer	0.5% FCS (2.5ml) and 2mM EDTA (0.3722 mg) in 1X PBS (500ml, Invitrogen). 50°C for 4-5 hours or RT overnight. Buffer is filtered and stored at 4°C	Cell separation with MACS Kits
P1 buffer (resuspension buffer)	50mM Tris-HCl (6.06g) and 10mM EDTA(3.72g $Na_2EDTA\ 2H_2O$) in 800 ml distilled water. Adjust pH to 8.0 with HCl and fill up to 1L. Finally add 100mg (100µg/ml) RNaseA	Miniprep
P2 buffer (lysis buffer)	200mM NaOH (8g) and 1% SDS(50ml 20% SDS w/v) in 1L distilled water	Miniprep
P3 buffer (neutralisation buffer)	3M Potassium-Acetate (294.5g) to pH5.5 with acetic acid, fill up to 1 liter	Miniprep
PBS/EDTA	2mM (0.3722mg) EDTA in 500 ml PBS. 50°C for 4-5 hours or RT overnight. Buffer is filtered and stored at 4°C	For tail blood collection
TBST (0.2%)	50mM Tris (6.05g) and 150mM NaCl (8.76g) in 800 ml distilled water. Adjust pH to 7.5 and fill up to 1L. Finally add 2ml Tween 20	Membrane wash in western blot
Transfer buffer	2.9 g glycine, 5.8 g Tris and 0.37 g SDS in 800ml distilled water. Adjust the volume to 1L with 200ml methanol	Western blot
Wash buffer	200ml 10X PBS in 1.8L distilled water. Add 1ml Tween20 (0.05%)	ELISA assay

2.1.4 Kits

Kit	Supplier	Application
BCA protein assay kit	Novagen	Measuring protein conc
CBA kit	BD	Cytokine measurement by FACS
CCL17 elisa kit	R&D	Elisa assay
CCL22 elisa kit	R&D	Elisa assay
$CD11c^+$ MACS separation kit	Miltenyi Biotech	DC isolation
CD19 MACS separation kit	Miltenyi Biotech	B cell isolation
$CD4^+CD25^+$ MACS separation kit	Miltenyi Biotech	Treg cell isolation
$CD4^+CD62L^+$ MACS separation kit	Miltenyi Biotech	Naïve/effector T cell isolation
CD43 MACS separation kit	Miltenyi Biotech	B cell isolation
DNeasy blood and tissue kit	Qiagen	DNA extraction
FoxP3 staining kit	eBioscience	Foxp3 staining
QIAfilter Plasmid Maxi kit	Qiagen	Plasmid for virus production
QIAquick Gel Extraction kit	Qiagen	DNA purification from gel
QIAquick PCR purification kit	Qiagen	DNA purification from buffer
Ready-Set-Go Elisa kit	eBioscience	Cytokine measurement
RNeasy kit	Qiagen	RNA extraction
Transcriptor first strand DNA synthesis kit	Roche	cDNA synthesis

2.1.5 Bacteria and cell line

Bacteria:

Bacteria	Supplier	Application
DH5α	Invitrogen	Transformation and cloning
MAX EfficiencyDH5α	Invitrogen	Transformation and cloning
Novablue	Invitrogen/ Merck/ Novagen	Transformation and cloning
One Shot TOP10	Invitrogen	Transformation and cloning

Cell line:

293 F cell line: is also called HEK 293 cell line. It is established from human embryonic kidney cells transformed with sheared adenovirus 5 DNA. 293 F cells are easy to culture and transfect. In this project, 293 F cells were used to generate lentivirus.

2.1.6 shRNA Sequences against *Ptpn22*

P1 (position 321): target-GTAGAGCTGTCTCTGTTAA
Fwd:
TGTAGAGCTGTCTCTGTTAATTCAAGAGATTAACAGAGACAGCTCTACTTTTTTC
Rev:
TCGAGAAAAAAGTAGAGCTGTCTCTGTTAATCTCTTGAATTAACAGAGACAGCTCTACA

P2 (position 345): target-GATGAGGATTCCAGTTATA
Fwd:
TGATGAGGATTCCAGTTATATTCAAGAGATATAACTGGAATCCTCATCTTTTTTC
Rev:
TCGAGAAAAAAGATGAGGATTCCAGTTATATCTCTTGAATATAACTGGAATCCTCATCA

P3 (position 1421): target-GGACAGGTATCACAATTCA
Fwd:
TGGACAGGTATCACAATTCATTCAAGAGATGAATTGTGATACCTGTCCTTTTTTC
Rev:
TCGAGAAAAAAGGACAGGTATCACAATTCATCTCTTGAATGAATTGTGATACCTGTCCA

P4 (position 1682): target-GCATCTGTACACATCTTTA
Fwd:
TGCATCTGTACACATCTTTATTCAAGAGATAAAGATGTGTACAGATGCTTTTTTC
Rev:
TCGAGAAAAAAGCATCTGTACACATCTTTATCTCTTGAATAAAGATGTGTACAGATGCA

P5 (position 2285): target-GAACTCCACATCTTCTAAA
Fwd:
TGAACTCCACATCTTCTAAATTCAAGAGATTTAGAAGATGTGGAGTTCTTTTTTC

Rev:
TCGAGAAAAAAGAACTCCACATCTTCTAAATCTCTTGAATTTAGAAGATGTGGAGTTCA

P6 (position 2562): target-GCAGATAAAGCTACTTGAA
Fwd:
TGCAGATAAAGCTACTTGAATTCAAGAGATTCAAGTAGCTTTATCTGCTTTTTTC
Rev:
TCGAGAAAAAAGCAGATAAAGCTACTTGAATCTCTTGAATTCAAGTAGCTTTATCTGCA

P7 (position 2578): target-GAATACTGCTATAATAATA
Fwd:
TGAATACTGCTATAATAATATTCAAGAGATATTATTATAGCAGTATTCTTTTTTC
Rev:
TCGAGAAAAAAGAATACTGCTATAATAATATCTCTTGAATATTATTATAGCAGTATTCA

P8 (position 2639): target-GAAAGCAATATGTGACAAA
Fwd:
TGAAAGCAATATGTGACAAATTCAAGAGATTTGTCACATATTGCTTTCTTTTTTC
Rev:
TCGAGAAAAAAGAAAGCAATATGTGACAAATCTCTTGAATTTGTCACATATTGCTTTCA

2.1.7 Antibodies

Antigen	FC	Company	Clone	Dilution
Actin		Sigma		
Annexin V	APC	BD		1:100
Annexin V	PE	BD		1:100
ArmHamster IgG1	Purified/FG	BD	G94-56	
B220 (CD45R)	APC	BD	RA3-6B2	1:300
B220 (CD45R)	PE	BD	RA3-6B2	1:300
B220 (CD45R)	APC eFluor 780	eBioscience	RA3-6B2	1:400
CD103	PerCP-Cy5.5	BioLegend	2E7	1:400
CD11b	PECy7	BD	MI/70	1:800
CD11b	eFluor 450	eBioscience	MI/70	1:1600
CD11c	PECy7	BD	HL3	1:1600
CD16/32 (FcgR3/2)	Purified/FG	eBioscience	93	1µl/ $1x10^6$ cells
CD19	eFluor 450	eBioscience	1D3	1:1600
CD23	PE	eBioscience	B3B4	
CD25	PECy7	BD	PC61	1:300
CD25	PerCP-Cy5.5	BioLegend	PC61	1:300
CD25	APC	eBioscience	PC61.5	1:300
CD25	PerCP-Cy5.5	eBioscience	PC61.5	1:300
CD25	Purified/FG	eBioscience	PC61.5	
CD273 (B7-DC)	PE	BD	TY25	1:800
CD274 (B7H1)	PE	BD	MIH5	1:800
CD28	Purified/FG	BD	37.51	
CD28	Purified/FG	eBioscience	37.51	
CD3ε	FITC	BD	145-2C11	
CD3ε	PE	BD	145-2C11	1:300

CD3ε	PerCP	BD	145-2C11	1:200
CD3ε	V500	BD	500A2	1:800
CD3ε	PerCP-Cy5.5	BioLegend	145-2C11	1:400
CD3ε	Brilliant Violet 421	BioLegend	145-2C11	1:400
CD3ε	Purified/FG	eBioscience	145-2C11	
CD3ζ	PE	Cedarlane	Cl7230	
CD4	Alexa 647	BD	RM-4-5	1:400
CD4	APC-Cy7	BD	GK1.5	1:800
CD4	PerCP-Cy5.5	BD	RM4-5	1:800
CD4	V500	BD	RM4-5	1:1600
CD4	Brilliant Violet 421	BioLegend	GK1.5	1:800
CD4	APC	eBioscience	RM4-5	1:800
CD4	Purified/FG	eBioscience	GK1.5	
CD40	Purified/FG	eBioscience	HM40-3	1:800
CD40L (CD154)	PE	BD	MR1	
CD44	FITC	BD	IM7	
CD44	PECy5	BD	IM7	1:3000
CD45	eFluor 780	eBioscience	30-F11	1:400
CD45RB	PE	eBioscience	C363.16A	1:1600
CD49b/Pan NK	FITC	BD	DX5	
CD5	PE	BD	53-7.3	1:300
CD62L	FITC	BD	MEL-14	
CD62L	PE	BD	MEL-14	1:200
CD62L	APC-Cy7	BioLegend	MEL-14	
CD69	PECy7	eBioscience	H1.2F3	1:300
CD8	PE-Cy7	BioLegend	53-6.7	
CD80	Biotin	BD	16-10A1	
CD80	APC	eBioscience	16-10A1	1:1600
CD86	Biotin	BD	GL1	
CD86	APC	eBioscience	GL1	1:1600
CD86	PE	eBioscience	GL1	1:1600
CD8a	APC	BD	53-6.7	1:800
CD8a	PE	BD	53-6.7	1:800
CD8a	PECy7	BD	53-6.7	1:800
CD8a	eFluor 450	eBioscience	53-6.7	1:1600
CD93 (AA4.1)	APC	eBioscience	AA4.1	
CTLA-4 (CD152)	PE	BD	UC10-4F10-11	1µg intrac
CTLA-4 (CD152)	PE	eBioscience	UC10-4B9	1µg intrac
F4/80	PECy5	eBioscience	BM8	1:400
F4/80	APC	eBioscience	BM8	
Foxp3	APC	eBioscience	FJK-16s	
Foxp3	PE	eBioscience	FJK-16s	
GITR	APC	eBioscience	DTA-1	1:300
GITR-L	Biotin	eBioscience	eBio YGL386	

goat IgG	PE	Santa Cruz		
I-A^b	PE	BD	AF6-120.1	
I-A^k	Biotin	BD	10-3.6	
ICAM-1 (CD54)	PE	BD	3E2	
IgD	PE	BD	11-26c.2a	
IgM	PE-Cy7	BD	R6-60.2	1:200
IgM F(ab)'2	purified	Jackson Immuno	115-006-020	
Klrg1 (MAFA)	PE	BioLegend	2F1/KLRG1	1:400
PLC-γ2 (pY759)	PE	BD		
PEP (Ptpn22)		From Dr. Chan		
PI	Purified/FG	BD		1μl/ 1x106 cells
rat IgG1 κ	APC	BD		
rat IgG1 κ	PE	BD		
rat IgG2a	APC	eBioscience	eBR2a	
rat IgG2a	Biotin	eBioscience	eBR2a	
RT1B (I-Ag7)	PerCP	BD	OX-6	1:800
SA	APC	BD		
SA	PE	BD		
SA	PerCP-Cy5.5	BD		
TCRβ	APC	BD	H57-597	1:300
TCRβ	Biotin	BD	H57-597	
TCRβ	APC eFluor 780	eBioscience	H57-597	
TCRβ	PerCP-Cy5.5	eBioscience	H57-597	1:300
tetR		Mobitec		
Zap70 pY319	Alexa 647	BD	17A/P-ZAP70	

2.2 Methods

2.2.1 293 F cell passage

The 293 F cell line is derived from human embryonic kidney cells, which is maintained in advanced DMEM medium supplemented with 5% FCS, glutamine and penicillin/ streptomycin (P/S) in 10 cm plates. The plates are maintained in the incubator at 37°C with 5% CO_2. After 3-day growth, exhausted medium is aspirated; cells are washed with 10ml PBS and then treated with 1ml trypsin for 2-3min. 9 ml media is then added to inactivate trypsin as well as to suspend cells. 1 ml cell suspension is added into new plates containing 9 ml fresh medium.

2.2.2 Cloning of inducible shRNA expression vector

Dr. Stephan Kissler had previously tested knock down efficiencies of 8 shRNAs in

the pLB backbone. Luciferase reporter assay demonstrated that shRNA P2 and P4 displayed the highest knock down efficiency. These two shRNA sequences were cloned into the inducible shRNA expression vector FH1t-UTG (kindly provided by Dr. MJ Herold). The inducible shRNA expression system consists of 2 vectors, pH1tet-flex and FH1tUTG. shRNAs are synthesized, phosphorylated and cloned into pH1tet-flex vector. The fragment containing the H1 promoter and tet-operator is cut and inserted into the final vector, FH1tUTG.

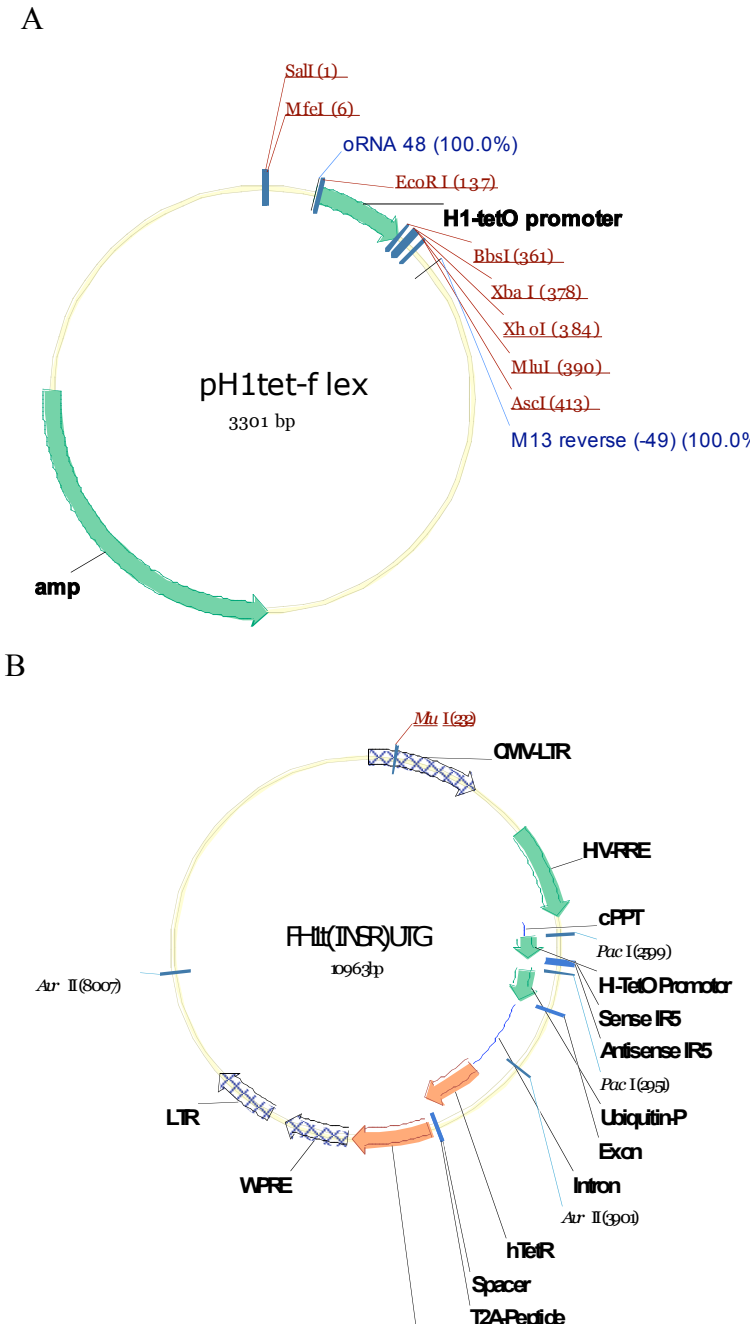

Fig 2.1 : Schematic diagram of the inducible shRNA expression system.

A: pH1tet-flex vector, B: FH1tUTG vector

First, forward and reverse oligos with BbsI and XhoI overhangs were synthesized (Sigma) and dissolved in ddH_2O at 100pmol/µl. Oligo phosphorylation is done in the following reaction condition:

6µl	oligos
1µl	PNK
1µl	T4 ligase buffer
2µl	ddH_2O

37°C for 1 hour.

Phosphorylated fwd and rev oligos were annealed in the PCR machine using the following conditions: 94°C 2min, 70°C 5min, and 4°C 10min. The annealed oligos were diluted in 600µl ddH_2O.

To insert shRNA oligos behind the human H1 promoter containing a tet-operator in the pH1tet-flex vector, the vector was digested with BbsI and XhoI:

30µl (3µg)	pH1tet-flex
2µl	BbsI
1µl	XhoI
0.5µl	BSA
5µl	NEB buffer 2
11.5µl	ddH_2O

37°C for 1.5 hour.

The digested DNA fragment was purified by Qiaquick PCR purification kit. Purified vector was ligated with annealed oligos:

10µl (3µg)	digested pH1tet-flex
1µl	diluted oligos
2µl	T4 ligase buffer
1µl	T4 ligase
6µl	ddH_2O

22°C for 2 hour.

The ligation products were used to transform DH5α competent bacteria. Competent bacteria were thawed on the ice, and then incubated with ligation product for 30min. Bacteria were heat-shocked at 42°C for 90s, and then kept on ice for 5min prior to being plated out. The positive clones are selected on ampicillin LB agar plates. Besides the positive clones, self-ligated vector without insert could also grow in the presence of ampicillin. To screen for positive clones, 10 clones for each construct were picked and cultured in 3ml ampicillin containing LB medium for 6-7h to prepare the miniprep.

2.2.3 Miniprep

Miniprep was used to isolate plasmid DNA from bacteria in a small scale. Miniprep was performed with P1, P2 and P3 buffers prepared in the laboratory (recipes mentioned in material section). Bacteria suspensions were transferred into eppendorf tube and spun down at 13000rpm for 5min to harvest bacteria. The pellet was resuspended at 150µl P1, followed by addition of 150µl P2, inverting several times, and incubating at RT for 2min. 150µl P3 was then added. The mixture was centrifuged at 13000rpm for 5min. The supernatant was transferred into a new eppendorf tube. 300µl isopropanol was added to precipitate plasmid DNA by centrifuging at 13000rpm for 10min. The DNA pellet was washed with 500µl 70% ethanol. DNA is air dried and dissolved in 30-50 µl ddH_2O.

The plasmid DNA was digested using restriction enzyme to screen the positive clones. In this case, when PacI enzyme was used, positive and negative clones should generate a 300bp and 23bp band, respectively.

42.5µl (24µg)	pH1tet-flex DNA
2µl	PacI
5µl	NEB buffer1
0.5µl	10X BSA

37°C for 2 hour.

In parallel, 5µg FH1tUTG vector was digested with PacI in the same condition. The reaction products are run in 1% agarose gel. FH1tUTG backbone and 300bp band from pH1tet-flex are cut and purified by Qiaquick gel purification kit, followed by

ligation, and transformed into component DH5α bacteria to prepare plasmid DNA by miniprep. The positive clones were screened by XhoI digest, and further sequenced with primer FUW1 (GACATAATAGCAACAGAC) to make sure the shRNA sequence is correct.

2.2.4 Luciferase reporter assay

To further validate that the shRNA sequence is correct, a luciferase reporter assay with psi-check2 vector was used to measure shRNA knockdown efficiency. In this dual luciferase vector, firefly luciferase is constitutively expressed and used to normalize data to the transfection efficiency. *Ptpn22* cDNA was inserted behind renilla luciferase mRNA, into the 3' UTR. The principle is if the shRNA works efficiently, the fusion mRNA will be degraded, resulting the reduction of renilla luciferase signal. Thus, the reduction of renilla luciferase should be an indicator of shRNA knock down efficiency.

In this assay, 2.5 x 10^5 293F cells were plated on a 24-well plate. The following day, cells were co-transfected with 100 ng psi-check 2 containing Ptpn22 cDNA, 300 ng shRNA constructs and 3 μl Genejammer. After 1 day, supernatant was aspirated and cells were washed once with 200 μl PBS. Cells were lysed with 150 μl passive lysis buffer at RT for 5min. 5 μl lysate was added into an opaque 96-well plate to measure firefly and renilla luciferase with a Fluostar Optima luminometer.

2.2.5 Maxiprep

The maxiprep was used to get a large amount of plasmid DNA for lentivirus production. Bacteria with correct P2 or P4 shRNA plasmid were grown in 100 ml ampicillin containing LB medium overnight. The maxiprep was performed with a Qiagen maxiprep kit according to the manufacturer's instructions. In principle, bacteria were lysed and neutralized. DNA bind to anion exchange resin under low salt and pH condtion and further washed by high salt buffer. Finally, DNA was dissolved in TE buffer at the concentration of 1μg/μl.

2.2.6 Lentivirus production and titration

Once a large amount of DNA was obtained by maxiprep, lentivirus was produced to

generate transgenic mice. To generate lentivirus, 8-9 x 10^6 293 F cells were plated in 20 cm plate. The next day, 3µg pCMV-VSVg, 3µg RSV-rev, 4µg pMDL-gag/pol, 5µg pAdvantage, 20µg shRNA construct along with 70µl Fugene HD were added into 2ml serum free media. The mixture was incubated at room temperature for 30 minutes, and then added onto cells. 2 days after transfection, supernatant was collected, spun down at 2300rpm for 7min and filtered. Viral medium was then ultracentrifuged at 25000rpm for 90min. The supernatant was carefully aspirated. 100µl PBS was added along the tube. The virus was recovered by overnight resuspension at 4°C. The next day virus was carefully resuspended, and aliquoted into 4tubes. The tubes were flash-frozen in liquid nitrogen and stored at -80°C.

Only lentivirus with high titers was used to inject single cell embryo. To titrate lentivirus, 4 x 10^5 293 F cells were plated into 6 well plates the day before titration. 1µl lentivirus is added into 1ml DMEM medium, and then further serially diluted to 1:10 and 1:100. After 1-day infection, supernatant is removed. Cells were washed twice with 1ml PBS, and then transferred into FACS tube. The percentage of GFP^+ cells is recorded by FACS CantoII.

2.2.7 Generation of lentiviral transgenic NOD mice

No ES cells were available in the NOD background until very recently (Nichols et al., 2009). To generate transgenic NOD mice, single cell NOD embryos were employed. Female mice were injected with pregnant mares serum (PMS), 48 hours later followed with human chorionic gonadotropin (HCG). Females were then mated with males overnight. The next morning, females were dissected to obtain oviducts. Single cell embryos were collected under a microscope.

Lentivirus with high titers (>1x10^8 particles/ ml) was injected into the perivitelline zone of embryos. Infected embryos were then implanted into pseudopregnant females to deliver transgenic pups. Since P2/P4 shRNAs were used to inducible knock down Ptpn22, transgenic mice carrying P2 and P4 shRNA are termed P2 and P4 mice, respectively.

2.2.8 Mouse genotyping

In the shRNA expression cassette, the ubiquitin promoter constitutively expresses GFP. Thus, GFP is a good indicator for transgenic mice. After pups were weaned, blood samples were collected from tail cut. Blood was treated with ACK buffer to remove red blood cells. Cells were washed twice with PBS 1% FCS, and then analysed by FACS to check the GFP expression in the lymphocytes.

2.2.9 Mouse treatment

Transgenic P2/P4 mice were treated with 200 µg/ml Doxycycline (Dox) to knock down *Ptpn22*. Meanwhile, WT and some P2/P4 mice were left untreated to test for leaky shRNA expression without Dox. Some WT mice were also treated with Dox to examine the effect of Dox in non-transgenic mice.

2.2.10 Knock down validation by qRT-PCR and western blot

When mice were 5-7 weeks old, they were treated with Dox for 7-10 days. Mice were then dissected to obtain lymph nodes. Lymph cells were treated with ACK buffer, filtered to make single cell suspensions. Lymph cells were used to prepare samples for qRT-PCR and western blot to validate knock down on the mRNA and protein levels.

qRT-PCR:

Total RNA was obtained using Qiagen RNeasy kit following manufacturer's instructions. cDNA was synthesized with a first strand cDNA synthesis kit from Roche. For each reaction:

1µg	Total RNA
1µl (2.5µm)	Anchored-oligo dT 18 primer
2µl (60µm)	Random hexames primers
variable	H_2O
13µl	Total volumn

The mixture was heated at 65°C for 10min, immediately cooled on ice. Adding master mix containing:

4µl	RT buffer 5X

0.5µl	DNase inhibitor
2µl	DNTP mix (10mM each)
0.5µl	Reverse transcriptase (20U/µl)

The 20 µl mixture was left in the PCR machine using program 25°C 10min, 55°C 30min, 85°C 5min and then 4°C forever. cDNA is diluted with H_2O to 1:3. qRT-PCR is done with Taqman probe and universal probe master mix (ROX) from Roche. The primer sequences and probe are as follows:
GAPDH: fwd 5'- agcttgtcatcaacgggaag-3', rev 5'-tttgatgttagtggggtctcg- 3', probe: #9
PTPN22: fwd 5'- cagaacgtgttcagccaaaa-3', rev 5'-ttggtcctttgcgttttgaa- 3', probe: #17

The PCR was performed in 384-well plates. For each reaction:

5µl	Roche master mix 2X
0.4µl	Fwd primer (10um)
0.4µl	Rev primer (10um)
2.1µl	ddH_2O
0.1µl	Probe

The PCR reaction was carried out with an ABI 7900HT (Applied Biosciences) instrument using the following conditions: 50°C 2min, 95°C 10min, 40 cycles of 95°C 15 seconds and 60°C 1min, lastly 60°C 1min.

Western blot

~ 5 x 10^6 lymph cells were used to prepare the western blot sample. Cells were washed once with PBS, and then lysed in 100µl RIPA buffer supplemented with 10% protease inhibitor cocktail on ice for 30min. The lysates were centrifuged at 14000rpm for 15min to remove cell debris. The supernatant was transferred into new eppendorf tubes. The protein concentration was measured with BCA protein assay kit (Novagen).

Western blot was done with BioRad Protean 3 system. Before loading samples into gel, the same amount of proteins was mixed with Laemmli buffer and boiled at 95°C for 10 minutes. Samples and protein ladders were run on a 12 % acrylamide gel. Once

protein ladder reached the bottom of the gel, samples were transferred onto a nylon membrane at 100V for 90min. After transfer, the membrane was blocked with a 5% fat-free milk solution for 1 hour at room temperature. The primary antibody was then added at 4°C overnight (anti-PEP: 1:1000; anti actin: 1:1000; anti-tetR: 1:1000). The following day, the membrane was washed with 0.2% TBST buffer 3 times for 20 minutes to remove excess antibody. The secondary antibody was diluted and incubated with membrane at room temperature for 1 hour, then washed with 0.2% TBST solution. The membrane was incubated in ECL reagent (PerkinElmer) for 1 minute. The membrane was then exposed to a camera to capture an image (Fluor Chem Q, Alpha Innotech).

2.2.11 Cell purification

Single cell suspensions were prepared from pooled peripheral lymph nodes and spleen for isolation of cell subpopulations. All the isolations were done with Miltenyi cell isolation kits according to the manufacturer's instructions. $CD4^+$ cells were purified using negative selection by removing magnetic bead bound CD8, B cells, DC, Macrophages, NK, NKT cells. CD25 is selectively highly expressed on Treg cells. To isolate Treg ($CD4^+CD25^+$) cells, $CD4^+$ cells were incubated with PE-conjugated anti-CD25 mAb and then anti-PE microbeads. To purify CD4 naïve and effector cells ($CD62L^{hi}$ and $CD62L^{lo}$, respectively), CD4+ cells were incubated with anti-CD62L beads, washed in the magnetic separator. CD4 effectors flowed through, while CD4 naïve T cells are retained in the column. For isolation of B cells, splenocytes were incubated with anti-CD19 or anti-CD43 microbeads by positive and negative isolation, respectively. Peritoneal exudates cells (PEC) were obtained by washing peritoneal cavity with PBS 1% FCS. PEC were incubated with anti-CD11b microbeads to purify PEC macrophages. Splenocytes were incubated with anti-CD11c microbeads to isolate dentritic cells (DC).

2.2.12 Cell differentiation

Depending on reaction conditions, naïve CD4 T cells can differentiate into Th1, Th2, Th17 and Treg cells *in vitro*. In this project, we tested the capacity of naïve T cells to differentiate into Treg cells. 2μg anti-CD3 was coated on a 24-well plate at 37°C for 3-4 hours. Unbound anti-CD3 was washed away with PBS. 0.4-0.5 x 10^6 naïve CD4

T cells were cocultured with 2μg/ml anti-CD28 and 0.5ng/ml TGF-β. 1μg/ml Dox was added when cells were prepared from Dox treated mice. After 3 days incubation, the frequency of $Foxp3^+$ cells was analyzed by intracellular Foxp3 staining.

2.2.13 Proliferation assay

Proliferation assays are determined by [^{3}H]-thymidine incorporation. When cells were prepared from Dox treated mice, 1μg/ml Dox was added to the culture medium. Proliferation of T cell subpopulations and thymocytes was performed by incubation with anti-CD3/CD28 Dynalbeads or PMA and ionomycin in 96-well plates. To test proliferation of Treg cells, Treg cells were cocultured with anti-CD3/28 Dynalbeads, or dendritic cells (along with 1μg/ml anti-CD3) in RMPI medium supplemented with 2000IU IL-2. To check the long-term expansion capacity of Treg cells, purified Treg cells were cocultured with anti-CD3/28 Dynalbeads, DC or PEC macrophages supplemented with IL-2. Every 2-3 days, half of the medium was carefully replaced with fresh medium. Cells were pulsed with 25μl [^{3}H]-thymidine (0.5 μCi/well) 16 hours before harvesting.

2.2.14 Suppression assay

A suppression assay was used to test Treg cell suppressive function *in vitro*. Purified wild type conventional T cells ($CD4^+CD25^-$, 2.5 x 10^4) were cocultured with different numbers of Treg cells along with irradiated (20 Gy) splenocytes (2.5 x 10^5). 1μg/ml anti-CD3 is added into wells to stimulate conventional T cell proliferation for 3 days. Cells are pulsed with 25μl [3H]-thymidine (0.5 μCi/well) 16 hours before harvesting.

2.2.15 B cell activation and proliferation

B cells were purified from splenocytes using anti-CD19 or anti-CD43 microbeads (Miltenyi). 1x10^5 purified B cells were stimulated with LPS, serially diluted anti-IgM F(ab)'2 or anti-CD40. 1 day after stimulation, cells were stained with PE-Cy7 conjugated anti-CD69 and APC conjugated anti-CD25 to measure B cell activation. 2 day after stimulation, cells are pulsed with 25μl [3H]-thymidine (0.5 μCi/well) 16 hours before harvesting to test for proliferative capacity.

2.2.16 PLC-γ2 phosphorylation during B cell activation

Mice were first treated with Dox for 1 month. Wild type and transgenic (GFP^+) B cells were mixed at 1:1 ratio, and then stained with pacific blue conjugated anti-CD19 mAb. Cells were resuspened in RPMI medium at 20 x 10^6/ml. Cells were warmed to 37°C for at least 10min. 25μl (0.5 x 10^6) cells were aliquoted into a 96-well plate, and then activated with 40μg/ml anti-IgM F(ab)'2 for 1, 3, 5, 10 min. Cells were immediately fixed with 150μl FixI (BD) at 37°C for 10min, then washed, and permeabilized with Perm III buffer (BD) on ice for 15min. Cells were washed with PBS 1%FCS, stained with PE-conjugated anti-PLC-γ2 mAb (pY759, 1:200 diluted) at 4°C for 30min. Cells were then washed again and analyzed by flow cytometry.

2.2.17 Flow cytometry

Flow cytometry utilizes fluorophore conjugated mAbs to simultaneously measure multiple protein expression levels within single cells. For cell surface staining, -5x10^5 cells in suspension were first incubated with CD16/32 mAb at 4°C for 10 min to reduce unspecific antibody binding. The mixture of desired antibodies was added to cells at 4°C for 30min. Cells were washed twice with PBS 1%FCS, and then analyzed by flow cytometry.

To detect intracellular protein expression levels, surface staining was first employed to identify extracellular markers. Cells were then fixed and permeabilized to allow antibody to access intracellular tissues. FoxP3 staining was performed using a FoxP3 staining kit (eBioscience) according to manufacturer's instruction.

For FACS analysis of cell apoptosis, cells were stained with 7-AAD and a Annexin V mAb. Annexin V recognize phosphatidylserine (PS) which is predominantly located in the inner leaflet of plasma membrane in live cells. During the early stage of apoptosis, PS moves to the extracellular membrane, which makes it detectable by Annexin V. Cell membrane is still intact to exclude viability dye 7-AAD. In the late stage of apoptosis, integrity of the cell membrane is compromised and unable to exclude 7-AAD. To analyze cell apoptosis, cells were first surface stained, washed and incubated with 50μl (diluted 1:50) 7-AAD at 4°C for 15min. Cells were washed again and analyzed by FACS.

2.2.18 anti-CD3 stimulation *in vivo*

To test T cell activation and proliferation *in vivo*, 10μg anti-CD3 was injected *i.v.* into 10 day Dox-treated wt and transgenic mice. 2 days later, mice were dissected to obtain peripheral lymph nodes and spleen. Lymph node cells and splenocytes were stained with anti-CD4, CD8, TCR, Ki-67, CD62L and CD44 mAbs to analyze the proportion of effector T cells and dividing cells.

2.2.19 Cytokine production by ELISA and CBA kit

Purified naïve and effector T cells were stimulated with anti-CD3/28 dynalbeads (Invitrogen) for 3 days. On day 4, 60μl supernatant was taken out from each well to measure IL-2, IL-17, IL-4, IL-10 and IFN-γ production using CBA kit (BD) and ELISA assay (eBioscience). The assays are carried out according to manufacturer's instructions.

2.2.20 Colitis induction

Mice homozygous for the SCID mutation lacks functional T and B cells. Thus, NOD.*scid* mice provide a lymphopenic environment allowing for expansion of exogenous cell populations. $CD4^+CD45RB^{hi}$ cells are purified and then transferred into NOD.*scid* mice to induce colitis. Briefly, $CD4^+$ T cells were isolated according to manufacturer's manual (Miltenyi). $CD4^+$ cells were incubated with biotinylated anti-CD45RB mAb (1:800) and CD16/32 at 4°C for 5min. Cells were washed twice and then incubated with anti-biotin microbeads. Cells retained in magnetic separator were $CD4^+CD45RB^{hi}$ cells. 0.5-1x10^6 cells are injected *i.v.* into NOD.*scid* mice. After 6-7 weeks, mice were dissected. The colon was cut into five pieces, fixed in 4% PFA at 4°C overnight. The colon tissues were then embedded in paraffin, cut and stained with H&E. The inflammation in colon was scored under microscope by Dr. Alma Zernecke.

2.2.21 Diabetes test

NOD mouse develops diabetes spontaneously. In some cases, diabetes was induced by adoptive transfer or Treg cell depletion. In this project, diabetes incidence was tested by the following three approaches:

Spontaneous diabetes: Nine groups of female NOD mice were used to test

spontaneous diabetes incidence: untreated WT, P2, P4, and WT, P2, P4 treated with Dox from 4 or 10 weeks old. Mice were tested for diabetes once a week using Diastix (Bayer). When mice were tested hyperglycemic in two consecutive tests, they were considered diabetic.

Cyclophosphamide (CY) induced diabetes: Cyclophosphamide can induce diabetes by depleting Treg and B cells. Male mice were treated with Dox for at least 1 month. Cyclophosphamide was prepared at 20 mg/ml in PBS. Mice were first weighed, and injected *i.p.* with 200μg CY/g body weight. Mice were tested for diabetes every 2 days with Diastix (Bayer).

CHAPTER 3

RESULTS

The gene *PTPN22* is widely associated with many human autoimmune diseases, including T1D (Bottini et al., 2004; Smyth et al., 2004; Ladner et al., 2005; Onengut-Gumuscu et al., 2004). The disease susceptibility is conferred by the SNP (C1858T), causing the substitution from arginine to tryptophan (R620W) (Bottini et al., 2004). Further studies have identified R620W in Lyp is a gain-of-function mutation, illustrated by the reduced responsiveness of T and B cells when carrying heterozygous *PTPN22* allele (Vang et al., 2005; Rieck et al., 2007; Aarnisalo et al., 2008;). In B6 mice, the corresponding mutation in Ptpn22 (Pep) is R619W. A recent paper reported the generation of a R619W knockin mouse. This transgenic mouse showed a similar phenotype to the Pep knockout mouse. Further experiments showed that this mutation accelerated Pep degradation, indicating that Pep-619W was a loss-of-function variant (Zhang et al., 2011). The controversial conclusions on the mutation in Lyp/Pep increase the difficulty of understanding the role of Lyp/Pep in autoimmune diseases. The aim of this project was to utilize inducible RNAi to explore the role of Pep in the pathogenesis of autoimmune diseases, especially in type 1 diabetes (T1D) and colitis. The reason for choosing these two autoimmune diseases is that Pep reversely modulates T1D and colitis (Vang et al., 2005; Frank et al., 2011; Rivas et al., 2011; Diaz-Gallo et al., 2011). If Lyp-620W is a gain-of-function variant, *Ptpn22* silencing should prevent or delay diabetes and exacerbate colitis in the inducible knockdown (KD) mice; if the opposite is true, *Ptpn22* silencing should accelerate diabetes and reduce the severity of colitis.

In this project, inducible RNAi is utilized to functionally study of *Ptpn22* in autoimmune diabetes and colitis. Backcrossing knockout B6 mice into the NOD background may introduce B6 genome fragments in addition to the *Ptpn22* KO allele, that can interfere with the interpretation of Pep's function in the NOD mouse. Compared to the KO technique, inducible RNAi has several advantages. Hypomorphic function and reduced expression of proteins are more common *in vivo*. RNAi provides a better mimick of the physiological states than complete loss of protein. Moreover, RNAi is a powerful tool to study the role of specific splice isoform (Gerold et al., 2011; Pecot et al., 2011; Kim et al., 2007). Since Pep is also involved in thymocyte selection and maturation, inducible knockdown, which can silence *Ptpn22* from 5-7 weeks of age when most thymocytes have already matured, can be used to mimick drug treatment in human patients.

Briefly, shRNAs were first designed, screened and cloned into the inducible shRNA expression vector. This vector was packaged into the lentivirus to generate lentiviral transgenic founders. The founders were then mated with WT NOD mice to separate the multiple copies of the integrated lentiviral transgene. To identify artifacts due to off-target effects of RNAi, in this project, two transgenic NOD mouse lines, which carried inducible P2 and P4 shRNA respectively, were generated, established and characterized.

3.1 shRNA design and validation

In this project, inducible RNAi was employed to study the role of Pep in the NOD mouse. In RNAi, there are two types of small RNAs, endogenous micro RNAs (miRNAs) and small interfering RNAs (siRNAs). The primary miRNAs usually come from the processing of long RNA transcripts. The primary miRNAs are cleaved by Drosha to remove the hairpin, followed by Dicer to remove loop and cut the miRNA into a mature miRNA of 21-23 base pairs. In the case of siRNAs, long double strand RNAs are cleaved into 21-23 base pairs by Dicer. The 21-23 base pairs are then unwound and disassociated. The anti-sense strand is loaded into RNA induced silencing complex (RISC). The perfect matching between anti-sense strand and complementary sequences in the target mRNAs results in the target mRNAs degradation. Imperfect matching leads to repression of mRNA translation and subsequent protein reduction.

To efficiently silence *Ptpn22*, 8 different shRNAs were designed by Dr. Stephan Kissler. These shRNA oligos were phosphorylated, annealed and then cloned into the pLB vector, in which shRNA was constitutively expressed from the CMV promoter. The shRNA knockdown efficiencies were tested by luciferase reporter assay.

In the luciferase reporter assay, 293 F cells were co-transfected with pLB and psi-check2 vector. In the psi-check2 vector, firefly luciferase is constitutively expressed and used to normalize results to account for variable transfection efficiency. *Ptpn22* cDNA was inserted behind renilla luciferase mRNA, into the 3' UTR. If shRNA works efficiently, the fusion mRNA will be degraded, resulting in the reduction of

renilla luciferase signal. Thus, the reduction of renilla luciferase should be an indicator of shRNA knockdown efficiency. Our results showed that shRNA P2 and P4 possessed the highest knockdown efficiencies, which were selected and inserted into the inducible shRNA expression vector (Fig 3.1).

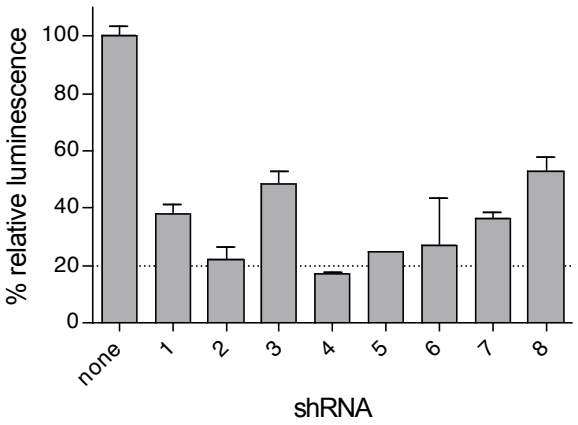

Fig 3.1 Validation of 8 *Ptpn22* shRNA knockdown efficiencies by luciferase reporter assay. Assay was done in duplicates against *Ptpn22* cDNA.

3.2 Generation and validation of inducible shRNA expression vector

The inducible shRNA expression vector FH1t-UTG was kindly provided by Dr. MJ Herold. By using an inducible shRNA expression vector, we can start the gene silencing at any time, just by adding Doxycycline (Dox) into the culture medium or the mouse's drinking water. Moreover, we can study phenotype recovery or duration after removing Dox from drinking water.

The basis for inducible RNAi is a tetracycline operator-repressor controlled promoter driving shRNA expression. In this dual promoter vector, shRNA is transcribed by the polymerase III H1 promoter containing tetracycline operator (TetO), and ubiquitin promoter constitutively expresses tetracycline repressor (TetR) and GFP. TetR blocks shRNA expression by binding to TetO. By adding Dox into mouse drinking water or food, TetR is removed and degraded. Thus, shRNA is allowed to be transcribed and to silence *Ptpn22* (Herold et al., 2008).

Luciferase reporter assays using the pLB backbone demonstrated that shRNAs P2 and P4 displayed the highest knockdown efficiencies. The next step was to clone these two shRNA sequences into the FH1t-UTG vector. shRNAs were synthesized,

annealed and first cloned into the pH1tet-flex vector. The fragment containing the H1 promoter and TetO was cleaved and inserted into the final vector, FH1t-UTG. The vectors were sequenced using the FUW1 primer to make sure the shRNA sequences were correct.

We again used a luciferase reporter assay to validate the inducible shRNA expression constructs. 293F cells were co-transfected with psi-check 2 and inducible shRNA vectors. 3μg/ml Dox was added to induce shRNA expression. However, in the absence of Dox, P2 and P4 shRNA still induced reporter knockdown. We reasoned it could be that shRNA had time to accumulate prior to expression of the TetR which subsequently represses shRNA transcription in the absence of Dox. To overcome this challenge, we first used the inducible shRNA expression vectors to generate a small amount of lentivirus, which we then used to infect 293 F cells in 6-well plates. The transduced cells were transfected with psi-check 2 vector with or without Dox. The renilla signal in no Dox cells was set to 100%. In the presence of Dox, P2 and P4 shRNAs showed high knockdown efficiencies similar to results obtained with the pLB vectors (Fig 3.2).

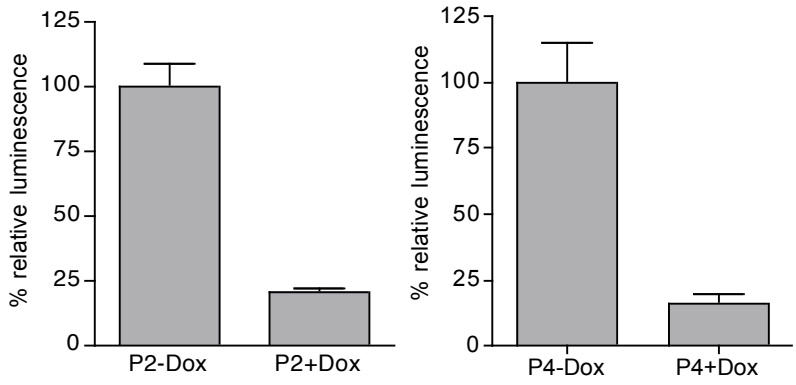

Fig 3.2 Validation of inducible P2 and P4 shRNA expression vectors by luciferase reporter assay. 293 F cells were first infected with lentivirus, and then transfected with psi-check 2 vector with or without Dox. Assay was done in duplicates.

3.3 Lentivirus generation and titration

Lentivirus, which is derived from HIV-1immunodeficiency virus, can efficiently incorporate its genetic material into genomic DNA in both dividing and non-dividing cells. Lentivirus provides a valuable research tool for studying gene function *in vivo*.

To generate lentivirus, 8-9 x 10^6 293 F cells were co-transfected with 3µg pCMV-VSVg, 3µg RSV-rev, 4µg pMDL-gag/pol, 5µg pAdvantage, 20µg inducible shRNA construct along with 70µl Fugene HD. 48 hours later, supernatant was collected, spun down and filtered. Lentivirus was then ultracentrifuged at 25000rpm for 90min. The Lentivirus was recovered in PBS at 4°C overnight. The next day virus was carefully aliquoted, flash-frozen in liquid nitrogen and stored at -80°C.

To titrate lentivirus, 0.01, 0.1, and 1µl lentivirus were used to infect 293 F cells. 24 hours later, cells were washed and run through flow cytometry to measure the percentage of GFP^+ cells. To calculate virus titer, we assumed that after 24h growth, 293 F cells had doubled in numbers to around 8 x10^5. The lentivirus titer was estimated as cell number x frequency of GFP^+ x 1000/ml. Hence, the titers of P2 and P4 lentiviruses were calculated as 3x 10^8 and 4x 10^8, respectively, which could be used to generate inducible transgenic NOD mice (Fig 3.3).

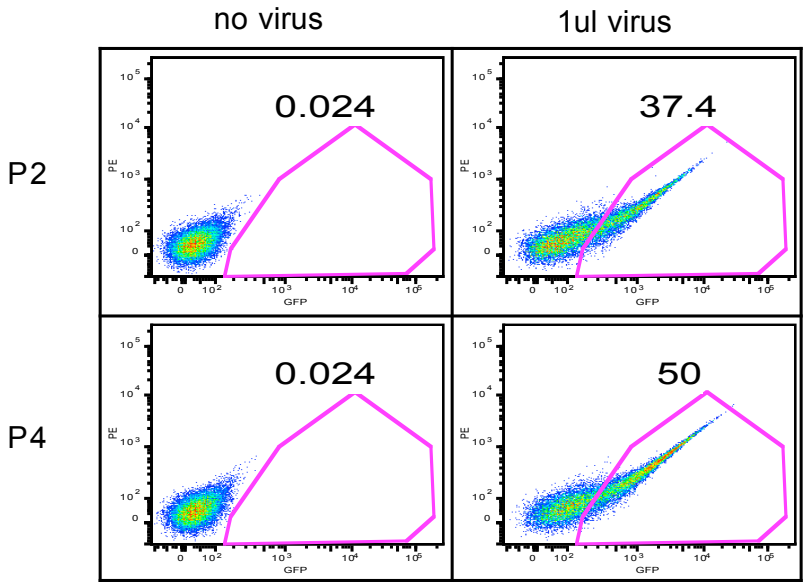

Fig 3.3 Lentivirus titration. 293 F cells were infected with 0.01, 0.1, and 1µl lentivirus to determine the virus titration. The frequencies of GFP^+ in cells with no virus and 1µl virus were shown. GFP+ frequencies in cells with 0.01 and 0.1µl viruses were in accordance with virus dilution.

3.4 Generation of transgenic P2 and P4 mouse lines

To generate lentiviral transgenic mice, single cell NOD embryos were microinjected with lentivirus. Female mice were injected with PMS, followed with hCG to induce ovum. After an overnight mating with males, females were euthanised and oviducts were dissected to collect single cell embryos. Lentivirus was injected into the

perivitelline space of embryos. Infected embryos were implanted into the uterus of pseudopregnant females to deliver transgenic pups. To control for possible off-target effects of RNAi, two transgenic mouse lines (P2 and P4), which carried P2 and P4 shRNAs respectively, were generated. The assumption was if similar phenotypes could be found in both P2 and P4 knockdown mice, our conclusion would be more convincing.

In the shRNA expression cassette, GFP was constitutively expressed by the ubiquitin promoter. Thus, GFP was a reliable marker for transgenic mice. Blood samples were collected to measure GFP expression. GFP positive founders were mated with WT NOD mice to segregate the multiple copies of the integrated lentiviral transgene. The number of functional transgene copies was determined by GFP^+ proportion in the offspring as well as peak numbers in GFP histogram. After breeding transgenic lines for 4 generations, the frequency of GFP^+ pups went down to ~50%, and single peak of GFP histogram could be observed in blood lymphocytes. All these data demonstrated that only one functional copy of the transgene was present in the P2 and P4 mouse lines. The lines were then expanded for inducible knockdown validation, diabetes test and functional studies.

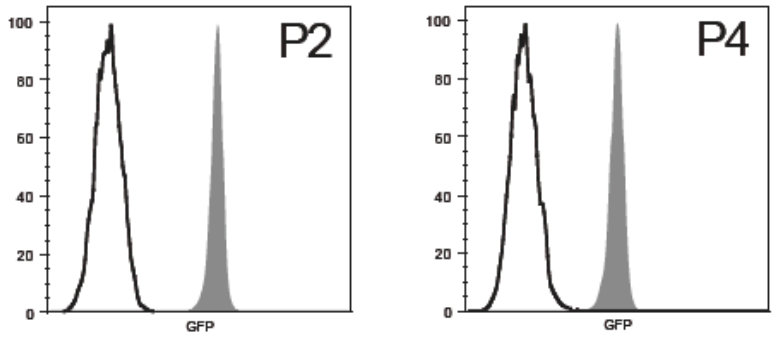

Fig 3.4 GFP expression in the blood lymph cells of established P2 and P4 mouse lines. Blood cells were treated with ACK buffer, washed and analyzed by flow cytometry. WT (open histogram) showed an negative control for GFP. P2 and P4 were showed in grey histogram.

3.5 Inducible knockdown validation

Next we validated that P2 and P4 shRNAs could silence *Ptpn22 in vivo*. To confirm that knockdown could be modulated in an inducible manner, six groups of mice were used: WT, P2, and P4 mice either treated with 200 μg/ml Dox for 7-10 days or left untreated. Untreated P2 and P4 mice were used to examine if shRNA expression was

leaky in the absence of Dox. Some WT mice were also treated with Dox to examine the effect of Dox in non-transgenic mice. 7-10 days later, mice were dissected to obtain lymph nodes. Lymph nodes were disaggregated and prepared for qRT-PCR and western blot.

qRT-PCR was carried out with Taqman probe and universal probe master mix (ROX). ROX, a passive reference dye, can compensate variations between wells to improve the precision of the results. Taqman probe consists of a quencher dye at the 3' end and a reporter dye at the 5' end that was quenched before PCR reaction. During the PCR reaction, the Taqman probe is cleaved by DNA polymerase, resulting in a corresponding increase of reporter dye intensity. The housekeeping gene *GAPDH* was used to normalize samples to amplification efficiency. The cycle threshold (Ct) values of *GAPDH* and *Ptpn22* were determined by the PCR program automatically. The abundance of *Ptpn22* in each group was calculated by Δ CT value (*Ptpn22* Ct value – *GAPDH* Ct value). To compare *Ptpn22* abundance in control mice (untreated WT, P2, P4 and Dox-treated WT) and Dox-treated P2, P4 mice, we calculated ΔΔCT value (Δ Ct value – WT Δ Ct value). The result showed that ΔΔCT values were comparable in untreated WT, P2, P4 and Dox-treated WT cells. The ΔΔCT values were increased by 1-2 cycles, indicating a 50-75% reduction of *Ptpn22* mRNA in Dox-treated P2 and P4 cells (Fig 3.5). These results confirmed that in the P2 and P4 mice, RNAi could be achieved on the mRNA level in an inducible manner. Moreover, Dox did not influence Ptpn22 mRNA transcription and stability.

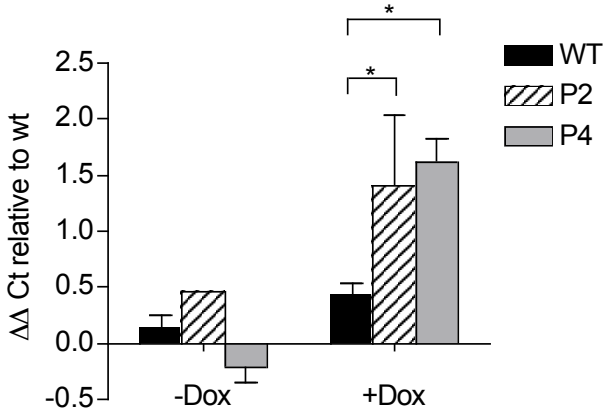

Fig 3.5 Validation of inducible RNAi by qRT-PCR. The abundance of *Ptpn22* in each group was calculated by ΔCT value (*Ptpn22* Ct value – *GAPDH* Ct value). ΔΔCT values (ΔCt value – WT ΔCt value) were used to compare *Ptpn22* abundance in control mice (untreated WT, P2, P4 and Dox-treated WT) and Dox-treated P2 and P4 mice.

We also validated inducible Pep knockdown by western blot. Lymph node cells were lysed in RIPA buffer (containing proteinease inhibitor cocktail) in ice for 30min. The lysates were spun down, and then incubated with BCA solution (Novagen) to measure protein concentrations. Proteins were separated and blotted with antibodies to detect actin, Pep and TetR. Similar to the the result in qRT-PCR, Pep levels were comparable in untreated WT and P2 mice, as well as in Dox treated WT mice. The reduction of Pep was only observed in the Dox-treated P2 mice. The strong bands of TetR confirmed P2 were lentiviral transgenic mice (Fig 3.6A). Along with qRT-PCR data, we confirm in our KD mice, *Ptpn22* can be inducibly silenced. Next P2 and P4 mice were treated with a serial concentration of Dox to compare knockdown efficiencies in P2 and P4 mice. With the increase of Dox in the drinking water, loss of Pep reached to ~80% of loss with 2 μg/ml Dox in P2 mice. A less knockdown efficiency in P4 mice could be observed (~60% of loss). The increase of Dox (from 2 μg/ml for P2, and from 20 μg/ml for P4) did not improve knockdown efficacy any more (Fig 3.6B). Dox will gradually degrade in the water. Unlike changing drinking water 3 times a week as Herold and colleagues did, in this project Dox is regularly added into mouse drinking water on every Monday without change. To maintain the maximal knockdown efficiency during the whole week, 200 μg/ml Dox is used in the treatment of mice in the subsequent experiments. The following studies showed that there are no differences between untreated WT and Dox-treated WT mice, indicating 200 μg/ml Dox does not exert any side effect on the NOD mouse.

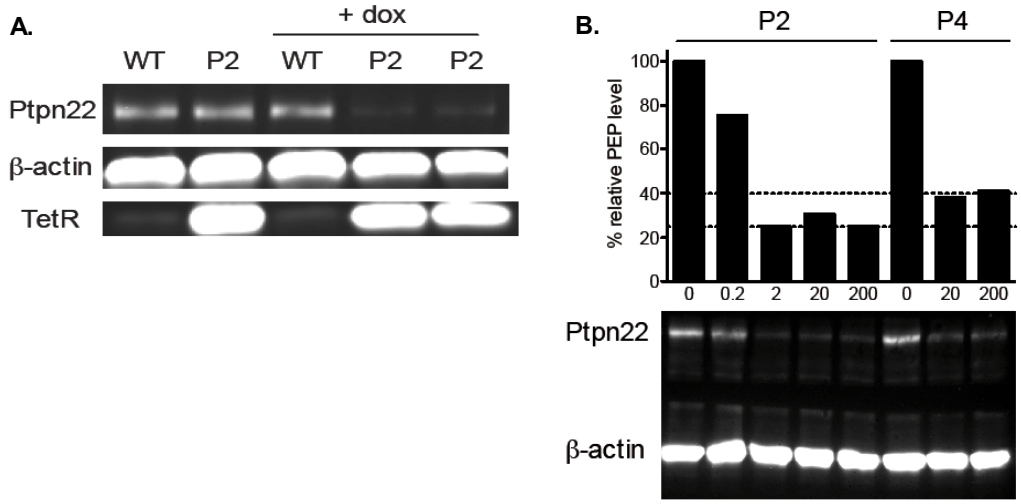

Fig 3.6 Validation of inducible RNAi by western blot. A. Western blot figure. Proteins were blotted with anti-actin, Pep and TetR antibodies to detect protein expression levels. B. Pep protein levels from KD mice treated with a serial concentration of Dox were quantified with Image J.

3.6 Prolonged Pep knockdown increases spleen cellularity

In the mouse**,** *Ptpn22* encodes a tyrosine phosphatase, Pep. The substrates of Pep have been identified, including Lck, Fyn and ZAP-70. Pep can attenuate TCR/BCR signaling by dephosphorylating the positive regulatory tyrosine phosphorylation in Lck, Fyn and ZAP-70. Thus, Pep is a negative regulator in T/B cell activation. Correspondingly, splenomegaly and lymphadenopathy occured in old, but not young Pep knockout and knockin B6 mice. Since *Ptpn22* silencing is detectable after 7-10 day Dox treatment, an interesting question was if we could see similar phenotype in our inducible knockdown mice.

To make sure the phenotype was due to the inducible knockdown, we usually utilized six groups of mice: untreated and 200μg/ml Dox treated WT, P2 and P4 mice. The mice were treated with Dox from 5-7 weeks of age for a duration of 4-5 months. The lymph nodes and spleen were then dissected to count cell numbers. The results showed that cell numbers in the lymph nodes were quite similar (data not shown). Similar to the *Ptpn22* KO and knockin mice, cellularities were significantly increased in the spleen of Dox-treated P2 and P4 mice. Moreover, in agreement with the higher KD efficiency in the Dox-treated P2 mice, more splenocytes could be found in the P2 KD than P4 KD mice (Fig 3.7). The similarities of increased spleen cellularity in KO, knockin and inducible KD mice strongly suggested that P2 and P4 mice were reliable models to explore the function of Pep in the NOD mouse.

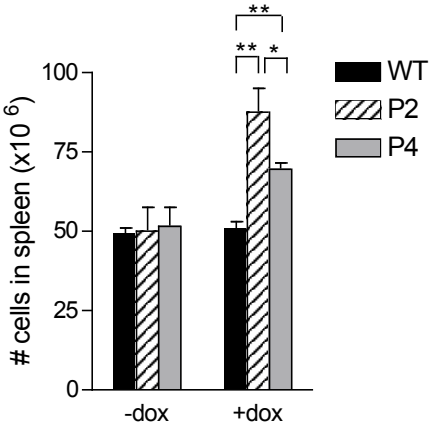

Fig 3.7 Prolonged *Ptpn22* silencing increased spleen cellularity. Mice were treated with Dox for 4-5 months, and then dissected to count cell numbers (*: P<0.05; **: P<0.01)

3.7 The effect of inducible *Ptpn22* silencing on T cell subsets

Since we saw that long-term *Ptpn22* silencing boosted the number of splenocytes, we next analyzed which cell populations were influenced. Considering *Ptpn22* was predominantly expressed in T and B cells, we first examined the role of *Ptpn22* silencing on T cell subsets.

T cells are matured in the thymus. During T cell development, positive selection and negative selections occur to protect the body from infection as well as to avoid self-tissue destruction. Double-positive immature thymocytes obtain the survival signal when reacting to self-antigen presented on thymic stromal cells. Surviving thymocytes undergo negative selection to deplete autoreactive T cells with high affinity to self-antigen. Mature T cells then upregulate CD62L and CCR7 to facilitate migration into secondary lymphoid organs. Once these T cells encounter antigen in the periphery, CD62L is down-regulated to slow down migration. T cells are then activated, converted into effector/memory T cells, followed with proliferation and secretion of cytokines. Another T cell subpopulation, regulatory T cell (Treg) cells, plays a vital role in the self-tolerance. In this project, we systematically examined the effect of inducible *Ptpn22* silencing on T cell development and on the function of T cell subsets.

3.7.1 Inducible *Ptpn22* silencing does not influence thymocyte development

Several papers reported that Lyp/Pep participates in T cell development. Hasegawa et al demonstrated that in the absence of Pep, positive selection in thymus was enhanced in the context of TCR transgene while negative selection was not affected (Hasegawa et al., 2004). CD5 expression was enhanced in the double positive (DP) thymocytes, indicating elevated TCR signaling in DP thymocytes (Hasegawa et al., 2004; Azzam et al., 1998). Thymocytes from *Ptpn22* knockin mice were hyperproliferative in response to anti-CD3/CD28 stimulation (Zhang et al., 2011). In this project, *Ptpn22* was silenced from 5-7 weeks of age, when most thymocytes have already matured (Scollay et al., 1980). In this scenario, thymocyte development should not be altered in our inducible P2 and P4 KD mice.

To test this hypothesis, WT, P2 and P4 mice were treated with Dox from 5-7 weeks of age for 1 month. Some mice were left untreated as a control. Thymocytes were then

obtained and stained with fluorophore-conjugated anti-CD4, CD8 and CD5 mAbs. The results showed that the frequencies of CD4 single positive, CD8 single positive and DP cells were similar in control (WT, P2, P4, and Dox-treated WT) and P2, P4 inducible KD mice. Furthermore, CD5 expression in DP thymocytes was not altered, indicating that TCR signaling was not affected in DP thymocytes (Fig 3.8).

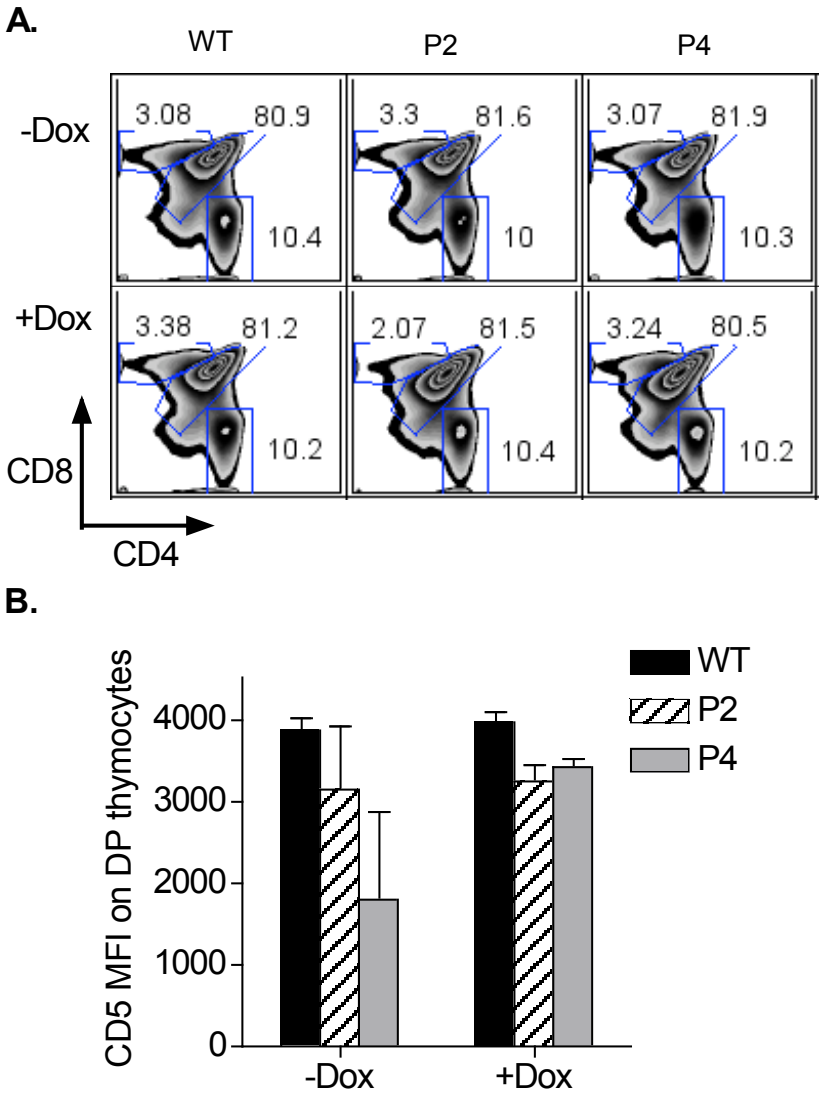

Fig 3.8 Inducible *Ptpn22* silencing didn't alter T cell development. A. The distribution of single CD4, CD8 and DP thymocytes. B. CD5 expression in DP cells.

In *Ptpn22* knockin mice, thymocytes were hyperresponsive to anti-CD3/CD28 stimulation (Zhang et al., 2011). Although cell staining in thymocytes did not show any discrepancies, we also tested the proliferative capacity of thymocytes after 1 month of Pep silencing. Thymocytes were stimulated with anti-CD3/CD28 dynabeads

(Invitrogen) at different bead:cell ratios. Cell proliferation was measured by the uptake of [^{3}H]-thymidine. We found comparable cell proliferation in control and Pep KD thymocytes (Fig 3.9). The unaltered cell distribution and CD5 expression in DP thymocytes suggests that inducible *Ptpn22* silencing from 5-7 weeks of age does not alter thymocytes development and proliferation.

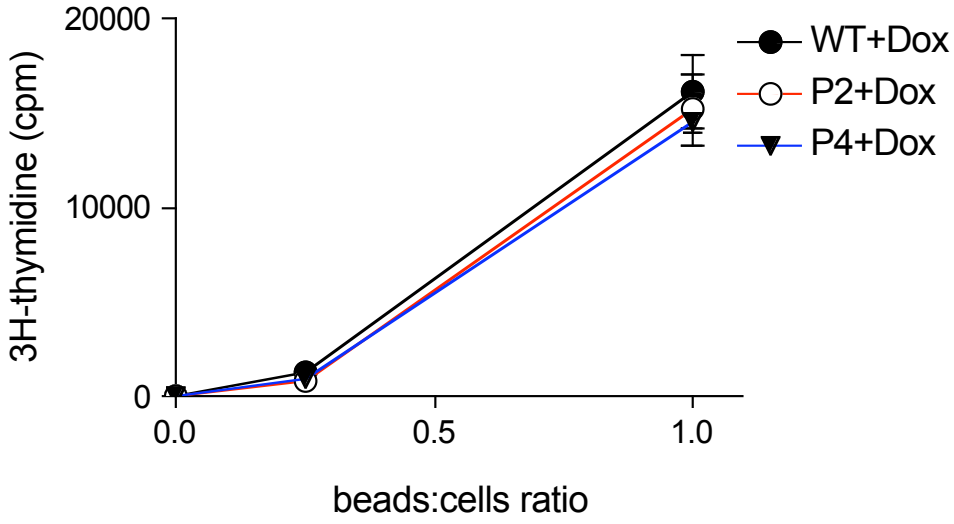

Fig 3.9 Proliferation of thymocytes were comparable. Thymocytes from control and inducible KD mice were stimulated with different numbers of anti-CD3/CD28 dynalbeads for 3 days. Proliferation was measured by the incorporation of [^{3}H]-thymidine.

3.7.2 The effect of inducible *Ptpn22* silencing on non-Treg T cells

3.7.2.1 *Ptpn22* silencing in adult mice does not boost effector T cells

When thymocytes mature, CD62L expression is upregulated to faciliate naïve T cells migrating into peripheral lymphoid organs. When naïve T cells encounter antigen and differentiate into effector/memory T cells in the periphery, CD62L is downregulated and CD44 expression is enhanced. Thus, effector/memory T cells are determined as CD44^{hi}CD62L^{lo}. Correspondingly, naïve T cells are marked as CD44^{lo}CD62L^{hi}.

Lyp/Pep negatively modulates T cell activation and the generation of effector/memory T cells. *In vitro*, *PTPN22* knockdown increased antigen-receptor signaling in Jurkat T-cell line, while overexpression suppressed T cell activation (Begovich et al., 2004; Cloutier et al., 1999). In the *Ptpn22* knockout and knockin mouse, effector/memory T cell pool was expanded, especially in the older mice (Hasegawa et al., 2004; Zhang et al., 2011).

To examine the role of *Ptpn22* silencing on effector/memory pool in our inducible knockdown mice, mice were treated from 5-7 weeks of age for 1month. Lymph nodes and spleen were obtained and prepared for FACS staining. To determine naïve, effector/memory and Treg cells in a single panel, cells were stained with fluorophore-conjugated anti-CD4, CD8, CD25, TCR, CD62L, CD44 and subsequently permeabilized and stained with anti-Foxp3 mAb. Cells were first gated with $CD4^+TCR^+$ to identify $CD4^+$ T cells. In $CD4^+$ T cells, Treg cell were gated as $Foxp3^+$, effector/memory T cells were determined as $CD62L^{lo}Foxp3^-$, and naïve T cells were identified as $CD62L^{hi}Foxp3^-$. We found proportions of effector/memory T cells were similar in each group, indicating that 1 month of Pep KD does not expand the effector/memory T cell pool (Fig 3.10A). We hypothesized that this could be due to the short duration of gene silencing, as the accumulation of effector/memory T cells was only observed in older KO mice. We therefore explored if effector/memory T cells would accumulate after a longer period of gene silencing. P2 and P4 mice were treated with Dox for 8 months. Similar to the results in 1-month treated mice, the effector/memory T cell pool was not affected in the lymph node compartment, and slightly increased in the splenic $CD4^+$ T cell compartment of P2 inducible KD mice (Fig 3.10B). Our data showed that if mice were treated with Dox from 5-7 weeks of age, *Ptpn22* silencing did not significantly boost the effector/memory T cell pool in either P2 or P4 inducible KD mice, which was distinct to *Ptpn22* KO and knockin mice.

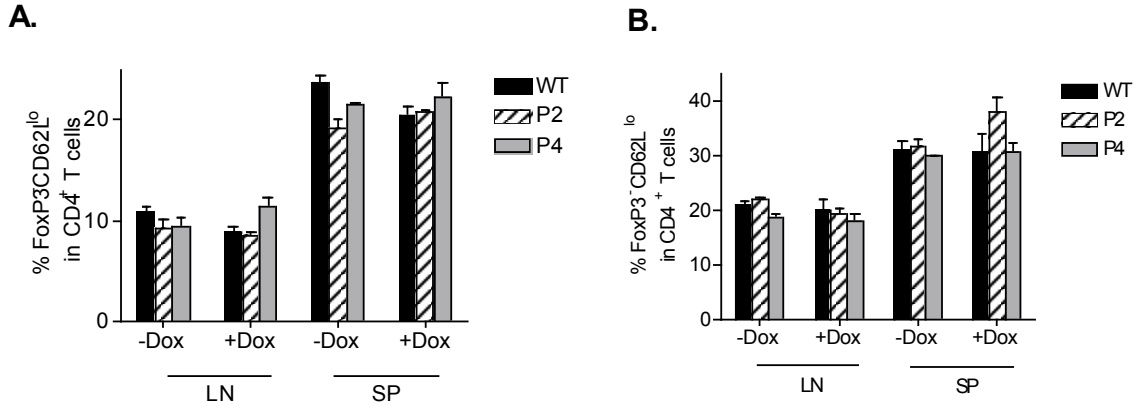

Fig 3.10 Retained effector/memory T cell pool in adult KD NOD mice. A. Mice were treated with Dox from 5-7 weeks old for 1month. B. Mice were treated with Dox for 8months. The proportion of effector/memory $CD4^+$ T cells in the LN and SP were shown. No significant differences could be observed.

3.7.2.2 *Ptpn22* silencing facilitates Teff T cell generation

We have shown that under homeostatic condition, *Ptpn22* silencing could not boost effector/memory pool, even in long-term treated mice. But we had not investigated the effect of *Ptpn22* silencing during T cell priming conditions. For this purpose, we decided to stimulate T cells *in vivo*. We used anti-CD3, a potent stimulator for all the T cells. 10μg anti-CD3 or PBS alone was injected *i.v.* into 10-day Dox treated WT and P4 mice. Two days later, mice were dissected to obtain lymph nodes and spleen. Cells were surface stained to check the effector/memory T cell pool in T cells, and then pemeabilized, stained with anti Ki-67 mAb to identify dividing cells. We found *Ptpn22* silencing facilitated effector/memory T cell generation under anti-CD3 priming (Fig 3.11). It seemed that under homeostatic condition, *Ptpn22* silencing may enhance TCR signaling, but not sufficiently to generate more effector/memory T cells. When *Ptpn22* KD T cells encountered antigen, they were converted into effector/memory T cells more efficiently.

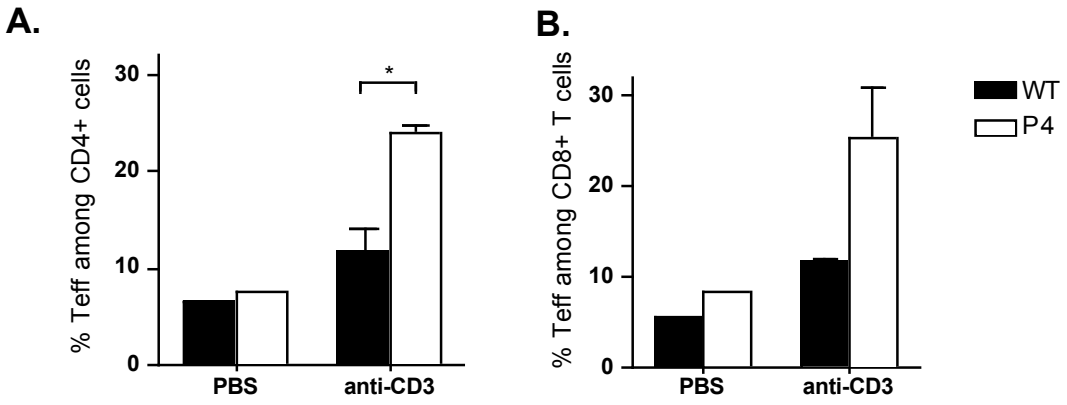

Fig 3.11 Inducible *Ptpn22* silencing facilitated effector/memory T cell generation under the priming condition. Mice were treated with Dox for 10 days to knockdown Pep, and then injected with anti-CD3 or PBS. The frequencies of effector/memory T cells in CD4 (A) and CD8 (B) T cells were shown.

3.7.2.3 *Ptpn22* silencing from birth boosts effector/memory T cell pool

In most experiments, *Ptpn22* silencing started from 5-7 weeks of age when most thymocytes have been matured (Scollay et al., 1980). In the KO and knockin mice, Pep has been confirmed to be involved in thymocyte education (Hasegawa et al., 2004; Zhang et al., 2011). We then asked if the expanded effector/memory T cells were related to the role of Pep in the thymic education. To test this hypothesis, WT, P2 and P4 mice were treated with Dox from birth for 2month. Surprisingly, similar to

Ptpn22 KO and knockin mice, effector/memory T cells were significantly increased in the spleen and to a lesser extent in the P2 inducible KD lymph nodes, indicating Pep may determine peripheral effector/memory T cell pool through thymocyte education (Fig 3.12).

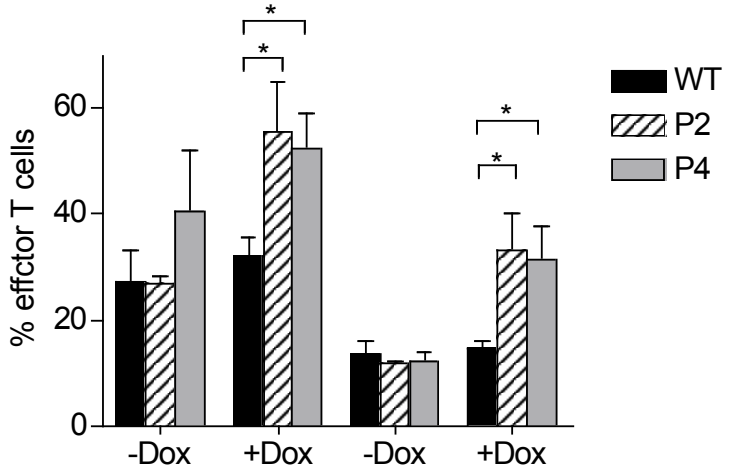

Fig 3.12 The expanded splenic effector/memory T cell pool when P2 and P4 mice were treated with Dox from birth for 2 months. (*: P<0.05)

3.7.2.4 *Ptpn22* silencing does not alter T cell proliferation

Lyp/Pep acts as an important negative regulator in TCR signaling. Hasegawa and collegues assayed the proliferation of naïve and effector/memory T cells from *Ptpn22* deficient mice. They found that loss of Pep only enhanced effector/memory T cell proliferation, but not that of naïve T cells (Hasegawa et al., 2004). In this project, we examined the proliferation of naïve and effector/memory T cells by different approaches.

In vitro, we assayed the proliferation of *Ptpn22* KD T cells in response to TCR stimulation. Effector and naïve $CD4^+$ T cells were isolated from 1 month Dox-treated mice using magnetic microbeads (Miltenyi) according to manufacturer's instructions. Naïve or effector $CD4^+$ T cells were stimulated by different numbers of anti-CD3/CD28 dynabeads (invitrogen). To continuously silence Pep, 1μg/ml Dox was added when cells were purified from Dox-treated mice. Cell proliferation was assayed by the uptake of [^{3}H]-thymidine. We found compared to control (WT, P2, P4 and Dox-treated WT) cells, KD naïve and effector T cells showed similar proliferation capacities, indicating *Ptpn22* silencing after thymocytes education didn't alter T cell

proliferation (Fig 3.14).

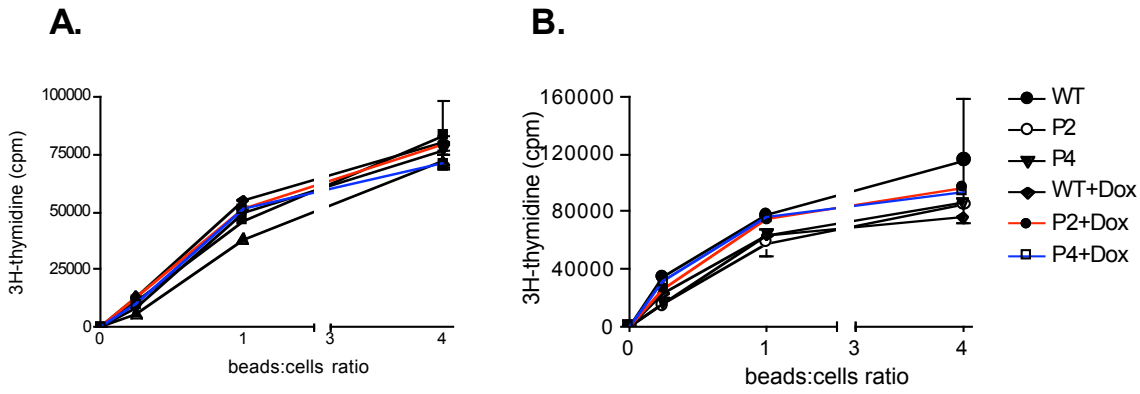

Fig 3.14 Naïve and effector/memory $CD4^+$ T cell proliferation. Mice were treated with Dox for 1 month. naïve (A) and effector/memory (B) T cells were isolated and stimulated with anti-CD3/CD28 dyanlbeads for 3 days. During the last 16h, 0.5 μCi [^{3}H]-thymidine was added.

Next we tested T cell proliferation *in vivo* using Ki-67 protein. Ki-67 is a nuclear protein associated with cell proliferation. Thus, Ki-67 is a cellular marker for proliferation. Mice were left untreated or treated with Dox from 5-7 weeks of age for 8 months, and then dissected to examine the frequency of dividing cells ($Ki\text{-}67^+$) in the naïve and effector $CD4^+$ T compartments. The results showed similar $Ki\text{-}67^+$ frequencies in naïve and effector $CD4^+$ T cells, suggesting that *Ptpn22* silencing didn't accelerate T cell proliferations under homeostatic condition (Fig 3.15).

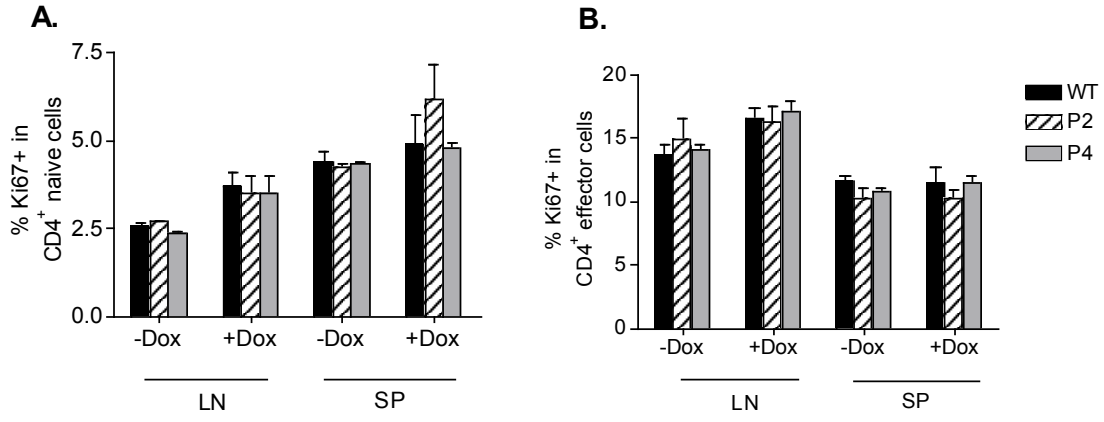

Fig 3.15 $Ki\text{-}67^+$ cells in naïve and effector/memory T cells. Mice were treated with Dox from 5-7 weeks for 8 months. Lymph node cells and splenocytes were stained with anti-Ki-67 mAb to determine the dividing cells in CD4 naïve (A) and effector (B) T cells.

Finally, we tested effector/memory T cell expansion potential *in vivo* by cell transfer into NOD.*scid* mice. Mice homozygous for the SCID mutation lack functional T and B cells. Thus, NOD.*scid* mice provide a lymphopenic environment allowing for expansion of exogenous cell populations. Lymph node cells were obtained from 1 month Dox-treated WT, P2 and P4 mice. Before the transfer, the proportions of effector/memory T cells were determined by CD4/CD44/CD62L staining.

To minimize environmental variations, WT cell were mixed with P2 or P4 cells at the ratio 1:1 and transferred into Dox-treated NOD.*scid*s. The recipients were dissected after 1 month cell transfer to obtain lymph nodes and spleens to measure effector/memory T cell pool. We found before and after cell transfer, effector/memory T cell pools were similar in WT and P2, P4 KD $CD4^+$ T cells, indicating *Ptpn22* silencing didn't enhance effector/memory T cell generation and expansion *in vivo* (Fig 3.16).

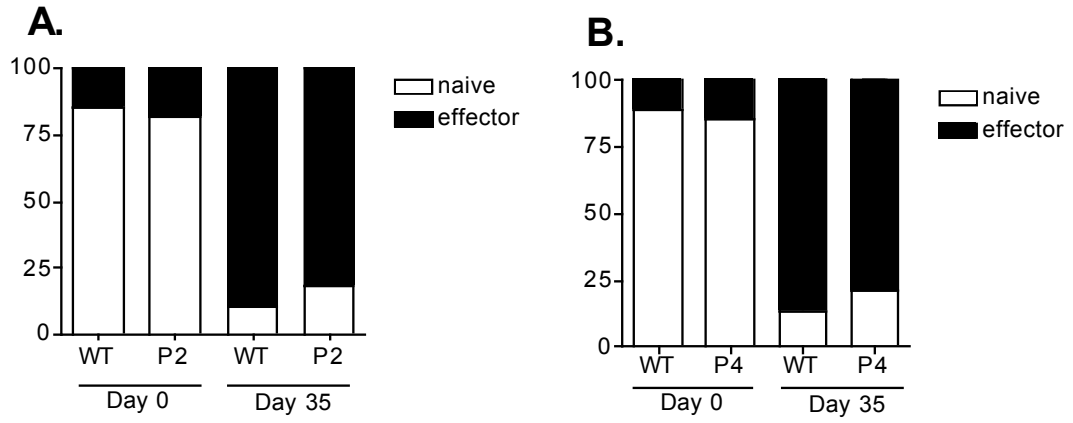

Fig 3.16 Effector T cell expansion in the NOD.*scid* mice. Dox-treated WT lymph cells were mixed with P2, or P4 cells, and then transferred into NOD-SCIDs. The effector/memory pool in $CD4^+$ T cells was measured before and after cell transfer.

3.7.2.5 *Ptpn22* silencing does not affect cytokine production

In addition to hyper-proliferation of effector/memory T cells, Pep deficiency also increased IL-2, IL-4 and IFN-γ production in the effector T cells (Hasegawa et al., 2004). To analyze the effect of *Ptpn22* silencing on the cytokines production of T cells, naïve and effector $CD4^+$ T cells were isolated from untreated or 1 month Dox-treated mice, and then stimulated by anti-CD3/CD28 dynabeads for 3 days. 60μl supernatant was taken out to measure cytokines using cytometric bead array (CBA)

kits. Supernatant was incubated with capture beads for IFN-γ, IL-2, IL-17A, IL-10 and IL-4, the representative cytokines of Th1, Th2, Th17 and Treg cells. Capture beads were then incubated with PE-detector beads. The capture beads were identified by the distinct combinations of APC and APC-Cy7 intensities. The standard curve could not be calculated due to problems during acquisition of standard samples. To overcome this challenge, cytokine concentrations were indicated by the geometric mean florescence intensity (MFI) of PE. We found *Ptpn22* silencing did not alter the production of IL-2, IFN-γ, IL-17A, IL-10 and IL-4 in naïve T cells. In the case of effector T cells, no big change in IFN-γ, IL-17A, IL-10 and IL-4 production could be observed, but IL-2 secretion was elevated in KD effector T cells (Fig 3.17).

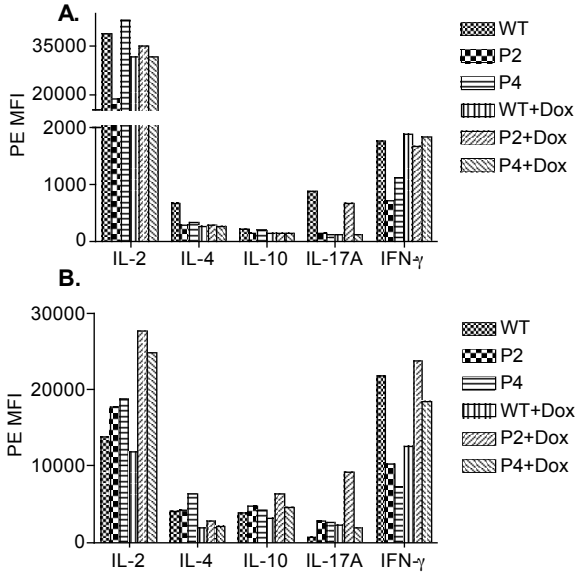

Fig 3.17 Cytokine measurement by CBA kit. Supernatant from stimulated naïve (A) and effector (B) CD4+ T cells were incubated with beads (CBA) to measure IL-2, IL-4, IL-10, IFN-γ and IL-17A. The concentration of cytokines were presented by the geometric mean florescence intensity of PE.

To further verify if *Ptpn22* silencing enhanced IL-2 production by effector T cells, we employed ELISA assay to detect IL-2 secretion. Capture antibody, which was precoated on the wells, could specifically bind to IL-2 in the supernatant. Wells were extensively washed, and then incubated with detection antibody. We found that, compared to effector T cells from untreated mice, IL-2 production was slightly increased in P2, but not P4 KD effector T cells (Fig 3.18). Similar to the CBA data, *Ptpn22* silencing did not alter cytokine production in naïve $CD4^+$ T cells. *Ptpn22* silencing may facilitate IL-2 production by effector $CD4^+$ T cells, but it did not affect

IL-4, IL-10, IL-17A and IFN-γ production.

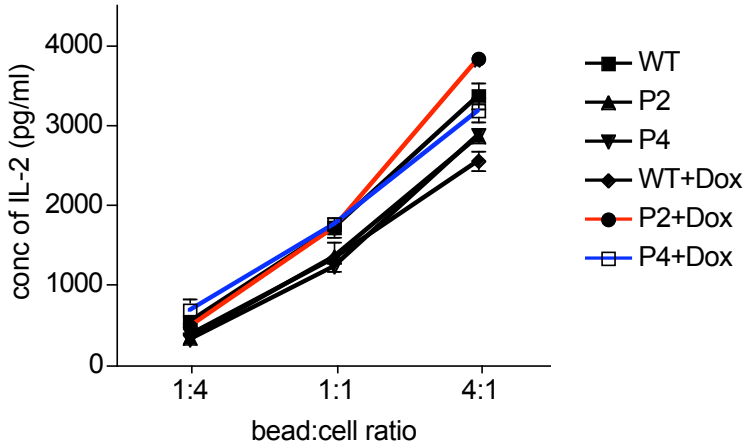

Fig 3.18 ELISA assay to detect IL-2 production of effector T cells. Effector T cells were stimulated with anti-CD3/CD28 dynalbeads at bead: cell ratio 1:4, 1:1 and 4:1. The supernatant was used in the ELISA assay to detect IL-2 concentration.

3.7.3 The effect of inducible *Ptpn22* silencing on Treg T cells

We have shown that *Ptpn22* silencing expanded effector/memory T cell pool only under priming but not under homeostatic conditions. Moreover, Pep deficient and knockin mice were reported to remain healthy without the development of autoimmune disease. These data suggested that *Ptpn22* silencing may also affect suppressive cell populations so that effector/memory T cell generation was under control. Treg cells, which are pivotal in maintaining peripheral tolerance, are the major cell type in suppressive cell populations. Furthermore, Treg cells are indispensable to control diabetes in the NOD mouse. Loss of Treg cells accelerates or exacerbates T1D (Salomon et al., 2000; Mellanby et al., 2007). On the contrary, increase of Treg cells by IL-2 treatment or by genetic approaches protects and even reverses T1D (Peng et al., 2004; Grinberg-Bleyer et al., 2010). Given the great importance of Treg cells in self-tolerance, we focused on the effect of *Ptpn22* silencing on Treg cells.

3.7.3.1 Long-term *Ptpn22* silencing increases Treg cells

Treg cells can be specifically identified by their unique transcription factor, FoxP3. To investigate the effect of *Ptpn22* silencing on Treg cells, WT, P2 and P4 mice were left untreated or treated with Dox from 5-7 weeks old for 1 month. We first examined the proportion of Treg cells in $CD4^+$ T cells. Lymph node cells and splenocytes were

first stained with cell surface markers, and then permeabilized, stained with anti-Foxp3 mAb, allowing Treg cells to be determined as $CD4^+TCR^+Foxp3^+$. Surprisingly, the frequencies of Treg cells in $CD4^+$ T cells were significantly increased in lymph node cells and splenocytes, which may explain why the effector/memory T cell pool was not increased when *Ptpn22* was silenced. Moreover, compared to the P4 KD mice, Treg cell expansion was increased in P2 KD mice (Fig 3.19). Our results were consistent with a very recent paper, reporting an increase of Treg cells in Pep KO B6 mice (Maine et al., 2012).

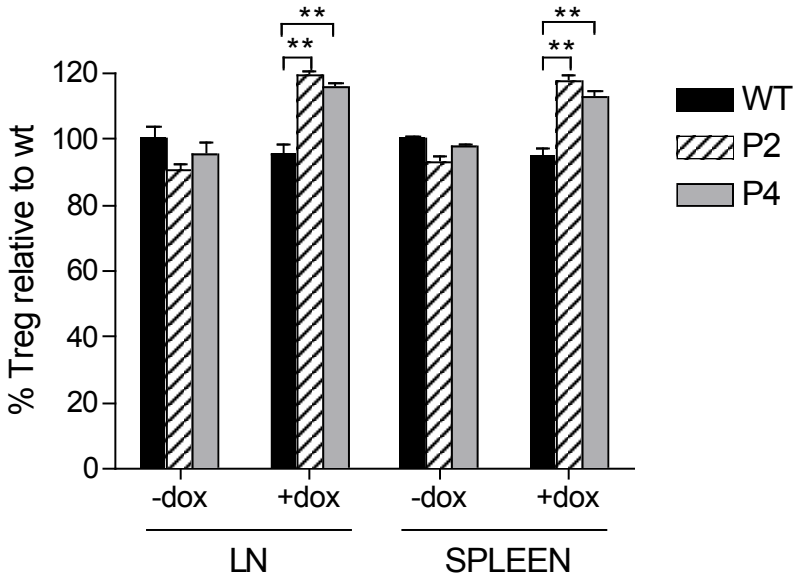

Fig 3.19 An increase of Treg cells in the lymph nodes and spleens of KD mice. Mice were left untreated, or treated with Dox from 5-7 weeks old for 1 month. Treg cells were identified as $CD4^+TCR^+Foxp3^+$ (**: $P<0.01$)

3.7.3.2 *Ptpn22* silencing enhances GITR expression on Treg cells

We have shown that *Ptpn22* silencing increased Treg cell numbers. We then characterized the phenotype of the expanded Treg cell compartment. Treg cells are characterized by the unique transcription factor FoxP3, as well as by high expression of several cell surface markers, including CD25, CTLA-4 and GITR. We measured the expression levels of these Treg cell markers by flow cytometry. We found that the expression levels of FoxP3, CD25 and CTLA-4 were comparable to WT. However, GITR expression was elevated in the P2 and P4 KD Treg cells (Fig 3.20).

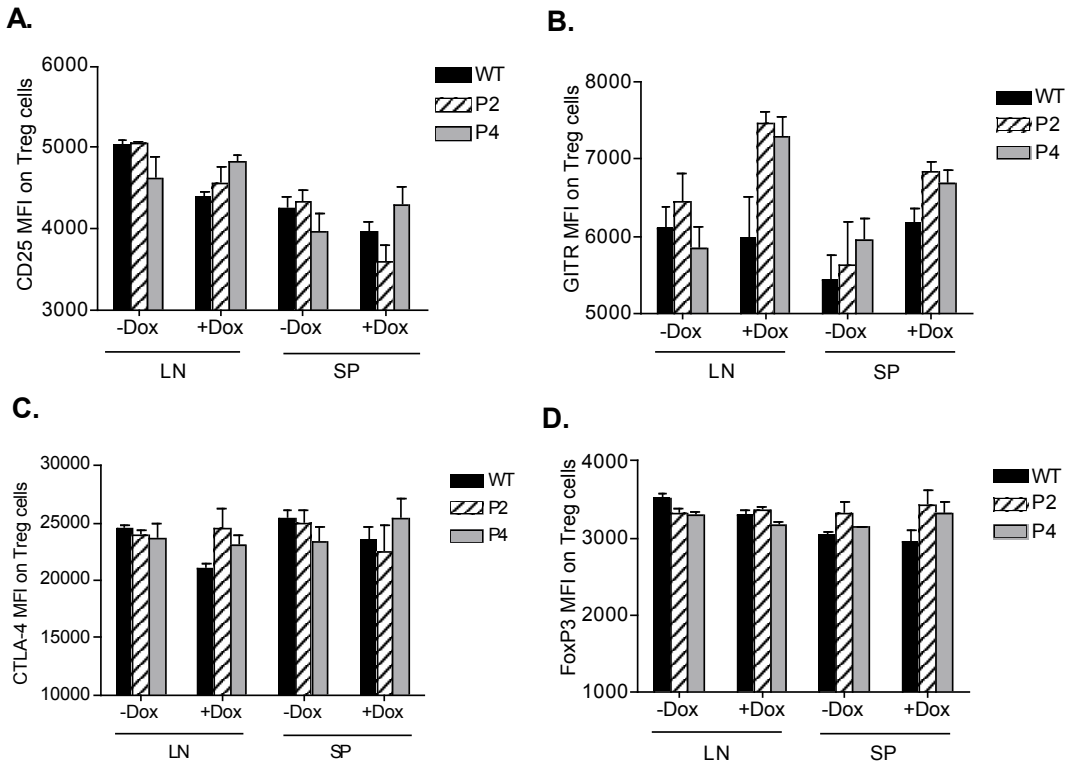

Fig 3.20 Characterization of P2 and P4 KD Treg cells. Mice were left untreated or treated with Dox from 5-7 weeks old for 1month. Lymph node cells and splenocytes were used to measure the expression levels of CD25 (A), GITR (B), CTLA-4 (C) and FoxP3 (D).

3.7.3.3 *Ptpn22* silencing does not disrupt Treg cell function

We have observed an increased Treg cell number as well as elevated GITR expression on *Ptpn22* KD Treg cells. Another important issue was the function of *Ptpn22* KD Treg cells. Treg cells can suppress the proliferation of conventional T cell by several ways: IL-2 consumption, secretion of suppressive cytokines, granzyme mediated cytolysis and modulation of antigen presenting cells (Shevach et al., 2009). To test the suppressive function of KD Treg cells, Treg cells were isolated from 1 month Dox-treated mice. Serially diluted Treg cells were cocultured with WT conventional T cells ($CD4^+CD25^-$) along with 1μg/ml anti-CD3. The proliferation of conventional T cells was assayed by the uptake of [^{3}H]-thymidine. We found P2 and P4 KD Treg cells were equally suppressive compared with WT Treg cells, indicating that *Ptpn22* silencing did not affect Treg cell function (Fig 3.21). Considering the increased number of Treg cells, overall Treg cell suppressive capacities were enhanced in P2 and P4 inducible KD mice.

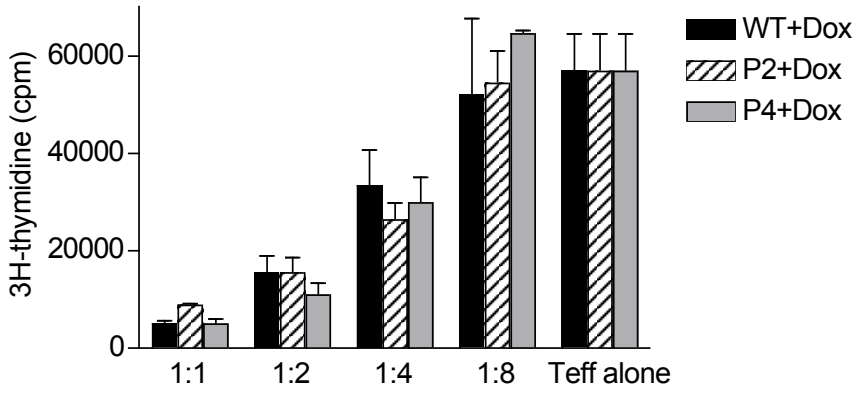

Fig 3.21 Treg assay. Treg cells were isolated and cocultured with Dox-treated WT conventional T cells to test the suppressive function of Treg cells. 1μg/ml anti-CD3 was used to stimulate conventional T cells to proliferate.

3.7.3.4 The increase of Treg cells is maintained after 2 month Dox removal

We have shown that 1 month *Ptpn22* silencing was sufficient to increase Treg cell numbers. An interesting question related to whether this increase is maintained following Dox withdrawal. By using the inducible shNRA expression system, gene knockdown can be reversed by removal of Dox from the drinking water. To test the lifetime of expanded *Ptpn22* KD Treg cells, all the mice were untreated or treated with Dox from 5-7 weeks of age for 1month to allow a Treg cell increase, some of WT, P2, and P4 mice were continuously treated for another 2 months. The other treated mice were given normal drinking water to shut down RNAi for another 2 months. All the mice were then dissected to check the Treg cell proportions in $CD4^+$ T cells. Interestingly, similar to mice treated continuously for 3 months with Dox, an increase of Treg cells remained in the P2 mice that had been treated for 1 month then left untreated for 2 months. In P4 mice treated for 1 month and then left untreated for 2 months, Treg cells were also increased in the lymph nodes and spleen, but numbers did not reached significance relative to Dox-treated WT (Fig 3.22). Our data indicate that once Treg cells were increased, *Ptpn22* silencing was not required to maintain this increase in P2 mice, at least for 2 months.

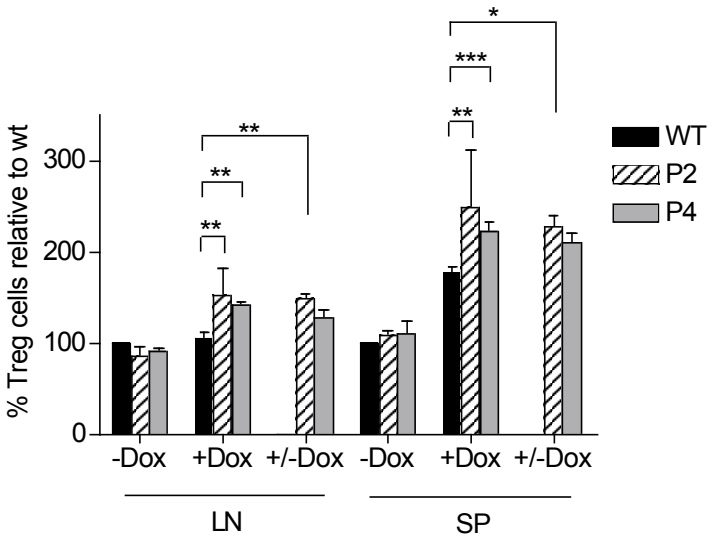

Fig 3.22 The duration of *Ptpn22* KD Treg cells. Mice were left untreated, or treated with Dox for 3month or treated with Dox for 1month followed with 2month RNAi shutdown. The proportion of Treg cells in the lymph nodes and spleen was analyzed by flow cytometry. (*: P<0.05; **: P<0.01; ***: P<0.001)

3.7.3.5 Identifying the source of increased Treg cells in KD mice

Our experiments have confirmed that *Ptpn22* silencing can boost Treg cell numbers. One question remained as to where the additional Treg cells came from. Similarly to the other T cells, Treg cells develop from progenitor cells from the bone marrow, following education in the thymus. Most Treg cells originate in the thymus (natural Treg/ nTreg), and these cells express high levels of helios. In the periphery, when naïve T cells encounter low-dose antigen, they can be induced to differentiate into Treg cells (induced Treg/ iTreg) with lower helios expression (Kretschmer et al., 2005). This differentiation can also occur by homeostatic conversion (Haribhai et al., 2009). *In vitro*, naïve $CD4^+$ T cells can convert into Treg cells in the presence of TGF-β and IL-2 (Chen et al., 2003; Fantini et al., 2004). We tested all these possibilities to find out the reason why *Ptpn22* silencing increased Treg cell numbers.

The increase of Treg cells was not due to the enhanced thymic output

We first investigated Treg cell development in the thymus to find out if *Ptpn22* silencing could enhance thymic Treg cell output. Mice were left untreated, or treated with Dox from 5-7 weeks of age for 1 month. Mice were dissected to obtain the

thymi. Thymocytes were stained with fluorophore-conjugated anti-CD4, CD8, CD25, FoxP3 mAbs to determine Treg cells (FoxP3+). We found similar frequencies of Treg cells in $CD4^+$ thymocytes, indicating *Ptpn22* silencing did not affect Treg cell development in thymus (Fig 3.23)

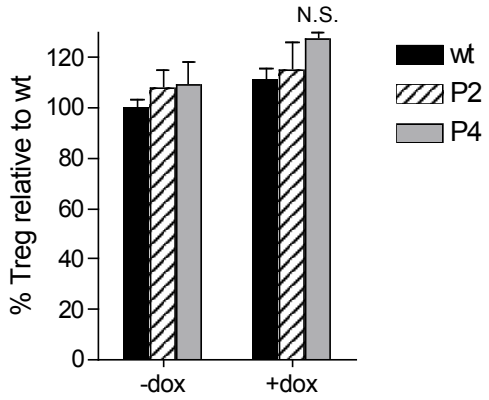

Fig 3.23 Natural Treg cells in the thymus. Mice were left untreated, or treated with Dox from 5-7 weeks old for 1month. The proportions of Treg cells in $CD4^+$ T cells are shown.

To further confirm the increase of Treg cells was not due to the enhanced thymic output, WT, P2 and P4 mice were treated with Dox from birth for 2 months. Mice were then dissected to measure % Treg cells in the $CD4^+$ thymocytes.

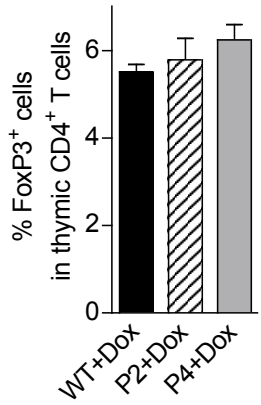

Fig 3.24 Natural Treg cells in the thymus. Mice were untreated, or treated with Dox from birth for 2month. The proportions of Treg cells in $CD4^+$ T cells were shown.

We found *Ptpn22* silencing from birth also didn't increase Treg cells in the thymus (Fig 3.24). Our data were distinct to a recent paper, reporting the increased Treg cells in Pep deficient B6 mice resulted from the enhanced thymic output (Maine et al., 2012). The discrepancy could be attributed to either the differences in the genetic backgrounds of the mice used, or to the differences in the techniques employed (KO

vs KD). In our mouse model, *Ptpn22* silencing from either 5-7 weeks old or birth, did not affect Treg cell development.

The increase of Treg cells was not due to a proliferative advantage

Lyp/Pep is a negative regulator of T cell activation, thus *Ptpn22* silencing likely enhances TCR signaling. Although *Ptpn22* KD naïve and effector T cells proliferated normally in response to TCR stimulation, we were not sure if *Ptpn22* silencing would enhance Treg cell proliferation and expansion. To test this possibility, Treg cells were isolated from untreated or 1 month Dox-treated mice. Treg cells were stimulated for 3 days with anti-CD3/CD28 dynabeads or dendritic cells (DCs) along with anti-CD3 Ab and IL-2. The proliferation of Treg cells was assayed by the uptake of [^{3}H]-thymidine. The result showed that P2 and P4 KD Treg cells proliferated normally (Fig 3.25A).

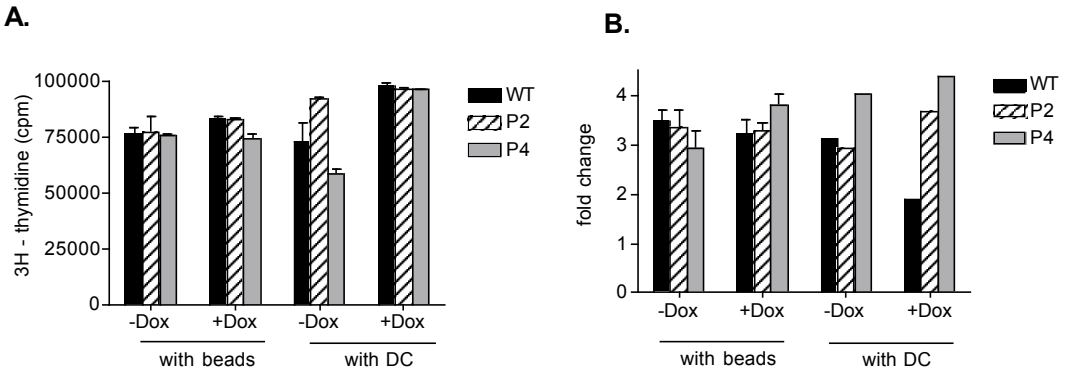

Fig 3.25 Treg cell proliferation and expansion *in vitro*. Treg cells were isolated from untreated or 1month Dox-treated WT, P2 and P4 mice. Treg cells were expanded with beads or DC/anti-CD3 in addition to IL-2 for 3 days (A) or 10 days (B).

Although we didn't see any difference in the 3-day culture, we decided to examine the long-term Treg cell expansion. Loss of Pep exerted its function in a slow manner, as illustrated by the expanded effector/memory T cells in the older KO mice (Hasegawa et al., 2004). In the case of Treg cells, *Ptpn22* silencing may slowly accelerate Treg cell turnover to increase the Treg cell number. To mimick this slow turnover *in vitro*, purified Treg cells were expanded with anti-CD3/CD28 dynalbeads or DC/anti-CD3 for 10 days. Every 2-3 days, half of the exhausted medium was replaced with fresh medium to maintain cell growth. On day 10, cell numbers were counted relative to input cell numbers. Similar to the 3-day expansion, no differences could be seen in

Treg cells after 10-day expansion, indicating *Ptpn22* silencing didn't enhance Treg cell proliferation and expansion (Fig 3.25B).

Finally we tested Treg cell proliferation capacity *in vivo* using Ki-67 protein. As mentioned above, Ki-67 could be a cellular marker for cell proliferation. Mice were left untreated or treated with Dox from 5-7 weeks old for 8 months, and then dissected to examine the dividing cells (Ki-67$^+$) among Treg cells. We found Ki-67$^+$ frequencies among Treg cells were comparable between WT and KD mice, indicating *Ptpn22* KD Treg cells divided normally *in vivo* (Fig 3.26). This observation coupled with the *in vitro* Treg cell expansion data, led us to believe that the increased Treg cell frequencies were not due to any proliferative advantage of KD Treg cells.

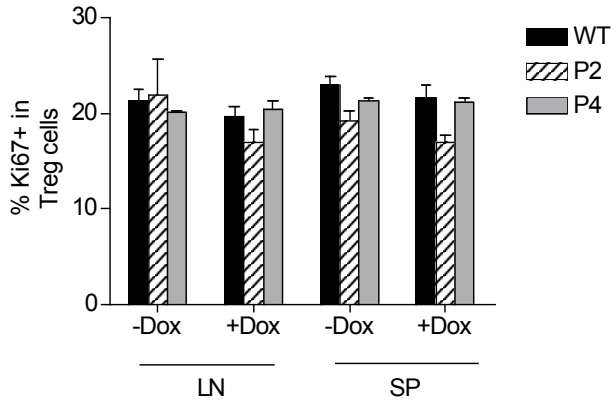

Fig 3.26 The frequencies of Ki-67$^+$ in Treg cells. Mice were untreated, or treated with Dox from 5-7 weeks old for 8months. Treg cells were gated on CD4$^+$FoxP3$^+$ cells. The frequenciese of Ki-67$^+$ in Treg cells are shown.

The increase of Treg cells was not due to increased naïve T cell conversion in vitro

Depending on culture conditions, naïve CD4+ T cells can differentiate into Th1, Th2, Th17 or Treg cells. When activated naïve CD4$^+$ T cells are cocultured with TGF-β and IL-2, they can convert into FoxP3+ Treg cells (Chen et al., 2003; Fantini et al., 2004). We investigated if the increase of Treg cells was due to enhanced naïve T cell conversion in response to TGF-β. Naïve CD4$^+$ T cells were purified and then induced to convert into Treg cells. 3 days later, cells were harvested and stained with anti-FoxP3 mAb. Comparable converted Treg cell percentages could be found in control (untreated and Dox-treated WT) and P2 KD cells (Fig 3.27). Thus, the Treg cell

increase could not be explained by differences in naïve T cell differentiation in response to TGF-β.

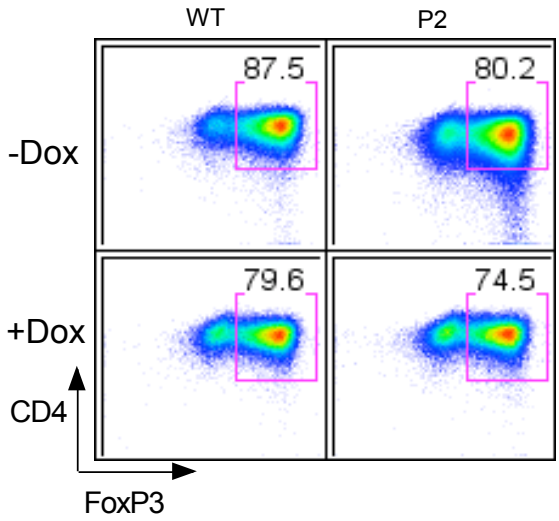

Fig 3.27 Naïve T cell differentiation into Treg *in vitro*. Naïve $CD4^+$ T cells were cocultured with TGF-β and IL-2 to induce conversion into Treg cells. 3 days later, cells were harvested and stained with anti-FoxP3 to analyze Treg cell proportion.

The increase of Treg cells was not due to enhanced homeostatic conversion *in vivo*

Our data have shown that the increase of Treg cells did not result from increased T cell development in the thymus, a proliferative advantage, or naïve T cell conversion in response to TGF-β. We next examined if the Treg cell increase was due to homeostatic conversion *in vivo*. By microarray analysis, Feuerer and colleagues found that homeostatically converted Treg cells could be defined as $CD103^+Klrg1^+$ Treg subset (Feuerer et al., 2010).

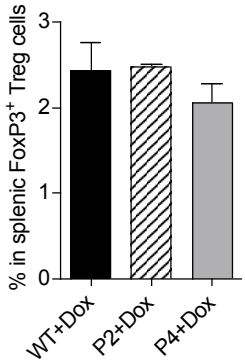

Fig 3.28 The proportions of homeostatic converted Treg cells. Mice were left untreated or treated with Dox for 1month. Splenocytes were stained with anti-CD103 and Klrg1 to determine homeostatic converted Treg cells ($CD103^+Klrg1^+$).

We stained lymph node cells and splenocytes with fluorophore-conjugated anti-CD103 and Klrg1 mAbs to measure the frequencies of homeostatically converted Treg cells. Again, no differences could be seen in the $CD103^{+}Klrg1^{+}$ Treg subset, indicating that *Ptpn22* silencing didn't enhance homeostatic conversion *in vivo* (Fig 3.28).

Since Helios is thought to be preferentially expressed in thymus-derived Treg cells, we additionally investigated Helios expression in Treg cells. Consistent with the results presented above, similar percentages of Helios negative Treg cells could be observed in KD mice with and without treatment (Fig 3.29). Thus, the increase of Treg cells was not due to enhanced homeostatic conversion *in vivo*.

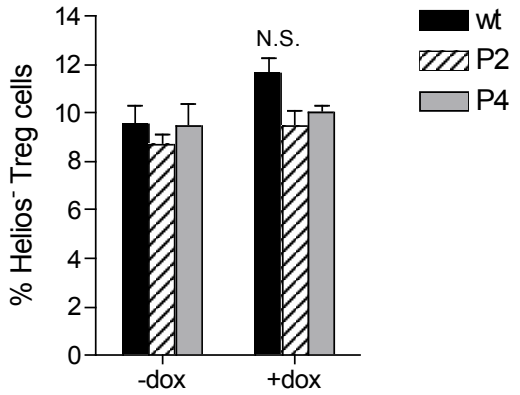

Fig 3.29 The proportions of Helios negative Treg cells. Mice were left untreated or treated with Dox for 1month. Splenocytes were stained with anti-CD4, FoxP3 and Helios mAbs to determine Helios negative Treg cells.

3.8 The effect of inducible *Ptpn22* silencing on chemokine receptors

Several papers have reported the importance of chemokines and chemokine receptors in the development off diabetes in the NOD mouse (Frigerio et al., 2002; Morimoto et al., 2004; Rhode et al., 2005; Grewal et al., 1997). Considering that *Ptpn22* is predominantly expressed in T and B lymphocytes, we focused on the expression of chemokine receptors in $CD4^{+}$ T cells. Chemokine receptors belong to the G-protein coupled receptor superfamily. Through the PI(3)K-Dock2-Rac pathway, chemokine receptors can induce cell cytoskeleton rearrangement, cell polarization, and cell migration (Weiss-Haljiti C et al., 2004; Viola A et al., 2007). Several chemokine receptors, such as CXCR3, CCR4, and CCR5, have been confirmed to play roles in

mediating T cell trafficking in diabetes pathogenesis. Loss of CXCR3 protected mice from LCMV infection induced diabetes (Frigerio et al., 2002). Similarly, CCR5 neutralization abrogated β cell destruction and diabetes (Carvalho-Pinto et al., 2004). Overexpression of CCL22, a CCR4 ligand, in the pancreas from birth accelerated diabetes (Kim et al., 2002), though its overexpression from 8 weeks of age prevented the disease through enhanced recruitment of Treg cells into pancreas (Montane et al., 2011).

Given the importance of chemokine receptors in the pathogenesis of T1D, we examined the effect of *Ptpn22* silencing on chemokine receptors in T cells. Lymph node cells and splenocytes were obtained from 1 month Dox-treated mice. Cells were stained with fluorophore-conjugated anti-CD4, CD25, CD62L, CCR4, CCR5 and CXCR3 mAbs to measure chemokine receptor expression on Treg and effector $CD4^+$ T cells. We found that the expression of CXCR3, CCR4 and CCR5 were not affected in lymph node cells (data not shown). More CCR4 and CXCR3 were expressed on the Treg ($CD4^+CD25^+$) cells from P2, but not P4 KD splenocytes. Interestingly, CCR4, CCR5 and CXCR3 were expressed normally on the P2 and P4 KD effector/memory T cells (Fig 3.30). Our data showed that *Ptpn22* silencing mainly affects chemokine receptor expression on Treg cells by enhancing CCR4 and CXCR3 expression.

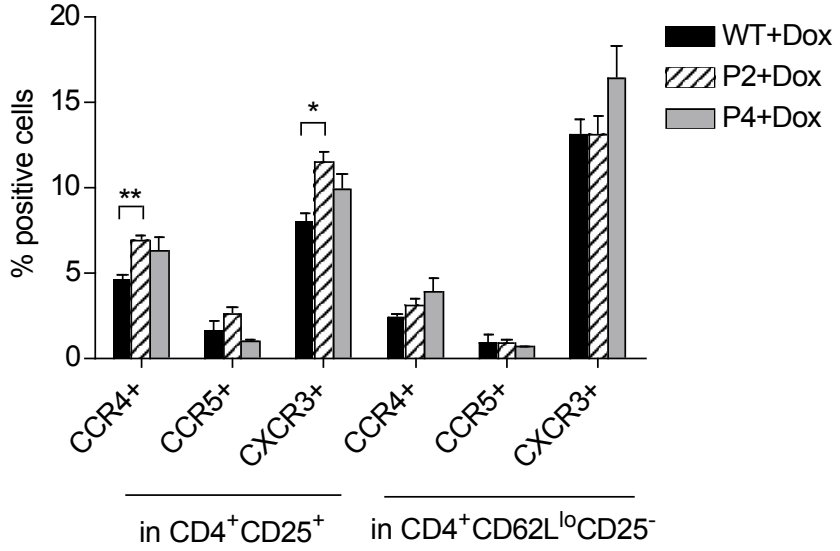

Fig 3.30 The expression of chemokine receptors, CCR4, CCR5 and CXCR3 on splenic Treg and effector/memory $CD4^+$ T cells. Mice were left untreated, or treated with Dox for 1month. Splenocytes were stained with fluorophore-conjugated anti-CD4, CD25, CD62L, CCR4, CCR5 and CXCR3 mAbs to measure chemokine receptor expression (**: $P<0.01$; *: $P<0.05$)

3.9 The effect of inducible *Ptpn22* silencing on B cells

In humans, several reports confirmed that Lyp changes the composition and function of the B cell compartment. Lyp participates in the removal of autoreactive B cells (Menard et al., 2011). Heterozygous subjects for Lyp R620W had more IgD^+CD27^- B cells (Habib et al., 2012) as well as reduced IgD^+CD27^+ (memory) B cells in peripheral blood (Rieck et al., 2007). BCR signaling was deficient, as illustrated by decreased phosphorylation, calcium flux and impaired proliferation (Arechiga et al., 2009). In mouse, loss of Pep enhanced B cell proliferation (Hasegawa et al., 2004). In this project, we investigated the effect of *Ptpn22* silencing on B cell activation, proliferation, survival as well as T-B interaction.

3.9.1 *Ptpn22* silencing enhances B cell activation and proliferation

As mentioned above, several papers have examined the role of Lyp/Pep on B cells. To investigate the role of Pep on B cells in the NOD mouse, we examined KD B cell activation and proliferation. Once cells were activated, CD69 expression was upregulated in the early response and then went down. Subsequently, CD25 expression was elevated.

B cell activation was assayed by activation markers CD25 and CD69. Mice were treated with Dox from 5-7 weeks of age for nearly 1 month. B cells were purified from splenocytes using anti-CD19 (positive selection) or anti-CD43 microbeads (negative selection) (Miltenyi). B cells were then stimulated with LPS, serially diluted anti-IgM F(ab)'2 or anti-CD40. 1 day later, cells were harvested, and stained with anti-CD25/CD69 mAbs to examine B cell activation. 2 days after stimulation, [^{3}H]-thymidine was added into wells to test B cell proliferation. We found in response to anti-IgM F(ab)'2 and anti-CD40, P2 and P4 KD B cells expressed more CD25 and CD69, illustrated by the increased MFI of CD25 and CD69, as well as elevated percentages of $CD25^+CD69^+$ B cells (Fig 3.31). Due to the higher KD efficiency in P2 KD mice, increased activation could be observed in P2 KD cells compared to P4 KD B cells.

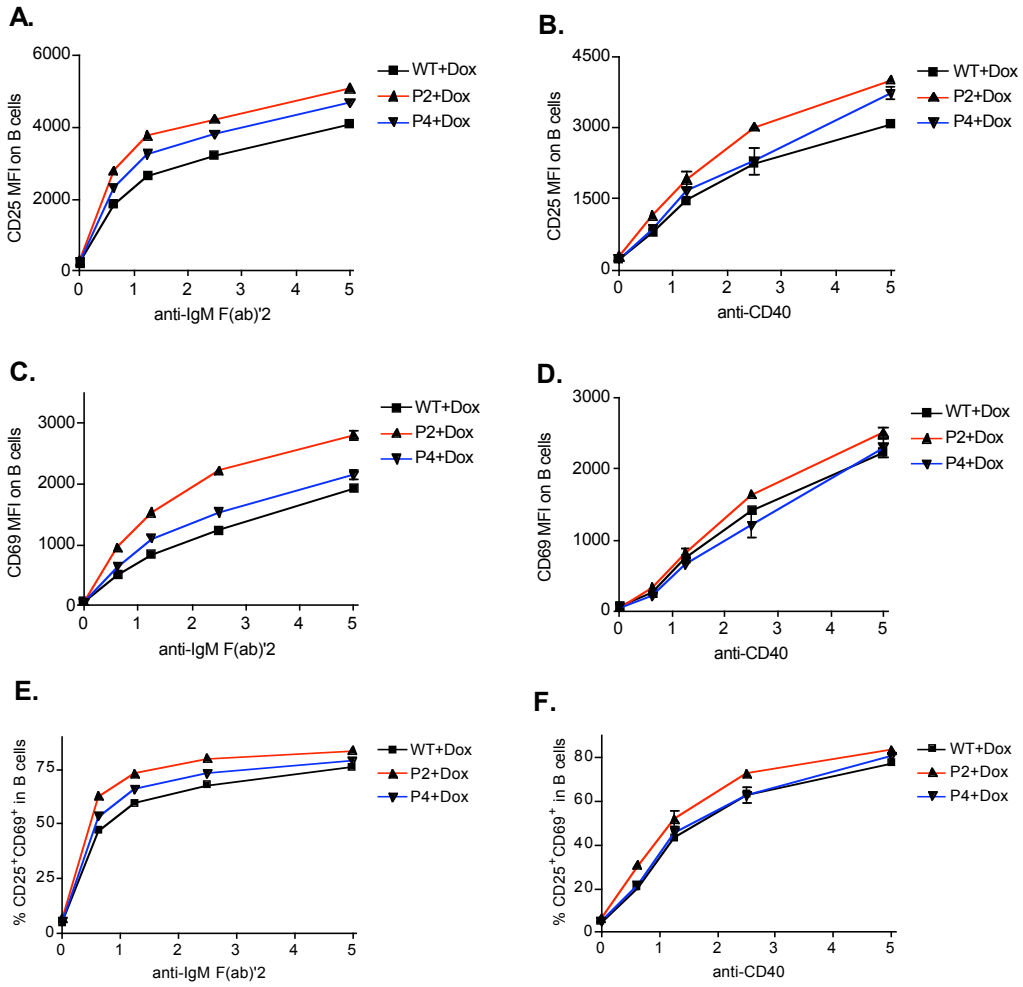

Fig 4.31 B cell activation. B cells were isolated from 1month Dox-treated mice, and then stimulated with LPS, serially diluted anti-IgM F(ab)'2 or anti-CD40. 1 day later, B cell activation was assayed by activation markers, CD25 and CD69. A. C. E shows CD25 MFI, CD69 MFI, and % $CD25^{+}CD69^{+}$ in B cells in response to anti-IgM F(ab)'2. B. D. F shows CD25 MFI, CD69 MFI, and % $CD25^{+}CD69^{+}$ in B cells in response to anti-CD40.

We assayed B cell proliferation after 2 day stimulation. Similar to the *Ptpn22* KO and knockin B cells, *Ptpn22* silencing enhanced P2 B cell proliferation in response to anti-IgM F(ab)'2 or anti-CD40 (Fig 3.32A,B). P2 and P4 KD B cells proliferated normally in response to LPS, a Toll-like receptor stimulant (Fig 3.32C).

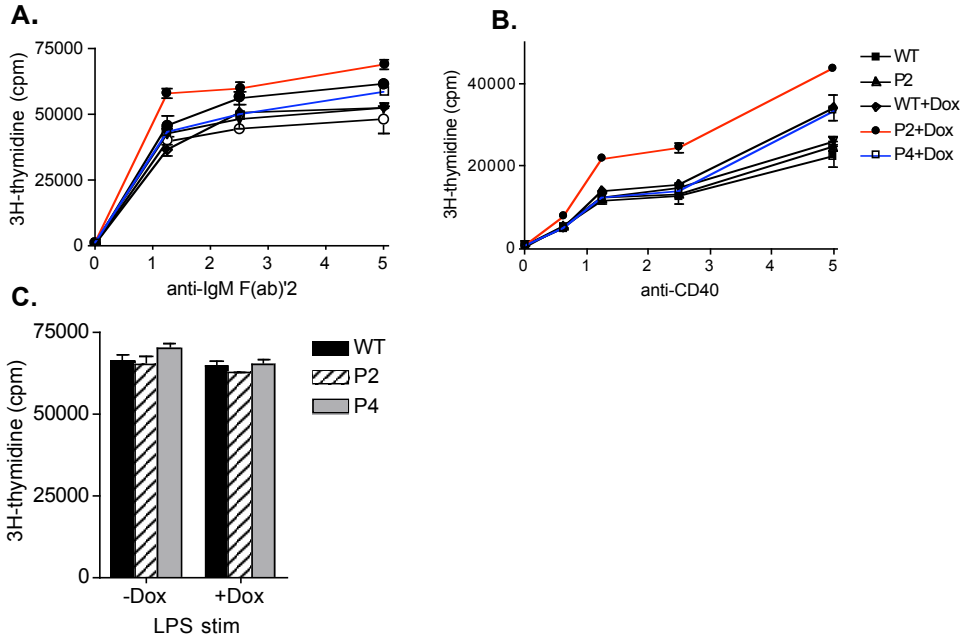

Fig 3.32 B cell proliferation. B cells were isolated from untreated or 1month Dox-treated mice, and then stimulated with LPS, serially diluted anti-IgM F(ab)'2 or anti-CD40. 2 days later, B cell activation was assayed by the uptake of [^{3}H]-thymidine. A. B cell proliferation in response to anti-IgM F(ab)'2; B. to anti-CD40; C. to LPS.

3.9.2 *Ptpn22* silencing facilitates PLC-γ2 phosphorylation

In humans, PLC-γ2 phosphorylation was attenuated when B cells carried *PTPN22* heterozygous allele (Arechiga et al., 2009; Habib et al., 2012). Since we saw enhanced B cell activation and proliferation when *Ptpn22* was silenced, to give more details, we decided to examine PLC-γ2 phosphorytion which was involved in the BCR signaling. For this purpose, splenocytes were prepared from untreated or 1 month Dox-treated mice, and stimulated with 20μg/ml anti-IgM F(ab)'2 for 1, 3, 5 or 10min. Cells were fixed immediately after stimulation, permeabilized and then stained with anti-CD19 and phos-PLC-γ2 mAbs. PLC-γ2 phosphorylation was determined by using the geometric mean fluorescence intensity of phos-PLC-γ2. We found phos-PLC-γ2 MFI dramatically went up in the first 1 min stimulation, and then decreased. *Ptpn22* silencing in P2 mice enhanced PLC-γ2 phosphorylation in almost all the time points we checked. We didn't see enhanced PLC-γ2 phosphorylation in P4 KD B cells, maybe due to the reduced KD efficiency in comparison to the P2 cells (Fig 3.33).

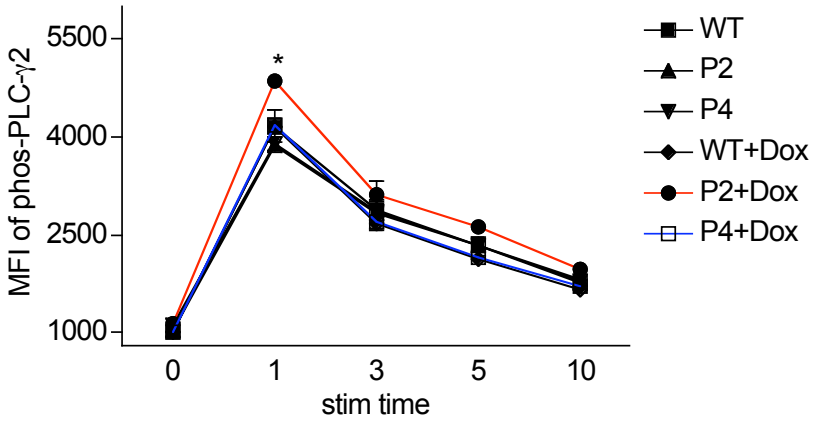

Fig 3.33 PLC-γ2 phosphorylation in response to anti-IgM F(ab)'2. Splenocytes were prepared from untreated or 1 month Dox-treated mice, and stimulated with 20μg/ml anti-IgM F(ab)'2 for different time intervals. Cells were fixed immediately after stimulation, permeabilized and then stained with anti-CD19 and phos-PLC-γ2 mAbs. PLC-γ2 phosphorylation was determined using the geometric MFI of phos-PLC-γ2.

3.9.3 *Ptpn22* silencing increases B cell apoptosis in response to stimulus

In humans, B cells bearing heterozygous *Ptpn22* allele survived better than WT B cells (Habib et al., 2012). We tested B cell apoptosis by using the cell viability dye 7-AAD. In late apoptotic cells, cell membrane is compromised allowing the uptake of 7-AAD. Hence, the late apoptotic cells were marked as 7-AAD$^+$.

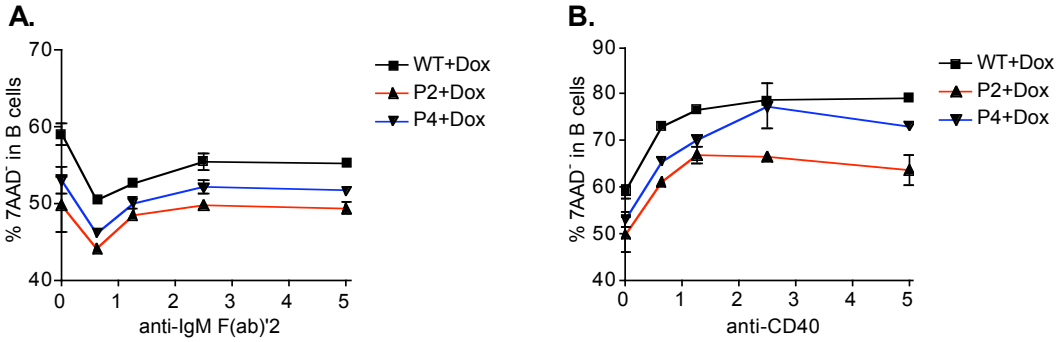

Fig 3.34 B cell apoptosis. B cells were isolated from 1month Dox-treated mice, and then stimulated with serially diluted anti-IgM F(ab)'2 (A) or anti-CD40 (B). 1 day later, the proportion of live (7-AAD$^-$) B cells was assayed.

We obtained spleens from 1-month Dox-treated mice. B cells were purified from splenocytes, and then stimulated with serially diluted anti-IgM F(ab)'2 or anti-CD40. 1 day after stimulation, apoptotic B cells were determined as B220$^+$7-AAD$^+$. Interestingly, *Ptpn22* silencing accelerated cell apoptosis in response to anti-IgM

F(ab)'2 and anti-CD40 stimulation. Moreover, more dead cells could be found in P2 KD than P4 KD B cells (Fig 3.34).

3.9.4 *Ptpn22* silencing doesn't alter B cell composition

B cells are a heterogeneous cell population. We have shown that *Ptpn22* silencing enhanced B cell activation, proliferation, apoptosis and PLC-γ2 phosphorylation in response to anti-IgM F(ab)'2 and anti-CD40. We further tested if *Ptpn22* silencing could alter B cell composition in bone marrow (BM), peritoneal cavity (PC) and spleen (SP). Since a stronger phenotype could be observed in P2 KD mice, we just compared cell compositions in Dox-treated WT and P2 mice.

B cell composition in BM

B cells mature in the bone marrow. According to their expression of IgD, IgM and B220, B cells in the BM can be divided into mature B cells ($IgM^{+}IgD^{+}$), immature B cells ($IgM^{+}IgD^{int}$), Pre B ($IgM^{-}IgD^{-}$ $B220^{-}$) and Pro B ($IgM^{-}IgD^{-}$ $B220^{+}$). We compared the proportions of each subset in BM. No differences could be observed in any of the subsets, indicating that *Ptpn22* silencing didn't alter cell composition in BM (Fig 3.35).

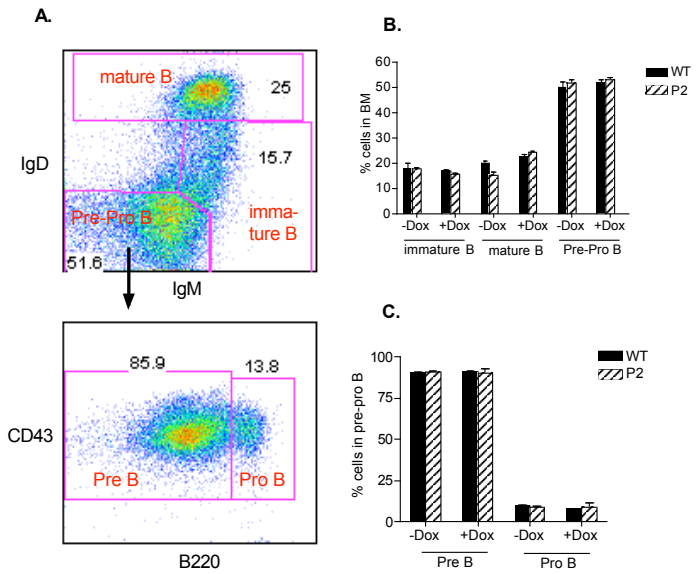

Fig 3.35 B Cell composition in BM of Dox-treated WT and P2 mice. The proportions of mature B cells (IgM^+IgD^+), immature B cells (IgM^+IgD^{int}), Pre B (IgM^-IgD^- $B220^-$) and Pro B (IgM^-IgD^- $B220^+$) are shown. A. Schematic of B cell subsets gating B.C. The statistics of each B cell subset.

B cell composition in PC

We next analyzed B cell subsets in the peritoneal cavity (PC), in which an abundance of B1a cells could be found. CD5 is selectively expressed on B1a cells. CD43 is not expressed on most B cells, which is used in the gating of B2 cells. Thus, B cells were first plotted against CD43 and CD5 to identify B1a ($CD5^+$), B1b ($CD43^+CD5^-$) and B2 ($CD43^-CD5^-$) cells. B2 cells were further plotted against CD21 and CD23 to determine marginal zone (MZ, $CD43^-CD5^-$ $CD23^-CD21^+$) and follicular (FO, $CD43^-$ $CD5^-$ $CD23^+CD21^+$) B cells. We found that the proportion of each subset was quite similar in Dox-treated WT and P2 mice, suggesting *Ptpn22* silencing didn't alter cell composition in PC (Fig 3.36).

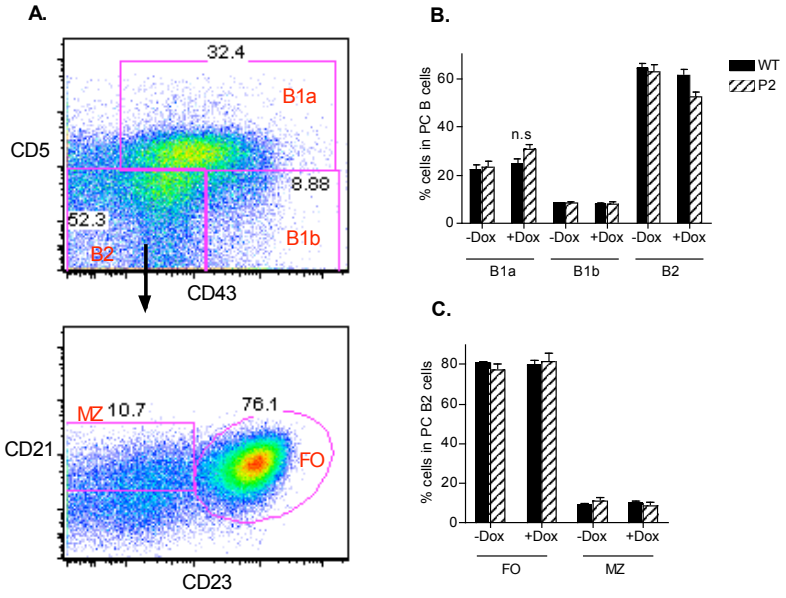

Fig 3.36 B Cell composition in PC of Dox-treated WT and P2 mice. The proportions of B1a ($CD5^+$), B1b ($CD43^+CD5^-$), B2 ($CD43^-CD5^-$), MZ ($CD43^-CD5^-CD23^-CD21^+$) and FO ($CD43^-CD5^-$ $CD23^+$ $CD21^+$) are shown. A. Schematic of B cell subsets gating B.C. The statistics of each B cell subset.

B cell composition in SP

We further analyzed B cell subsets in spleen (SP) by two different approaches. We measured mature (IgM^+IgD^+) and immature (IgM^+IgD^-) B cells by anti-IgM and IgD staining. Again, no difference could be observed (Fig 3.37).

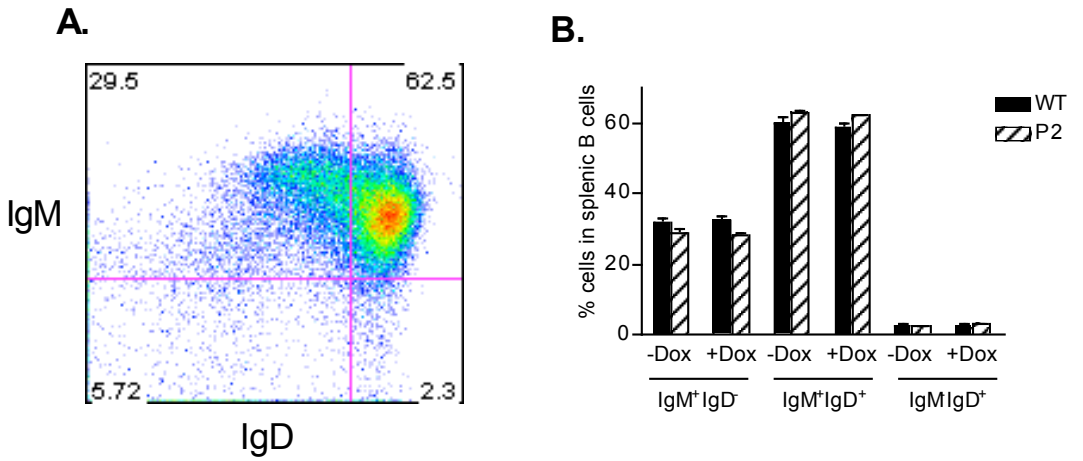

Fig 3.37 Mature and immature B cells in spleen. The proportions of mature B cells (IgM^+IgD^+) and immature B cells (IgM^+IgD^-) are shown. A. Schematic of B cell subsets gating B. The statistics of each B cell subset.

In the second approach, B cells were first plotted against CD1d/CD5 to determine regulatory B cells ($CD1d^{hi}CD5^+$) or CD43/CD5 to identify B1a ($CD5^+$), B1b ($CD43^+CD5^-$) and B2 ($CD43^-CD5^-$) cells. B2 cells were next plotted against CD93 and CD23 to determine T1 ($CD43^-CD5^-$ $CD23^-CD93^+$), T2 ($CD43^-CD5^-$ $CD23^+CD93^+$) and MZ+FO ($CD43^-CD5^-$ $CD93^-$) B cells. MZ+FO B cells were further plotted against CD23 and CD21 to identify FO ($CD43^-CD5^-$ $CD93^-$ $CD23^+CD21^{int}$) and MZ ($CD43^-CD5^-$ $CD93^-CD23^-CD21^+$) B cells. Interestingly, elevated FO and reduced MZ B cells could be found in the Dox-treated P2 splenocytes. Other cell subsets, like B1a, B1b, regulatory B cells and total B cells were not altered (Fig 3.38).

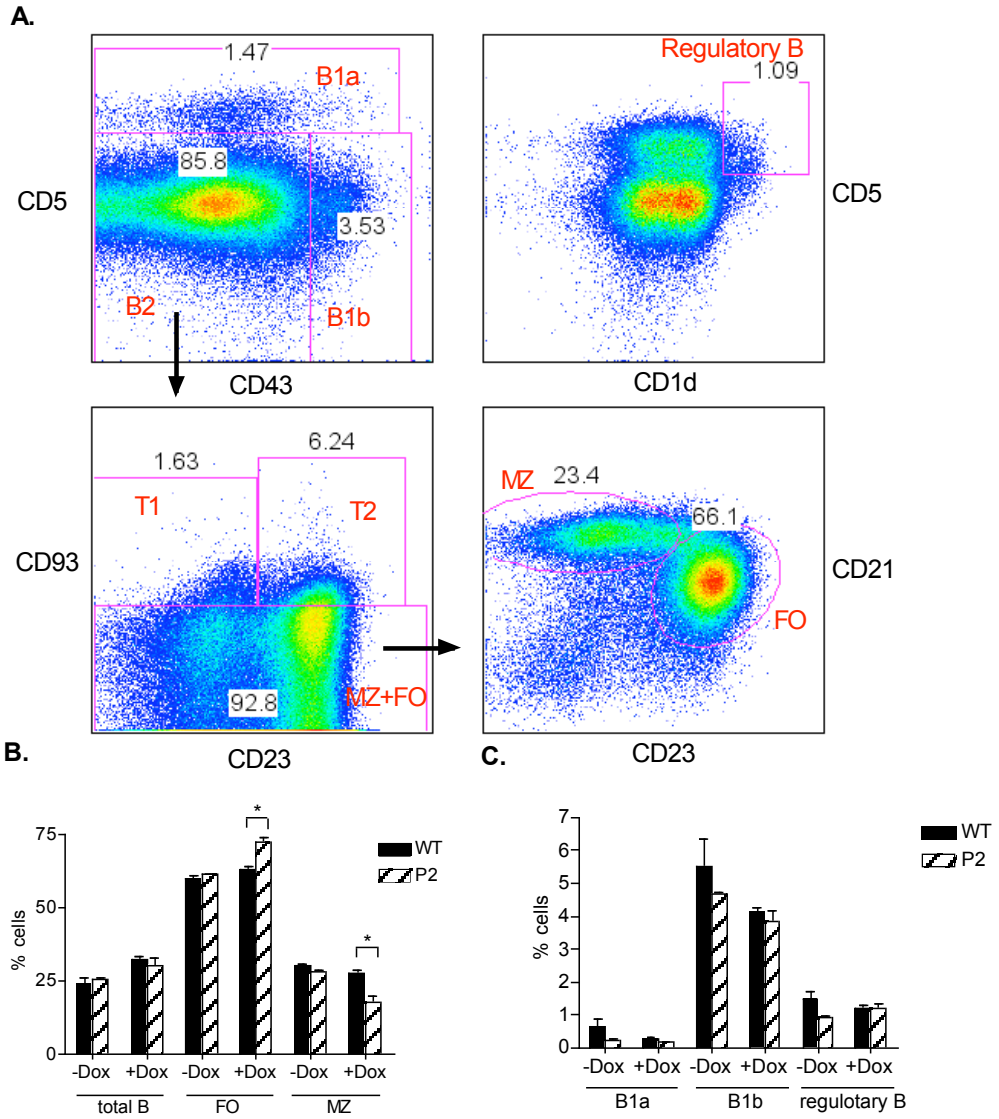

Fig 3.38 B Cell composition in spleen of Dox-treated WT and P2 mice. The proportions of regulatory B cells ($CD1d^{hi}CD5^{+}$), B1a ($CD5^{+}$), B1b ($CD43^{+}CD5^{-}$), FO ($CD43^{-}CD5^{-}$ $CD93^{-}CD23^{+}CD21^{int}$), MZ ($CD43^{-}CD5^{-}$ $CD93^{-}CD23^{-}CD21^{+}$) and total B cells are shown. A. Schematic of B cell subsets gating B. The statistics of each B cell subset (*,: $P<0.05$).

3.9.5 *Ptpn22* silencing doesn't affect T-B interactions in GC

As a subset of antigen presenting cells (APCs), B cells present both costimulatory and inhibitory signals to induce T cell activation or anergy (Alegre et al., 2001) (Fig 4.39). We investigated the role of *Ptpn22* KD on the interaction between B cells and T cells. To examine if *Ptpn22* silencing could affect the expression of costimulatory and inhibitory molecules on B cells, B cells were prepared from 4-5 month Dox-treated WT and P2 mice. B cells were then stained with fluorophore-conjugated anti-CD80, CD86, MHC, CD40, PD-L1 and PD-L2 mAbs to analyze costimulatory and inhibitory

signals on B cells. The results showed that the expression levels of CD80, CD86, CD40, MHCII, PD-L1, and PD-L2 were comparable between Dox-treated WT and P2 B cells, indicating that *Ptp22* silencing did not affect the antigen presenting ability of B cells (Fig 4.40).

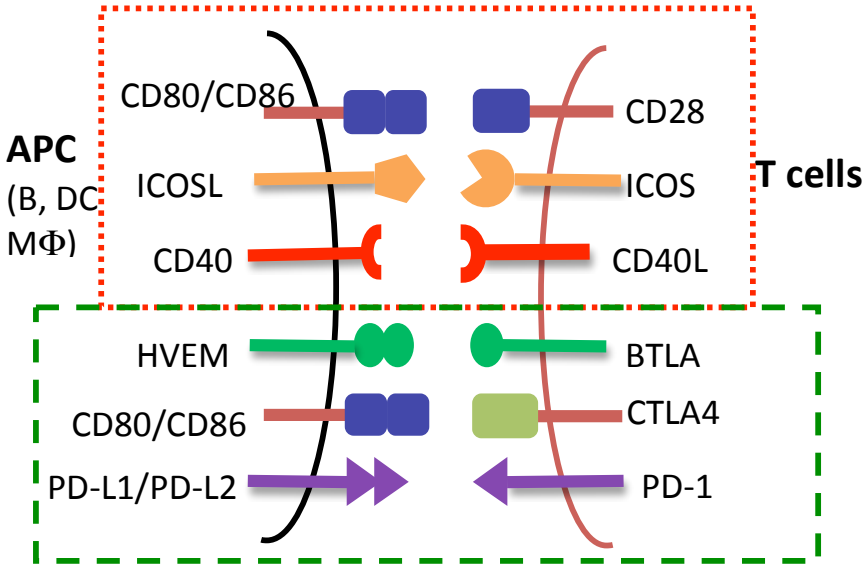

Fig 3.39 Costimulatory and inhibitory molecules on APCs, including B cells. Costimulatory signals are in the red rectangle, and inhibitory signals are shown in the green rectangle.

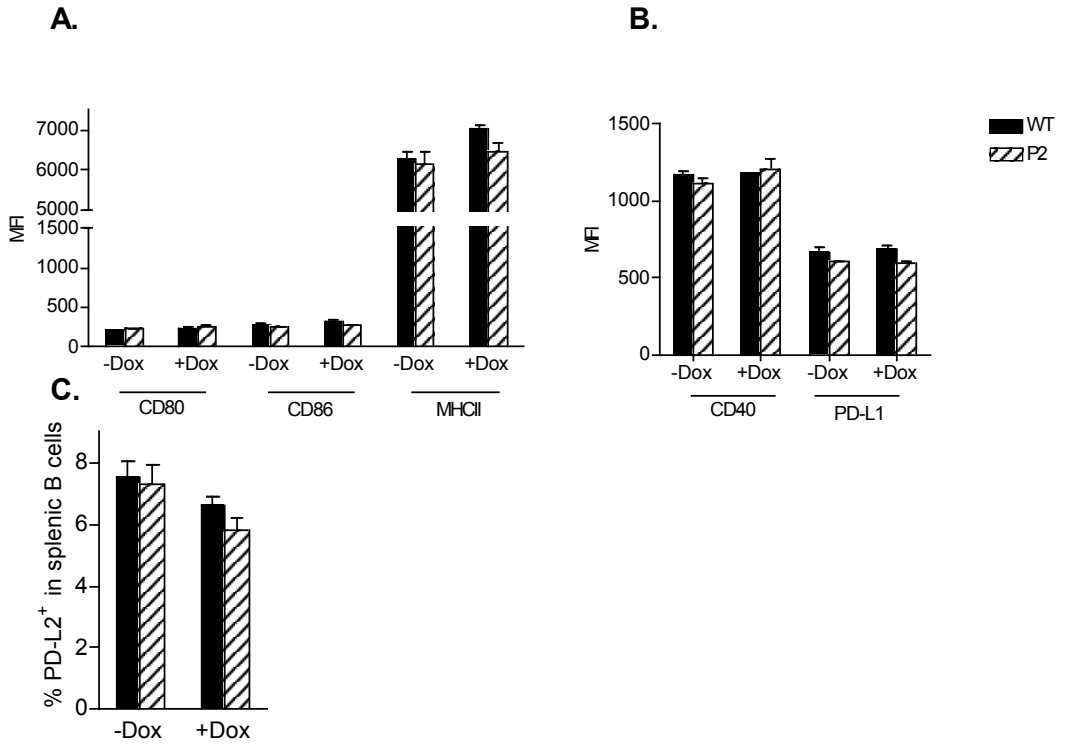

Fig 3.40 Costimulatory and inhibitory molecules on B cells. Mice were treated with Dox for 4-5 months. B cells were stained with mAbs to measure the expression levels of CD80, CD86, MHCII (A), CD40, PD-L1 (B). The % of PD-L2$^+$ in B cells were shown in (C).

We further analyzed T-B cell interaction in the germinal center (GC). Follicular helper T (T_{FH}) cells, which highly express CXCR5 and Bcl-6, represents a T cell subset preferentially in the germinal center. T_{FH} cells provide crucial signals to germinal center B cells (peanut agglutinin positive, PNA$^+$) to regulate humoral immunity (Chung et al., 2011; Linterman et al., 2011; Oestreich et al., 2012). We analyzed Treg and effector CD4$^+$ T cells of T_{FH} cells in 5 month Dox-treated mice, as well as the germinal center B cells in 8 month Dox-treated mice. The results showed that *Ptpn22* silencing did not alter the frequencies of follicular Treg or effector CD4$^+$ T cells (Fig 3.41A,B). The proportions of PNA$^+$ germinal center B cells were also similar in Dox-treated WT and P2 mice (Fig 3.41C). These data demonstrated that *Ptpn22* silencing did not affect T-B interactions in the germinal center.

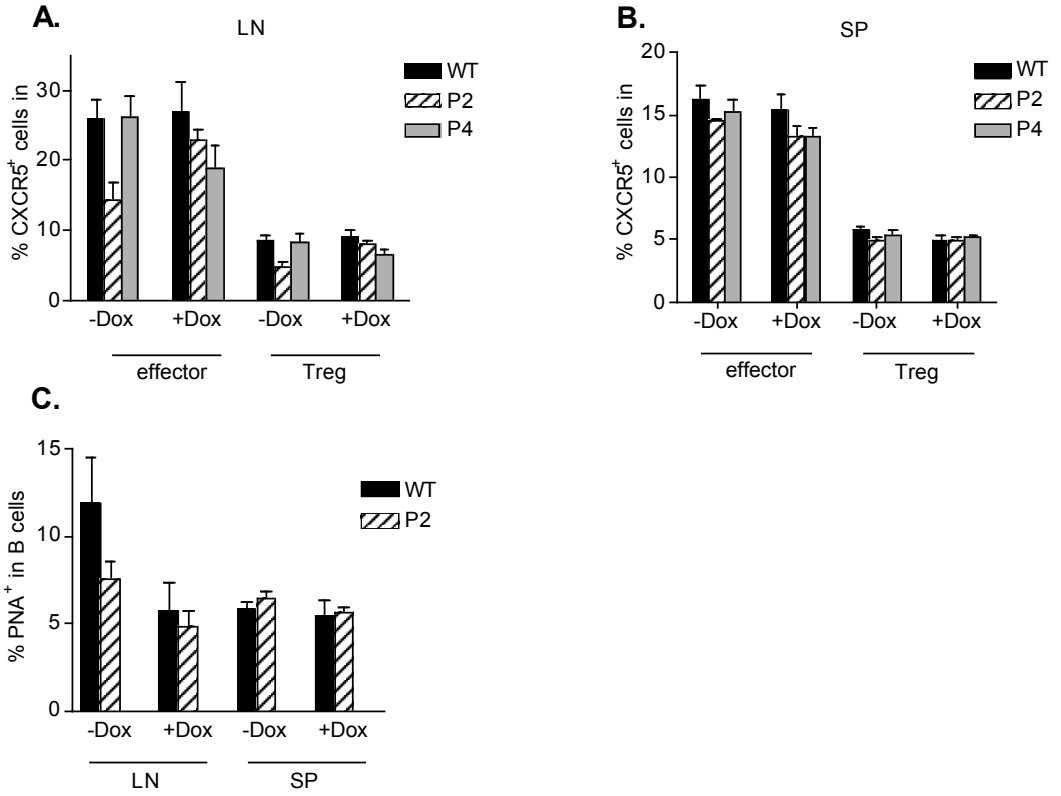

Fig 3.41 The follicular Treg, follicular effector T cells and germinal center B cells in the KD mice. Mice were treated with Dox for 5 or 8 months. Effector and Treg cells of CXCR5+ follicular helper T cells in lymph nodes (A) and spleen (B) are shown. The frequencies of germinal center (PNA$^+$) B cells in the splenocytes were compared in Dox-treated WT and P2 mice.

To sum up, we observed enhanced B cell activation, proliferation and apoptosis in response to anti-IgM F(ab)'2 or anti-CD40. An elevated PLC-γ2 phosphorylation could be detected in the P2 KD B cells. Moreover, increased FO B cells and reduced MZ B cells could be detected in P2 KD splenocytes. *Ptpn22* silencing did not alter B cell composition in the peritoneal cavity, bone marrow as well as costimulatory and inhibitory signals on B cells. The T-B interaction in germinal center was also unaffected.

In humans, several reports showed that in subjects bearing heterozygous Lyp R620W, BCR signaling was deficient, as illustrated by decreased PLC-γ2 phosphorylation, calcium flux and impaired proliferation (Arechiga et al., 2009; Habib et al., 2012). In mouse, loss of Pep enhanced B cell proliferation (Hasegawa et al., 2004). Our results support the proposal that the Lyp R620W variant in humans is a gain-of-function mutation, as *Ptpn22* silencing in the NOD mice showed an opposite phenotype to that observerd in humans.

3.10 The effect of inducible *Ptpn22* silencing on DC and MΦ

As mentioned above, antigen presenting cells (APCs) are essential for T cell activation and immune tolerance. Both co-stimulatory and inhibitory molecules are expressed on APCs (Alegre et al., 2001).

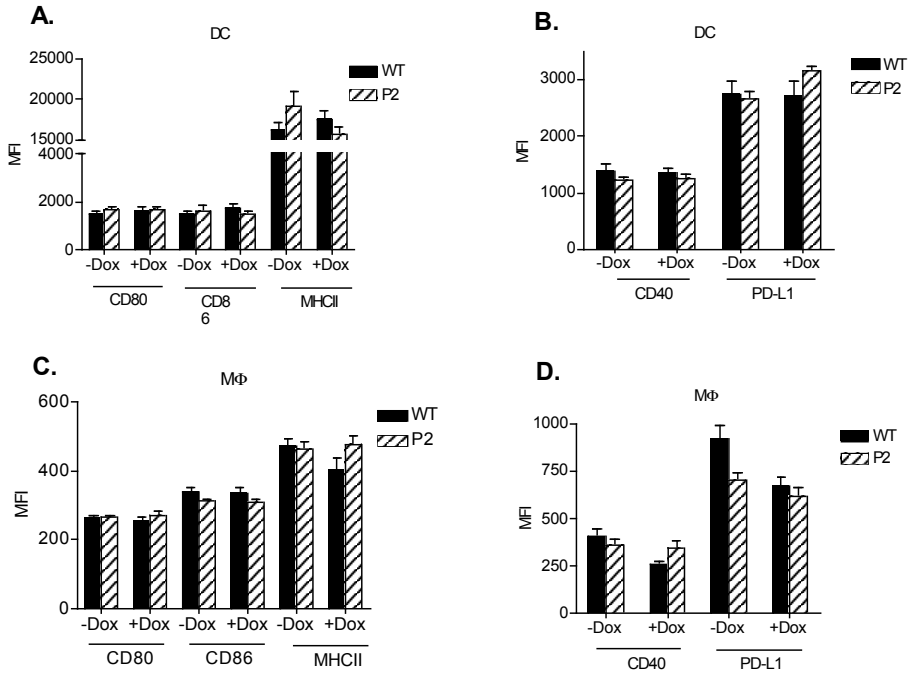

Fig 3.42 Costimulatory and inhibitory molecules on DC and MΦ. Mice were left untreated or treated with Dox from 5-7 weeks old for 4-5 months. Splenic DC and MΦ were stained with mAbs to measure the expression levels of CD80, CD86, MHCII (A,C), CD40 and PD-L1 (B,D).

Besides T and B cells, *Ptpn22* can also modulate dentric cells (DCs) and macrophages (MΦ). Zhang and colleagues reported that in the *Ptpn22* knockin mouse, more CD40 was expressed on DCs, which may facilitate effector/memory T cell generation (Zhang et al., 2011). In this project, we examined APC function by measuring costimulatory and inhibitory molecules in untreated or 4-5 month Dox-treated mice. Contrary to the *Ptpn22* knockin mouse, *Ptpn22* silencing did not affect costimulatory and inhibitory molecules on DC and MΦ (Fig 3.42).

3.11 The effect of inducible *Ptpn22* silencing on colitis and diabetes

In humans, Lyp-620W variant increased disease susceptibility to type 1 diabetes, arthritis, and many other autoimmune diseases. However, the *Ptpn22* knockout and knockin mice were healthy in spite of increased effector/memory T cell pool and enhanced B cell responsiveness, which failed to explain the increased disease susceptibility in humans. Moreover, so far it is controversial whether Lyp-620W is a gain- or loss-of-function variant (Vang et al., 2005; Rieck et al., 2007; Aarnisalo et al., 2008; Zhang et al., 2011). In this project, we investigated the role of *Ptpn22* in two autoimmune diseases using inducible RNAi: type 1 diabetes and colitis. The reason why we chose these two diseases is that the Lyp-620W allele modulates diabetes and colitis in antagonitic ways in humans: the 620W variant increases susceptibility to diabetes but protects from Crohn's disease (Bottini, et al., 2004; Smyth et al., 2004; Ladner et al., 2005; Onengut-Gumuscu et al., 2004; Diaz-Gallo et al., 2011). By using these two autoimmune disease models, we aimed to interpret the role of *Ptpn22* more precisely.

Ptpn22 silencing exacerbated colitis in a T cell transfer model

To investigate the role of Pep in colitis, $CD4^+CD45RB^{hi}$ cells were purified from 2 month Dox-treated WT, P2 and P4 mice. Briefly, $CD4^+$ T cells were first isolated from splenocytes using $CD4^+$ T cell isolation kit (Miltenyi). $CD4^+$ T cells were then incubated with biotinylated anti-$CD45RB^{hi}$, washed and separated using anti-biotin

microbeads. Purified $CD4^{+}CD45RB^{hi}$ cells were injected *i.v.* into NOD.*scid* mice. 6-7 weeks after transfer, the recipients were dissected to obtain the colon. Colon tissues were fixed, embedded in paraffin, cut and stained with Haematoxylin and Eosin solutions (H&E).

Haematoxylin specifically stains the chromatin and nuclear membrance within nucleus of the cells, Eosin stains cytoplasm, muscle fibers and collagen to define cell and tissue shapes. Under microscope, dark reddish orange colors identified red blood cells; ligher pastel pink determined collagen; and bright pink identified smooth muscle. By using H&E staining, we could score the inflammation and cell infiltrations in the colon (with kind help from Dr. Alma Zernecke). Our results showed that 6-7 weeks after transfer, $CD4^{+}CD45RB^{hi}$ cells could efficiently induce colitis in the NOD.*scid* mice. Compared to the recipients with WT cells, increased severity was seen in mice transferred with the P4 KD cells (Fig 3.43).

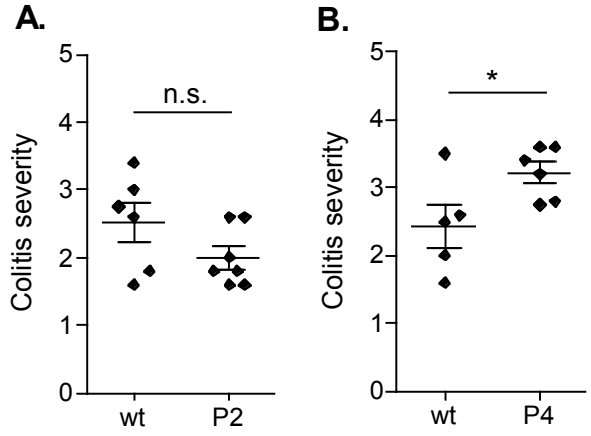

Fig 3.43 Inflammation severity in the colon of NOD.*scid* recipients. NOD.*scid* mice were transferred with Dox-treated WT, P2 and P4 $CD4^{+}CD45RB^{hi}$ cells. 6-7 weeks after transfer, colon tissues were obtained and scored by H&E staining.

Ptpn22 silencing protected P2 mice from diabetes

Ptpn22 silencing exacerbated colitis in the NOD.*scid* transfer model. We further explored the role of *Ptpn22* in autoimmune diabetes by two different approaches: spontaneous diabetes and CY induced diabetes. In the spontaneous diabetes test, WT, P2 and P4 mice were left untreated, or treated with Dox from 4 or 10 weeks old to determine the time window for Pep function. The results from P2/WT mice treated

with Dox from 4 weeks were not entirely reliable, due to observed effect on diabetes frequency in WT mice. This was absent in mice treated from 10 weeks. Only results from P2 groups treated from 10 weeks are shown. Compared to the untreated WT, P2, and Dox-treated WT, diabetes incidence was significantly decreased in the Dox-treated P2 mice (Fig 3.44A). However, this protection could only be observed in the Dox-treated P2, but not P4 KD mice from 10 weeks old (Fig 3.44B), and even in the P4 KD mice treated from an earlier time point of 4 weeks old (Fig 3.44C). The discrepancy between P2 and P4 KD mice will be discussed later.

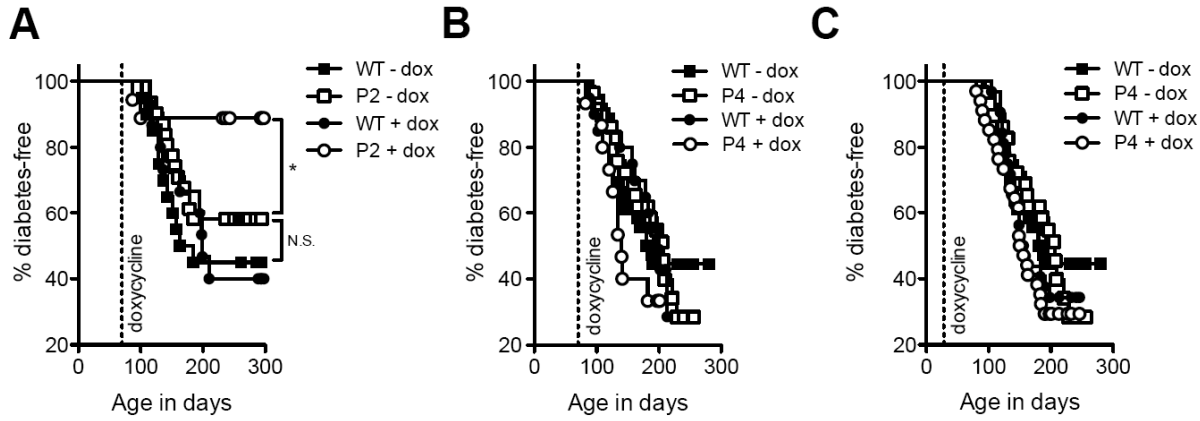

Fig 3.44 Spontaneous diabetes test. WT, P2 and P4 mice were left untreated, or treated with Dox from 10 weeks of age (A, B) or 4 weeks old (C). *A*: WT-dox n=20 ; P2-dox n=31 ; WT+dox n=15; P2+dox n=18; *B*: WT-dox n=36 ; P4-dox n=29 ; WT+dox n=20 ; P4+dox n=15; *C*: WT-dox n=36 ; P4-dox n=29 ; WT+dox n=32; P4+dox n=34; Log-rank test for *A*: WT-dox vs. P2-dox P=0.26 ; WT+dox vs. P2+dox P=0.006; P2-dox vs. P2+dox P=0.0418. Mice were tested diabetes from 3 months of age once a week until they became diabetic or reached 7 months of age (*: $P<0.05$)

Given the significant role played by Treg cells in immune tolerance, it was likely that the diabetes protection in P2 KD mice was due to the increased numbers of Treg cells. Cyclophosphamide (CY) can induce diabetes by reducing Treg cells. The idea was *Ptpn22* silencing increased Treg cells in the KD mice. After CY treatment, more Treg cells would remain in the KD mice, and thereby protect from or delay diabetes. Since we only saw the diabetes protection in the P2 KD mice, WT and P2 mice were treated with Dox for at least 1 month, and then injected *i.p.* with 200μg CY/g body weight. Consistent with the spontaneous diabetes result, P2 KD mice were protected from CY induced diabetes (Fig 3.45).

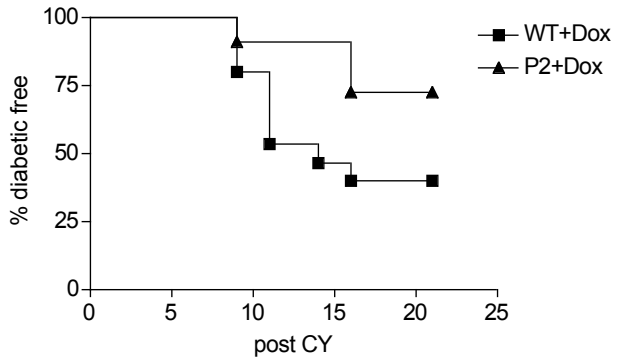

Fig 3.45 Cyclophosphamide induced diabetes in the 1month Dox-treated WT and P2 mice. Mice were tested for diabetes every two days with Diastix (Bayer). WT+dox n=15; P2+dox n=11.

CHAPTER 4
DISCUSSION

Autoimmune diseases are characterized by the dysfunction of the immune system – the failure of the immune system to remain tolerant to self-antigen and its subsequently aberrantly attack of self-tissues or -organs. There are a multitude of autoimmune diseases, including type 1 diabetes, rheumatoid arthritis (RA), juvenile idiopathic arthritis (JIA), systemic lupus erythematosus (SLE), Graves' disease, generalized vitiligo and Hashimoto's thyroiditis. Type 1 diabetes is characterized by the infiltration of immnue cells into the pancreas and by the permanent destruction of insulin producing β cells. Unlike for many other autoimmune diseases, men and women are almost equally susceptible to type 1 diabetes. The mean age of disease onset is 12 years old. Although multiple factors, including diet, commensal bacterial and viral infection, can influence the susceptibility to type 1 diabetes, the disease predisposition in children is mainly imparted by genetics.

To identify the genetic variations linked to the disease susceptibility, genome-wide association studies (GWAS) have been carried out. GWAS provides a powerful tool to dramatically accelerate the discovery of new risk genetic factors in type 1 diabetes. So far, more than fifty single-nucleotide polymorphisms (SNPs) have been identified according to the growing database (www.t1dbase.org). Among these 50 loci, the gene *PTPN22* ranks first in the non-HLA genetics risk factors. The disease susceptibility of *PTPN22* is imparted by the SNP (C1858T), which causes a substitution from arginine to tryptophan at the 620 position (Lyp-620R to Lyp-620W). Besides type 1 diabetes, the disease associated variant Lyp-620W is a strong risk factor in many other autoimmune diseases, including rheumatoid arthritis (RA) (Orozco et al., 2005; van Oene et al., 2005; Wesoly et al., 2005), juvenile idiopathic arthritis (JIA) (Hinks et al., 2005), systemic lupus erythematosus (SLE) (Kyogoku et al., 2004), Wegener's granulomatosis (Jagiello et al., 2005), Graves' disease (Velaga et al., 2004) and generalized vitiligo (Canton et al., 2005). Very interestingly, Lyp-620W is a protective allele in Crohn's disease, however, the mechanism of this protection is unknown (Frank et al., 2011; Rivas et al., 2011; Diaz-Gallo et al., 2011).

Although nearly 50 risk factors have been identified, little is known about how most of these genetic variants accelerate or exacerbate type 1 diabetes. In this project, we chose to study the role of *PTPN22* in type 1 diabetes, because of its broad association with multiple autoimmune diseases. Substantial efforts have been made to clarify how

the disease susceptible variant contributes to the pathogenesis of autoimmune diseases. The first study in 2004 found that Lyp-620W disrupted the interaction between Lyp and CSK (Bottini, et al., 2004). Subsequent studies demonstrated that T cells, as well as B cells from peripheral blood of subjects heterozygous at *PTPN22*, are less responsive, illustrated by the reduced phosphorylation in the TCR/BCR signaling compenents, reduced IL-2 production, impaired calcium flux and proliferation deficit in response to stimulation (Vang et al., 2005; Rieck et al., 2007; Aarnisalo et al., 2008; Habib et al., 2012). When two Lyp variants were transfected into Jurkat T cells, Lyp-620W showed decreased NF-AT/AP-1 activity (Vang et al., 2005). Notably, an inhibitor against Lyp could recover TCR/BCR deficit as found in heterozygous subjects. These data strongly support the notion that Lyp-620W is a gain-of function variant. Recently, a notable study indicated that Lyp-620W might instead be a loss-of-function variant. In support of this hypothesis, Pep-619W (the mouse homolog of human Lyp-620W) knockin mice resemble the KO phenotype, possibly due to the accelerated Lyp protein degradation (Zhang et al., 2011). Zikherman and colleagues also found enhanced Erk phosphorylation when Lyp-620W was introduced into Jurkat T cells (Zikherman., 2009). So far, whether Ptpn22 R620W is a gain- or loss-of-function mutation is still controversial. To address this issue, we generated two transgenic NOD mouse lines (P2 and P4) in which *Ptpn22* can be inducibly silenced.

PTPN22 encodes a negative regulator of TCR/BCR signaling. Loss of *Ptpn22* boosts effector/memory T cells and serum antibody levels, especially in older mice (Hasegawa et al., 2004). Despite being predisposed to autoimmunity, KO mice are healthy and even protected from EAE, which may be due to increased Treg cell numbers in the thymus and periphery (Maine et al., 2012). Similarly, we observed an increase of Treg cells in the lymph nodes and spleens of KD mice. Contrary to the findings in KO mice, the elevated thymic Treg cells could not be observed in either adult KD mice or KD mice treated from birth. Notably, complete loss of *Ptpn22* causes a more substantial increase of Treg cells than *Ptpn22* KD. These differences could be due to the partial loss of *Ptpn22* in our inducible KD mice and additive effect of greater thymic output in the KO mice. Nevertheless, the increase of Treg cells in the peripheral organs of KD mice demonstrates that *Ptpn22* participates in the regulation of peripheral homeostasis of Treg cells.

Most Treg cells are derived from the thymus ($Foxp3^+Helios^+$). In the periphery, naïve CD4 T cells can convert into Treg cells (iTreg) under some circumstances. Since we did not observe elevated output of thymic Treg cells, we focused on whether *Ptpn22* silencing could specifically increase iTreg cell numbers in the periphery. Interestingly, we found that *Ptpn22* silencing did not increase naïve T cell conversion into iTreg cells, as illustrated by comparable numbers of iTreg cells ($Helios^-$) *in vivo*, comparable iTreg cell conversion by TGF-β *in vitro*, and no change in homeostatically converted iTreg cells ($CD103^+Klrg1^+$). Although recent studies reported that some iTreg cells also express Helios, the frequency of Helios negative Treg cells remains almost the same, indicating nTreg and iTreg cells are equally increased (Gottschalk et al., 2012). The increase of Treg cells in KD mice might not be due to the elevated proliferative capacity. First, *in vitro* we did not observe the enhanced proliferation either during 3-day or 10-day expansion. Second, *in vivo* the proportion of dividing Treg cells ($Ki\text{-}67^+$) was comparable after *Ptpn22* silencing. We think the increase of Treg cells might be due to the enhanced responsiveness to IL-2. Grinberg-Bleyer and colleagues reported that a low dose of IL-2 administration reverses diabetes by specifically increasing Treg cells (Grinberg-Bleyer et al., 2010). We found that IL-2 production by P2 KD effector T cells is slightly increased, which could constitute a source of IL-2 for Treg cells in KD mice. In addition, *Ptpn22* silencing could enhance homeostatic TCR signaling and decreases the requirement of Treg cell for IL-2, which then slowly accelerates the turnover of Treg cells and increase Treg cell numbers (Josefowicz et al., 2012).

We think the disease resistance in P2 KD mice is imparted, at least partially, by the increased frequency of Treg cells. In support of this notion, P2 KD mice are still protected from diabetes after Cyclophosphamide (CY) administration. CY induces diabetes by depleting Treg cells. After CY depletion, more Treg cells remained in P2 KD mice, imparting disease protection. This suggests a link between the increased number of Treg cells and the observed protection from autoimmune diabetes, similar to the protection from EAE observed in the KO mice.

Some discrepancies can be observed between KO and KD mice. Unlike its effect on Treg cells, *Ptpn22* silencing did not affect the expansion of effector T cells in adult KD mice. We observed similar effector/memory T cell pools in adult WT and KD

mice treated for up to 8 months Dox. In support of this observation, we found *Ptpn22* KD effector and naïve CD4 T cells proliferate normally *in vitro*, with similar frequencies of dividing (Ki-67^{+}) cells *in vivo*. Our findings in *Ptpn22* KD mice are distinct from those in KO and knockin mice, in which enhanced effector T cell expansion was observed both *in vitro* and *in vivo*. This difference could be due to the incomplete loss of *Ptpn22*, but more likely, due to the unaltered thymocyte development in our KD adult mice. In this project, *Ptpn22* was silenced from 5-7 weeks of age, when most thymocytes have already matured (Scollay et al., 1980). In support of this hypothesis, *Ptpn22* silencing from birth significantly boosts effector/memory T cells after 2 months of treatment, resembling the effector T cell phenotype found in KO and knockin mice. Indeed, *Ptpn22* is involved in the thymus selection and loss of *Ptpn22* enhances positive selection, but does not alter negative selection (Hasegawa et al., 2004). Our data suggest that Pep modulates effector T cell generation and expansion mainly at the level of thymic development. Future experiments with TCR transgenic mice on the NOD background will help explore if *Ptpn22* silencing can alter positive and negative selections in the NOD mice. Alternative approaches will also be applied to examine if TCR repertoire is changed after *Ptpn22* silencing. For example, we can use FACS staining to investigate the TCR beta chain utilization, or compare the proliferative capacity of thymocytes from WT/KD mice treated from birth.

Although the effector/memory T cell pool is retained in adult KD mice, we found that *Ptpn22* silencing indeed increases homeostatic TCR signaling in effector T cells. *In vivo* anti-CD3 stimulation strongly induced effector T cell generation in KD mice pretreated for 10 days. The enhanced effector T cell generation depended on TCR stimulus, as it was not seen in the setting of lymphopoenia-induced expansion when lymph node cells were transferred into NOD.*scid* mice. It seems that *Ptpn22* silencing elevates homeostatic signals in both effector and Treg cells. But in adult KD mice, effector T cells fail to expand possibly due to the increased Treg cell numbers. To test this hypothesis in future, the effector/memory T cell pool will be investigated in Treg depleted mice (by administrating CD25 depletion antibody).

Interestingly, our data provide the first evidence for a role of *Ptpn22* in chemokine receptor expression. Some chemokine receptors, like CCR4 and CXCR3, are

selectively upregulated on KD Treg cells, but not on KD effector T cells. Chemokines and chemokine receptors play crucial roles in cell trafficking, lymph cell homing and even in autoimmune diseases. They also play essential roles in the pathogenesis of type 1 diabetes, considering T cells normally reside in pancreatic lymph node, not directly in the pancreatic islets. We propose that the elevated CCR4 and CXCR3 expression on P2 KD Treg cells facilitates their migration into the pancreas. We have preliminary data analyzing the frequency of Treg cells in the pancreas, though further repeats are required to consolidate it. Another interesting question is how *Ptpn22* silencing specifically enhances CCR4 and CXCR3 expression on Treg cells. Is it due to the enhanced chemokine production by antigen presenting cells or is it a cell intrinsic effect? In this project, we examined CCR4, CCR5 and CXCR3 expression, as these three have been reported to be involved in the modulation of type 1 diabetes. In future work, it may be of interest to comprehensively examine the expression of many other chemokine receptors to give an overall picture of how *Ptpn22* silencing affects chemokine receptor expression.

Besides T cells, *Ptpn22* silencing enhanced B cell activation, proliferation and PLC-γ2 phosphorylation in response to anti-IgM F(ab)'2 or anti-CD40. Strikingly, enhanced apoptosis could be found in KD B cells in response to stimulus, which is consistent with findings of reduced apoptosis observed in human B cells carrying the disease-allele, supporting the idea that Lyp-620W is a gain-of-function variant (Habib et al., 2012). B cells play important roles in diabetes. Depletion of B cells either by genetic approach or antibody mediated depletion, protects mice from diabetes (Serreze et al., 1996. Hu et al., 2007). Although the B cell proportions are normal in the lymph nodes and spleens of KD mice, KD B cells may survive less in the pancreas where they are stimulated similar to anti-IgM F(ab)'2 or anti-CD40 stimulus. Notably, a stronger phenotype can be found in P2 KD compared to P4 KD B cells, as KD efficiency is higher in P2 mice. Interestingly, the lack of diabetes resistance in P4 KD mice may correlate with a lesser dysfunction of B cells. Further work is required to determine the association between B cell apoptosis and diabetes protection, and to further clarify the relative contributions of increased number of Treg cells and enhanced B cell apoptosis to diabetes resistance.

Unlike the upregulated CD40 expression on dendritic cells (DC) in Lyp-619W

knockin mice, the expression of costimulatory and inhibitory signals on antigen presenting cells (B cells, DC and macrophages) were not altered in KD mice. Similarly, we did not find increased frequencies of germinal centers and the dysregulation of follicular T cells, as illustrated by the normal Peanut agglutinin (PNA) positive B cells as well as CXCR5 positive T cells. Right now, we cannot explain the failure to replicate these phenotypes. The differences between KI and KD mice could be accounted for by the different genetic background of the mice used, or by the differences in *Ptpn22* levels. Interestingly, although the proportions of B cell subsets are normal in the bone marrow and the peritoneal cavity, more follicular (FO) B cells and less marginal zone (MZ) B cells can be found in the spleens of long-term treated P2 mice. Non-circulating MZ B cells are distributed in the marginal zone of the spleen, constituting the first line of defense to trap antigens. FO B cells reside in follicles of B cell zone in the white pulp of the spleen, are involved in T-B cell interaction and in memory B cell generation. So far, we do not know if the imbalance between MZ and FO splenic B cells is related to disease protection. Further work is required to clarify this issue.

So far, whether Lyp R620W is a gain- or loss-of-function mutation is still controversial. To resolve this issue, we applied inducible RNAi to study the role of *Ptpn22* in type 1 diabetes and in colitis that are reversely modulated by *Ptpn22*. The rational was that if Lyp-620W is a gain-of-function variant, *Ptpn22* silencing should prevent or delay diabetes and exacerbate colitis; if the opposite is true, *Ptpn22* silencing should accelerate diabetes and reduce the severity of colitis. We found reduced diabetes incidence in the P2 KD mice, but this protection could not be seen in the P4 KD mice. This discrepancy could be due to the higher KD efficiency observed in the P2 mice, resulting in subsequently enhanced B cell apoptosis and more chemokine receptors on Treg cells in the P2 KD mice. Our observation that *Ptpn22* silencing does not increase diabetes risk in either transgenic line strongly supports the notion that Lyp-620W is a gain-of-function variant. Moreover, investigators at Cambridge University and at the Benaroya Research Institute in Seattle found that the accelerated Lyp protein degradation reported by Siminovitch and colleagues is possibly due to the failure of the antibody used in these experiments to recognize the Lyp-620W variant. Thus, our data support and further confirm that the disease associated variant Lyp-620W is a gain-of-function allele.

In humans, Lyp-620W is a pathogenic allele in diabetes but a protective variant in Crohn's disease. Since P2 KD mice are protected from diabetes, we further tested the effect of *Ptpn22* silencing on colitis using an adoptive transfer model. NOD.*scid* mice were injected with purified Dox-treated WT, P2 or P4 $CD4^{+}CD45RB^{hi}$ cells to induce colitis. Interestingly, elevated disease severity could be observed only in the recipients transferred with P4, but not P2 KD $CD4^{+}CD45RB^{hi}$ cells. These results will need further confirmation. Of note, colitis was induced with $CD4^{+}CD45RB^{hi}$ cells alone. Further experiments will be required to examine the role of *Ptpn22* in colitis under more complex conditions. For example, colitis could be induced with $CD4^{+}CD45RB^{hi}$ in the presence of Treg cells, or using an alternative model, the Dextran Sodium Sulfate (DSS) colitis model.

Although there are some limitations to lentivirus mediated RNAi, such as possible off-target effects and insertional effects of the transgene (where for example lentiviral integration could disrupt endogenous gene expression), we believe the phenotypes we observed in KD mice was specifically due to *Ptpn22* silencing. First, we generated two transgenic mouse lines bearing different shRNA sequences to control off-target effects. In almost all the cases, we found similar results in P2 and P4 KD mice. Due to the higher KD efficiency in the P2 mice, stronger phenotype can be found in P2 KD mice, such as the more substantial hyperreactivity of P2 KD B cells in response to stimulus. We also believe that Dox itself doesn't have a big impact on mice, as there are no differences between WT and Dox-treated WT mice. Second, our inducible KD system provides a good control for the insertional effects. In all cases, no difference was observed between untreated P2/P4 and WT mice. Third, our findings in inducible KD mice replicate several phenotypes in B6 KO mice, including splenomegaly and the increase of Treg cell numbers. KO mice are predisposed to autoimmunity, imparted by the expanded effector T cell population and elevated serum antibodies. Interestingly, KO mice are healthy and even protected from EAE compared to the WT B6 mice (Maine et al., 2012). Similarly, strong *Ptpn22* silencing in P2 mice protects from autoimmune diabetes.

Treg cells play a pivotal role in immune tolerance. On one hand, loss of Treg cells accelerates or exacerbates T1D (Salomon et al., 2000; Mellanby et al., 2007). On the

other hand, a boost in Treg cells provides a potential therapy for autoimmune patients. In the mouse, several approaches have been reported to increase Treg cells to prevent or cure type 1 diabetes, for example a lose dose of IL-2 administration, or overexpression of TGF-β under control of the insulin promoter (Peng et al., 2004; Grinberg-Bleyer et al., 2010). In humans, since the frequency of Treg cells in peripheral blood is quite low (1-5% in $CD4^+$ cells), Treg cells can be isolated, expanded *ex vivo* and then infused back into autoimmune patients, which is time-consuming and costly. Here, we show that Lyp can be a valuable target for the treatment of autoimmunity. *Ptpn22* inhibition in adult NOD mice specifically increases Treg cell numbers, without altering naïve and effector T cell cells. Our findings that once Treg cell number is increased, *Ptpn22* inhibition is not required to maintain this increase at least for 2 months make it more appealing. Meanwhile, more GITR is expressed on Treg cells to maintain its suppressive function. This specific effect on Treg cells suggests that *Ptpn22* inhibition (using a small molecule inhibitor) could be a valuable approach to increase Treg cells with limited adverse effects. Since several inhibitors against Lyp have been developed, it will be worth testing the disease protective effect of these inhibitors *in vivo*. Alternatively, these inhibitors may be used in the Treg cell expansion *ex vivo*, considering *Ptpn22* inhibition enhances homeostatic TCR signaling which can facilitate Treg cell expansion.

In sum, we generated two inducible KD mouse lines: P2 and P4. The inducible KD NOD mice replicated many of the phenotypes described for KO and knockin mice, including splenomegaly, hyperreactivity of B cells and increased Treg cell numbers. Of note, our findings of diabetes resistance in P2 KD mice, hyperreactivity and enhanced apoptosis of B cells are in agreement with the proposal that Lyp-620W is a gain-of-function variant. Thus, Lyp could be a valuable target for the treatment of autoimmune diseases.

CHAPTER 5
REFERENCES

Aarnisalo J, Treszl A, Svec P, Marttila J, Oling V, Simell O, et al. Reduced $CD4^+$T cell activation in children with type 1 diabetes carrying the PTPN22/Lyp 620Trp variant. *J Autoimmun* (2008). 31:13–21.

Acha-Orbea H, McDevitt HO. The first external domain of the nonobese diabetic mouse class II I-A beta chain is unique. *Proc Natl Acad Sci USA* (1987). 84:2435–2439.

Akimova T, Beier UH, Wang L, Levine MH, Hancock WW. Helios expression is a marker of T cell activation and proliferation. *PLoS One* (2011). 6(8):e24226.

Alard P, Manirarora JN, Parnell SA, Hunkins JL, Clark SL, Kosiewicz MM. Deficiency in NOD Antigen-Presenting Cell Function May Be Responsible for Suboptimal $CD4^+CD25^+$ T-Cell–Mediated Regulation and Type 1 Diabetes Development in NOD Mice. *Diabetes* (2006). 55:2098-2105.

Alegre ML, Frauwirth KA, Thompson CB. T cell regulation by CD28 and CTLA-4. *Nat Rev Immunol* (2001). 1(3):220-228.

Amur S, Parekh A, Mummaneni P. Sex differences and genomics in autoimmune diseases. *J Autoimmun* (2012). 38(2-3):J254-65.

Anderson MS, Bluestone JA. THE NOD MOUSE: A model of immune dysregulation. *Annu Rev Immunol* (2005). 23:447–485.

Arechiga AF, Habib T, He Y, Zhang X, Zhang ZY, Funk A, Buckner JH. The PTPN22 Allelic Variant Associated with Autoimmunity Impairs B Cell Signaling. *J Immunol* (2009). 182: 3343-3347.

Asano M, Toda M, Sakaguchi N, Sakaguchi S. Autoimmune disease as a consequence of developmental abnormality of a T cell subpopulation. *J Exp Med* (1996). 184:387–396.

Atkinson MA, Wilson SB. Fatal attraction: chemokines and type 1 diabetes. *J Clin*

Invest (2002). 110:1611–1613.

Azzam HS, Grinberg A, Lui K, Shen H, Shores EW, Love PE. CD5 expression is developmentally regulated by T cell receptor (TCR) signals and TCR avidity. *J Exp Med* (1998). 188(12):2301-2311.

Bach JF. Insulin-dependent diabetes mellitus as an autoimmune disease. *Endocr Rev* (1994). 15:516–542.

Bach JF. The effect of infections on susceptibility to autoimmune and allergic diseases. *N Engl J Med* (2002). 347: 911–920.

Baekkeskov S, Warnock G, Christie M, Rojotte RV, Larsen PM, Fey S. Revelation of specificity of 64K autoantibodies in IDDM serums by high-resolution 2-D gel electrophoresis. Unambiguous identification of 64K target antigen. *Diabetes* (1989). 38:1133-1341.

Barrett JC, Clayton DG, Concannon P, Akolkar B, Cooper JD, Erlich HA, Julier C, Morahan G, Nerup J, Nierras C, Plagnol V, Pociot F, Schuilenburg H, Smyth DJ, Stevens H, Todd JA, Walker NM, Rich SS, The Type 1 Diabetes Genetics Consortium. Genome-wide association study and meta-analysis find that over 40 loci affect risk of type 1 diabetes. *Nat Genet* (2009). 41: 703 – 707.

Becker KG, Simon RM, Bailey-Wilson JE, Freidlin B, Biddison WE, McFarland HF, Trent JM. Clustering of non-major histocompatibility complex susceptibility candidate loci in human autoimmune diseases. *Proc Natl Acad Sci USA* (1998). 95:9979–9984.

Beeson PB. Age and sex associations of 40 autoimmune diseases. *Am J Med* (1994). 96:457-462.

Begovich AB, Carlton VE, Honigberg LA, Schrodi SJ, Chokkalingam AP, Alexander HC, et al. A missense single-nucleotide polymorphism in a gene encoding a protein tyrosine phosphatase (PTPN22) is associated with rheumatoid arthritis. *Am J Hum*

Genet (2004). 75:330–337.

Bell GI, Horita S, Karam JH. A polymorphic locus near the human insulin gene is associated with insulin-dependent diabetes mellitus. *Diabetes* (1984). 33:176–183.

Bell GI, Selby MJ, Rutter WJ. The highly polymorphic region near the human insulin gene is composed of simple tandemly repeating sequences. *Nature* (1982). 295: 31-35.

Bennett ST, Lucassen AM, Gough SCL, Powell EE, Undlien DE, Pritchard LE, Merriman ME, Kawaguchi Y, Dronsfield MJ, Poclot F, Nerup J, Bouzekri N, Cambon-Thomsen A, Rønningen KS, Barnett AH, Bain SC, Todd JA. Susceptibility to human type 1 diabetes at *IDDM2* is determined by tandem repeat variation at the insulin gene minisatellite locus. *Nat Genet* (1995). 9: 284-292.

Boitard C, Yasunami R, Dardenne M, Bach JF. T cell-mediated inhibition of the transfer of autoimmune diabetes in NOD mice. *J Exp Med* (1989). 169:1669–1680.

Bottini N, Musumeci L, Alonso A, Rahmouni S, Nika K, Rostamkhani M, MacMurray J, Meloni GF, Lucarelli P, Pellecchia M, Eisenbarth GS, Comings D, Mustelin T. A functional variant of lymphoid tyrosine phosphatase is associated with type I diabetes. *Nat Genet* (2004). 36:337–338.

Brdicka T, Pavlistova D, Leo A, Bruyns E, Korinek V, Angelisova P, et al. Phosphoprotein associated with glycosphingolipid-enriched microdomains (PAG), a novel ubiquitously expressed transmembrane adaptor protein, binds the protein tyrosine kinase csk and is involved in regulation of T cell activation. *J Exp Med* (2000). 191:1591–1604.

Burn GL, Svensson L, Sanchez-Blanco C, Saini M, Cope AP. Why is PTPN22 a good candidate susceptibility gene for autoimmune disease? *FEBS Lett* (2011). 585:3689-3698.

Cameron MJ, Arreaza GA, Grattan M, Meagher C, Sharif S, Burdick MD, Strieter RM, Cook DN, Delovitch TL. Differential Expression of CC Chemokines and the

CCR5 Receptor in the Pancreas Is Associated with Progression to Type I Diabetes. *J Immunol* (2000). 165:1102-1110.

Canton I, Akhtar S, Gavalas NG, Gawkrodger DJ, Blomhoff A, Watson Carvalho-Pinto C, García MI, Gómez L, Ballesteros A, Zaballos A, Flores JM, Mellado M, Rodríguez-Frade JM, Balomenos D, Martínez-AC. Leukocyte attraction through the CCR5 receptor controls progress from insulitis to diabetes in non-obese diabetic mice. *Eur J Immunol* (2004). 34:548-557.

Carvalho-Pinto C, García MI, Gómez L, Ballesteros A, Zaballos A, Flores JM, Mellado M, Rodríguez-Frade JM, Balomenos D, Martínez-AC. Leukocyte attraction through the CCR5 receptor controls progress from insulitis to diabetes in non-obese diabetic mice. *Eur J Immunol* (2004). 34:548-557.

Caton AJ, C Cozzo, Larkin J III, Lerman MA, Boesteanu A, Jordan MS. $CD4^{+}CD25^{+}$ regulatory T cell selection. *Ann NY Acad Sci* (2004). 1029: 101–114.

Cantón I, Akhtar S, Gavalas NG, Gawkrodger DJ, Blomhoff A, Watson PF, Weetman AP, Kemp EH. A single-nucleotide polymorphism in the gene encoding lymphoid protein tyrosine phosphatase(PTPN22) confers susceptibility to generalised vitiligo. *Genes Immun* (2005). 6(7):584-7.

Cedebom L, Hall H, Ivars F. CD4+CD25+ regulatory T cells down-regulate co-stimulatory molecules on antigen-presenting cells. *Eur J Immunol* (2000). 30:1538-1543.

Chapman SJ, Khor CC, Vannberg FO, Maskell NA, Davies CWH, Hedley EL et al. PTPN22 and invasive bacterial disease. *Nat Genet* (2006). 38:499-500.

Charlton B, Zhang MD, Slattery RM. B lymphocytes not required for progression from insulitis to diabetes in non-obese diabetic mice. *Immunol Cell Biol* (2001). 79:597-601.

Chen W, Jin W, Hardegen N, Lei KJ, Li L, Marinos N, McGrady G, Wahl SM. Conversion of peripheral CD4+CD25- naive T cells to CD4+CD25+ regulatory T cells by TGF-beta induction of transcription factor Foxp3. *J Exp Med* (2003). 198(12):1875-86.

Chung Y, Tanaka S, Chu F, Nurieva RI, Martinez GJ, Rawal S, Wang YH, Lim H, Reynolds JM, Zhou XH, Fan HM, Liu ZM, Neelapu SS, Dong C. Follicular regulatory T cells expressing Foxp3 and Bcl-6 suppress germinal center reactions. *Nat Med* (2011) 17(8):975-982.

Cloutier J, Veillette A. Association of inhibitory tyrosine protein kinase $p50^{csk}$ with protein tyrosine phosphatase PEP in T cells and other hemopoietic cells. *EMBO J* (1996). 15:4909–4918.

Cloutier JF, Veillette A. Cooperative inhibition of T-cell antigen receptor signaling by a complex between a kinase and a phosphatase. *J Exp Med* (1999). 189:111-121.

Concannon P, Onengut-Gumuscu S, Todd JA, Smyth DJ, Pociot F, Bergholdt R, Akolkar B, Erlich HA, Hilner JE, Julier C, Morahan G, Nerup J, Nierras CR, Chen WM, Rich SS; Type 1 DiabetesGenetics Consortium. A human type 1 diabetes Susceptibility locus maps to chromosome 21q22.3. *Diabetes* (2008). 57(10):2858-61.

Cooper JD, Smyth DJ, Smiles AM, Plagnol V, Walker NM, Allen JE, Downes K, Barrett JC, Healy BC, Mychaleckyj JC, Warram JH, Todd JA. Meta-analysis of genome-wide association study data identifies additional type 1 diabetes risk loci. *Nat Genet* (2008). 40:1399–1401.

Copeman JB, Cucca F, Hearne CM, Cornall RJ, Reed PW, Rønningen KS, Undlien DE, Nisticò L, Buzzetti R, Tosi R, et al. Linkage disequilibrium mapping of a type 1 diabetes susceptibility gene (IDDM7) to chromosome 2q31-q33. *Nat Genet* (1995). 9:80-85.

Curiel TJ, Coukos G, Zou L, Alvarez X, Cheng P, Mottram P, Evdemon-Hogan M, Conejo-Garcia JR, Zhang L, Burow M, Zhu Y, Wei S, Kryczek I, Daniel B, Gordon

A, Myers L, Lackner A, Disis ML, Knutson KL, Chen L, Zou W. Specific recruitment of regulatory T cells in ovarian carcinoma fosters immune privilege and predicts reduced survival. *Nat Med* (2004); 10: 942–9.

Curiel TJ, Coukos G, Zou L, Alvarez X, Cheng P, Mottram P, Evdemon-Hogan M, Conejo-Garcia JR, Zhang L, Burow M, Zhu Y, Wei S, Kryczek I, Daniel B, Gordon A, Myers L, Lackner A, Disis ML, Knutson KL, Chen L, Zou W. Specific recruitment of regulatory T cells in ovarian carcinoma fosters immune privilege and predicts reduced survival. *Nat Med* (2004); 10: 942–9.

D'Cruz, LM, Klein L. Development and function of agonist-induced CD25+Foxp3+ regulatory T cells in the absence of interleukin 2 signaling. *Nat Immunol* (2005). 6: 1152–1159.

D'Alise AM, Auyeung V, Feuerer M, Nishio J, Fontenot J, Benoist C, Mathis D. The defect in T-cell regulation in NOD mice is an effect on the T-cell effectors. *Proc Natl Acad Sci USA* (2008). 105:19857-19862.

Davidson D, Cloutier JF, Gregorieff A, Veillette A. Inhibitory tyrosine protein kinase $p50^{csk}$ is associated with protein-tyrosine phosphatase PTP-PEST in hemopoietic and non-hemopoietic cells. *J Biol Chem* (1997). 272:23455–23462.

Delovitch TL, Singh B. The nonobese diabetic mouse as a model of autoimmune diabetes: immune dysregulation gets the NOD. *Immunity* (1997). 7:727-738.

Diaz-Gallo LM, Espino-Paisán L, Fransen K, Gómez-García M, van Sommeren S, Cardeña C, Rodrigo L, Mendoza JL, Taxonera C, Nieto A, Alcain G, Cueto I, López-Nevot MA, Bottini N, Barclay ML, Crusius JB, van Bodegraven AA, Wijmenga C, Ponsioen CY, Gearry RB, Roberts RL, Weersma RK, Urcelay E, Merriman TR, Alizadeh BZ, Martin J. Differential association of two PTPN22 coding variants with Crohn's disease and ulcerative colitis. *Inflamm Bowel Dis* (2011). 17:2287-2294.

Fantini MC, Becker C, Monteleone G, Pallone F, Galle PR, Neurath MF. TGF-beta induces a regulatory phenotype in CD4+CD25- T cells through Foxp3 induction and

down-regulation of Smad7. *J Immunol* (2004). 172: 5149-5153.

Feuerer M, Hill JA, Kretschmer K, von Boehmer H, Mathis D, Benoist C. Genomic definition of multiple ex vivo regulatory T cell subphenotypes. *Proc Natl Acad Sci USA* (2010). 107:5919-24.

Feuerer M, Jiang W, Holler PD, Satpathy A, Campbell C, Bogue M, Mathis D, Benoist C. Enhanced thymic selection of FoxP3^{+} regulatory T cells in the NOD mouse model of autoimmune diabetes. *Proc Natl Acad Sci USA* (2007). 104:18181-18186.

Fiorillo E, Orrú V, Stanford SM, Liu Y, Salek M, Rapini N, Schenone AD, Saccucci P, Delogu LG, Angelini F, Manca Bitti ML, Schmedt C, Chan AC, Acuto O, Bottini N. Autoimmune-associated PTPN22 R620W variation reduces phosphorylation of lymphoid phosphatase on an inhibitory tyrosine residue. *J Biol Chem* (2010). 285:26506-26518.

Fitzpatrick F, Lepault F, Homo-Delarche F, Bach JF, Dardenne M. Influence of castration, alone or combined with thymectomy, on the development of diabetes in the nonobese diabetic mouse. *Endocrinology* (1991). 129:1382-1390.

Foulis AK, Farquharson MA, Meager A. Immunoreactive alpha-interferon in insulin-secreting beta cells in type 1 diabetes mellitus. *Lancet* (1987). 2: 1423–1427.

Fox HS. Androgen treatment prevents diabetes in nonobese diabetic mice. *J Exp Med* (1992). 175:1409-1412.

Franke A, McGovern DP, Barrett JC, Wang K, Radford-Smith GL, Ahmad T, Lees CW, Balschun T, Lee J, Roberts R, Anderson CA, Bis JC, Bumpstead S, Ellinghaus D, Festen EM, Georges M, Green T, Haritunians T, Jostins L, Latiano A, Mathew CG, Montgomery GW, Prescott NJ, Raychaudhuri S, Rotter JI, Schumm P, Sharma Y, Simms LA, Taylor KD, Whiteman D, Wijmenga C, Baldassano RN, Barclay M,

Bayless TM, Brand S, Büning C, Cohen A, Colombel JF, Cottone M, Stronati L, Denson T, De Vos M, D'Inca R, Dubinsky M, Edwards C, Florin T, Franchimont D, Gearry R, Glas J, Van Gossum A, Guthery SL, Halfvarson J, Verspaget HW, Hugot JP, Karban A, Laukens D, Lawrance I, Lemann M, Levine A, Libioulle C, Louis E, Mowat C, Newman W, Panés J, Phillips A, Proctor DD, Regueiro M, Russell R, Rutgeerts P, Sanderson J, Sans M, Seibold F, Steinhart AH, Stokkers PC, Torkvist L, Kullak-Ublick G, Wilson D, Walters T, Targan SR, Brant SR, Rioux JD, D'Amato M, Weersma RK, Kugathasan S, Griffiths AM, Mansfield JC, Vermeire S, Duerr RH, Silverberg MS, Satsangi J, Schreiber S, Cho JH, Annese V, Hakonarson H, Daly MJ, Parkes M. Genome-wide meta-analysis increases to 71 the number of confirmed Croh's diseasesusceptibility loci. *Nat Genet* (2010). 42(12):1118-25.

Frigerio S, Junt T, Lu B, Gerard C, Zumsteg U, Holländer GA, Piali L. β cells are responsible for CXCR3-mediated T-cell infiltration in insulitis. *Nat Med* (2002). 8:1414-1420.

Fung EY, Smyth DJ, Howson JM, Cooper JD, Walker NM, Stevens H, Wicker LS, Todd JA. Analysis of 17 autoimmune disease-associated variants in type 1 diabetes identifies 6q23/TNFAIP3 as a susceptibility locus. *Genes Immun* (2009). 10:188–191.

Garton AJ, Flint AJ, Tonks NK. Identification of $p130^{CflS}$ as a substrate for the cytosolic protein tyrosine phosphatase PTP-PEST. *Mol Cell Biol* (1996). 16:6408-6418.

Gerold KD, Zheng P, Rainbow DB, Zernecke A, Wicker LS, Kissler S. The soluble CTLA-4 splice variant protects from type 1 diabetes and potentiates regulatory T-cell function. *Diabetes* (2011). 60(7):1955-63.

Gjörloff-Wingren A, Saxena M, Williams S, Hammi D, Mustelin T. Characterization of TCR-induced receptor-proximal signaling events negatively regulated by the protein tyrosine phosphatase PEP. *Eur J Immunol* (1999). 29:3845-3854.

Gomez LM, Anaya JM, Martin J. Genetic influence of PTPN22 R620W

polymorphism in tuberculosis. *Human Immunology* (2005). 66:1242-1247.

Gottschalk RA, Corse E, Allison JP. Expression of Helios in peripherally induced Foxp3+ regulatory T cells. *J Immunol* (2012). 188:976-980.

Grewal IS, Rutledge BJ, Fiorillo JA, Gu L, Gladue RP, Flavell RA, Rollins BJ. Transgenic monocyte chemoattractant protein-1 (MCP-1) in pancreatic islets produces monocyte-rich insulitis without diabetes. *J Immunol* (1997). 159:401–408.

Grewal IS, Rutledge BJ, Fiorillo JA, Gu L, Gladue RP, Flavell RA, Rollins BJ. Transgenic monocyte chemoattractant protein-1 (MCP-1) in pancreatic islets produces monocyte-rich insulitis without diabetes. *J Immunol* (1997). 159:401–408.

Grinberg-Bleyer Y, Baeyens A, You S, Elhage R, Fourcade G, Gregoire S, Cagnard N, Carpentier W, Tang Q, Bluestone J, Chatenoud L, Klatzmann D, Salomon BL, Piaggio E. IL-2 reverses established type 1 diabetes in NOD mice by a local effect on pancreatic regulatory Tcells. *J Exp Med* (2010). 207:1871-1878.

Gupta S, Manicassamy S, Vasu C, Kumar A, Shang W, Sun Z. Differential requirement of PKC-theta in the development and function of natural regulatory T cells. *Mol Immunol* (2008). 46:213-214.

Habib T, Funk A, Rieck M, Brahmandam A, Dai X, Panigrahi AK, Luning Prak ET, Meyer-Bahlburg A, Sanda S, Greenbaum C, Rawlings DJ, Buckner JH. Altered B Cell Homeostasis Is Associated with Type I Diabetes and Carriers of the PTPN22 Allelic Variant. *J Immunol* (2012). 188:487-496.

Hakonarson H, Grant SFA, Bradfield JP, Marchand L, Kim CE, Glessner JT, Grabs R, Casalunovo T, Taback SP, Frackelton EC, Lawson ML, Robinson LJ, Skraban R, Lu Y, Chiavacci RM, Stanley CA, Kirsch SE, Rappaport EF, Orange JS, Monos DS, Devoto M, Qu HQ, Polychronakos C. A genome-wide association study identifies KIAA0350 as a type 1 diabetes gene. *Nature* (2007). 448: 591–594.

Hakonarson H, Qu HQ, Bradfield JP, Marchand L, Kim CE, Glessner JT, Grabs R, Casalunovo T, Taback SP, Frackelton EC, Eckert AW, Annaiah K, Lawson ML, Otieno FG, Santa E, Shaner JL, Smith RM, Onyiah CC, Skraban R, Chiavacci RM, Robinson LJ, Stanley CA, Kirsch SE, Devoto M, Monos DS, Grant SF, Polychronakos C. A novel susceptibility locus for type 1 diabetes on Chr12q13 identified by a genome-wide association study. *Diabetes* (2008). 57(4):1143-1146.

Haribhai D, Lin W, Edwards B, Ziegelbauer J, Salzman NH, Carlson MR, Li SH, Simpson PM, Chatila TA, Williams CB. A central role for induced regulatory T cells in tolerance induction in experimental colitis. *J Immunol* (2009). 182(6):3461-348.

Hasegawa K, Martin F, Huang G, Tumas D, Diehl L, Chan AC. PEST Domain-Enriched Tyrosine Phosphatase (PEP) Regulation of Effector/Memory T Cells. *Science* (2004). 303: 685-689.

Herold MJ, Brandt JVD, Seibler J, Reichardt HM. Inducible and reversible gene silencing by stable integration of an shRNA-encoding lentivirus in transgenic rats. *Proc Natl Acad Sci USA* (2008). 105:18507-18512.

Hinks A, Barton A, John S, Bruce I, Hawkins C, Griffiths CE, Donn R, Thomson W, Silman A, Worthington J. Association between the PTPN22 gene and rheumatoid arthritis and juvenile idiopathic arthritis in a UK population: Further support that PTPN22 is an autoimmunity gene. *Arthritis Rheum* (2005). 52:1694– 9.

Hu CY, Rodriguez-Pinto D, Du W, Ahuja A, Henegariu O, Wong FS, Shlomchik MJ, Wen L. Treatment with CD20-specific antibody prevents and reverses autoimmune diabetes in mice. *J Clin Invest* (2007). 117:3857-3867.

Hu Y, Nakagawa Y, Purushotham KR, Humphreys-Beher MG. Functional changes in salivary glands of autoimmune disease-prone NOD mice. *Am J Physiol Endocrinol Metab* (1992). 263:E607–614.

Huehn J, Siegmund K, Lehmann JC, Siewert C, Haubold U, Feuerer M, Debes GF, Lauber J, Frey O, Przybylski GK, Niesner U, de la Rosa M, Schmidt CA, Bräuer R, Buer J, Scheffold A, Hamann A. Developmental stage, phenotype, and migration distinguish naive- and effector/memory-like CD4+ regulatory T cells. J Exp Med (2004). 199(3):303-13.

Hutchings PR, Cooke A. The transfer of autoimmune diabetes in NOD mice can be inhibited or accelerated by distinct cell populations present in normal splenocytes taken from young males. *J Autoimmun* (1990). 3:175–185.

Ichikawa M, Koh CS, Inaba Y, Seki C, Inoue A, Itoh M, Ishihara Y, Bernard CC, Komiyama A. IgG subclass switching is associated with the severity of experimental autoimmune encephalomyelitis induced with myelin oligodendrocyte glycoprotein peptide in NOD mice. *Cell Immunol* (1999). 191:97–104.

Iellem A, Mariani M, Lang R, Recalde H, Panina-Bordignon P, SinigagliaF, D'Ambrosio D. Unique chemotactic response profile and specific expression of chemokine receptors CCR4 and CCR8 by CD4+CD25+ regulatory T cells. *J Exp Med* (2001). 194: 847–53.

Imai T, Nagira M, Takagi S, Kakizaki M, Nishimura M, Wang J, Gray PW, Matsushima K, Yoshie O. Selective recruitment of CCR4-bearing Th2 cells toward antigen-presenting cells by the CC chemokines thymus and activation-regulated chemokine and macrophage-derived chemokine. *Int Immunol* (1999). 11: 81–8.

Ishida T, Ishii T, Inagaki A, Yano H, Konmatsu H, Lida S, Inagaki H, Ueda R. Specific recruitment of CCR4-positive regulatory T cells in Hodgkin lymphoma fosters immune privilege. *Cancer Res* (2006). 66: 5716–22.

Ishida T, Ueda R. CCR4 as a novel molecular target for immunotherapy of cancer. *Cancer Sci* (2006). 97: 1139–46.

Jagiello P, Aries P, Arning L, Wagenleiter SEN, Csernok E, Hellmich B, Gross WL, Epplen JT. The *PTPN22* 620W allele is a risk factor for Wegener's granulomatosis.

Arthritis Rheum (2005). 52:4039– 4043.

Josefowicz SZ, Lu L-F, Rudensky AY. Regulatory T cells: mechanisms of differentiation and function. *Ann Rev Immunol* (2012). 30:531-564.

Jordan MS, Boesteanu A, Reed AJ, Petrone AL, Holenbeck AE, Lerman MA, Naji A, Caton AJ. Thymic selection of $CD4^+CD25^+$ regulatory T cells induced by an agonist self-peptide. *Nat Immunol* (2001). 2: 301–306.

Julier C, Hyer RN, Davies J *et al*. Insulin-IGF2 region on chromosome 11p encodes a gene implicated in HLA-DR4-dependent diabetes susceptibility. *Nature* (1991). 354: 155-159.

Julier C, Lucassen A, Villedieu P, Delepine M, Levy-Marchal C, Danzé PM, Bianchi F, Boitard C, Froguel P, Bell J, Lathrop GM. Multiple DNA variant association analysis: application to the insulin gene region in type 1 diabetes. *Am J Hum Genet* (1994). 55: 1247-1254.

Kanagawa O, Martin SM, Vaupel BA, Carrasco-Marin E, Unanue ER. Autoreactivity of T cells from nonobese diabetic mice: an I-Ag7-dependent reaction. *Proc Natl Acad Sci USA* (1998). 95:1721–1724.

Kanazawa Y, Komeda K, Sato S, Mori S, Akanuma K, Takaku F. Non-obesediabetic mice: immune mechanisms of pancreatic beta-cell destruction. *Diabetologia* (1984). 27 Suppl:113-115.

Karjalainen J, Martin JM, Knip M, Ilonen J, Robinson BH. A bovine albumin peptide as a possible trigger of insulin-dependent diabetes mellitus. *N Engl J Med* (1992). 327:302–307.

Katz J, Benoist C, Mathis D. Major histocompatibility complex class I molecules are required for the development of insulitis in non-obese diabetic mice. *Eur J Immunol* (1993). 23:3358-3360.

Kaufman DL, Erlander MG, Clare-Salzler M, Atkinson MA, Maclaren NK, Tobin AJ. Autoimmunity to two forms of glutamate decarboxylase in insulin-dependent diabetes mellitus. *J Clin Invest* (1992). 89: 283–292.

Kawabuchi M, Satomi Y, Takao T, Shimonishi Y, Nada S, Nagai K, et al. Transmembrane phosphoprotein Cbp regulates the activities of Src-family tyrosine kinases. *Nature* (2000). 404:999–1003.

Kennedy GC, German MS, Rutter WJ. The minisatellite in the diabetes susceptibility locus *IDDM2* regulates insulin transcription. *Nat Genet* (1995). 9: 293-298.

Kikutani H, Makino S. The murine autoimmune diabetes model: NOD and related strains. *Adv Immunol* (1992). 51:285–322.

Kim DH, Rossi JJ. Strategies for silencing human disease using RNA interference. *Nat Rev Genet* (2007). 8: 173-184.

Kim S, Wairkar YP, Daniels RW, DiAntonio A. The novel endosomal membrane protein Ema interacts with the class C Vps-HOPS complex to promote endosomal maturation. *J Cell Biol* (2010). 188:717-734.

Kim SH, Cleary MM, Fox HS, Chantry D, Sarvetnick N. CCR4-bearing T cells participate in autoimmune diabetes. *J Clin Invest* (2002). 110:1675-1686.

Kishimoto H, Sprent J. A defect in central tolerance in NOD mice. *Nat Immunol* (2001). 2:1025–1031.

Kissler S, Stern P, Takahashi K, Hunter K, Peterson LB, Wicker LS. In vivo RNA interference demonstrates a role for Nramp1 in modifying susceptibility to type 1 diabetes. *Nat Genet* (2006). 38:479-483.

Klemetti P, Savilahti E, Ilonen J, Akerblom HK, Vaarala O. T-cell reactivity to wheat gluten in patients with insulin-dependent diabetes mellitus. *Scand J Immunol* (1998). 47:48–53.

Kouki T, Gardine CA, Yanagawa T, Degroot LJ. Relation of three polymorphisms of the CTLA-4 gene in patients with Graves' disease. *J Endocrinol Invest* (2002). 25:208-213.

Kretschmer K, Apostolou I, Hawiger D, Khazaie K, Nussenzweig MC, von Boehmer H. Inducing and expanding regulatory T cell populations by foreign antigen. *Nat Immunol* (2005). 6:1219-27.

Kyogoku C, Langefeld CD, Ortmann WA, Lee A, Selby S, Carlton VE, Chang M, Ramos P, Baechler EC, Batliwalla FM, Novitzke J, Williams AH, Gillett C, Rodine P, Graham RR, Ardlie KG, Gaffney PM, Moser KL, Petri M, Begovich AB, Gregersen PK, Behrens TW. Genetic association of the R620W polymorphism of protein tyrosine phosphatase PTPN22 with human SLE. *Am J Hum Genet* (2004). 75:504-507.

Ladner MB, Bottini N, Valdes AM, Noble JA. Association of the single necleotide polymorphism C1858T of the PTPN22 gene with type 1 diabetes. *Hum Immunol* (2005). 66(1):60-4.

Lan MS, Wasserfall C, Maclaren NK, Notkins AL. IA-2, a transmembrane protein of the protein tyrosine phosphatase family, is a major autoantigen in insulin-dependent diabetes mellitus. *Proc Natl Acad Sci USA* (1996). 93: 6367–6370.

Lee KM, Chuang E, Griffin M, Khattri R, Hong DK, Zhang W, Straus D, Samelson LE, Thompson CB, Bluestone JA. Molecular basis of T cell inactivation by CTLA-4. *Science* (1998). 282:2263-2266.

Lejon K, Fathman CG. Isolation of self antigen-reactive cells from inflamed islets of nonobese diabetic mice using CD4 high expression as a marker. *J Immunol* (1999). 163:5708–5714.

Lennon GP, Bettini M, Burton AR, Vincent E, Arnold PY, Santamaria P, Vignali DAA.T Cell Islet Accumulation in Type 1 Diabetes Is a Tightly Regulated, Cell-Autonomous Event. *Immunity* (2009). 31: 643-653.

Lepault F, Gagnerault MC. Characterization of peripheral regulatory $CD4^+$ T cells that prevent diabetes onset in nonobese diabetic mice. *J Immunol* (2000). 164:240–247.

Li W, Ley RE, Volchkov YP, Stranges PB, Avanesyan L, Stonebraker AC, Hu C, Wong FS, Szot GL, Bluestone JA, Gordon JI, Chervonsky AV. Innate immunity and intestinal microbiota in the development of Type 1 diabetes. *Nature* (2008). 455:1109-1113.

Linterman MA, Pierson W, Lee SK, Kallies A, Kawamoto S, Rayner TF, Srivastava M, Divekar DP, Beaton L, Hogan JJ, Fagarasan S, Liston A, Smith KG, Vinuesa CG. Foxp3+ follicular regulatory T cells control the germinal center response. *Nat Med* (2011). 17(8):975-82.

Lohmann T, Leslie RD, Londei M. T cell clones to epitopes of glutamic acid decarboxylase 65 raised from normal subjects and patients with insulin-dependent diabetes. *J Autoimmun* (1996). 9:385–389.

Lowe CE, Cooper JD, Brusko T, Walker NM, Smyth DJ, Bailey R, Bourget K, Plagnol V, Field S, Atkinson M, Clayton DG, Wicker LS, Todd JA. Large-scale genetic fine mapping and genotype-phenotype associations implicate polymorphism in the IL2RA region in type 1 diabetes. *Nat Genet* (2007). 39:1074–1082.

Lucassen AM, Julier C, Beressi JP, Boitard C, Froguel P, Lathrop M, Bell JI. Susceptibility to insulin-dependent diabetes mellitus maps to a 4.1 kb segment of DNA spanning the insulin gene and associated VNTR. *Nat Genet* (1993). 4: 305-310.

Lucassen AM, Screaton GR, Julier C, Elliot TJ, Lathrop M, Bell JI. Regulation of insulin gene expression by IDDM associated, insulin locus haplotype. *Hum Mol Genet* (1995). 4: 501-506.

Luther SA, Bidgol A, Hargreaves DC, Schmidt A, Xu Y, Paniyadi J, Matloubian M, Cyster JG. Differing Activities of Homeostatic Chemokines CCL19, CCL21, and CXCL12 in Lymphocyte and Dendritic Cell Recruitment and Lymphoid Neogenesis. *J Immunol* (2002). 169: 424-433.

Magistrelli g, Jeannin P, Herbault N, Benoit DCA, Gauchat JF, Bonnefoy JY, Delneste Y. A soluble form of CTLA-4 generated by alternative splicing is expressed by nonstimulated human T cells. *Eur J Immunol* (1999). 29:3596-3602.

Maine CJ, Hamilton-Williams EE, Cheung J, Stanford SM, Bottini N, Wicker LS, Sherman LA. PTPN22 Alters the Development of Regulatory T Cells in the Thymus. *J Immunol* (2012). 188(1):5267-75.

Makino S, Kunimoto K, Muraoka Y, Katagiri K. Effect of castration on the appearance of diabetes in NOD mouse. *Jikken Dobutsu* (1981). *30*:137-140.

Makino S, Kunimoto K, Muraoka Y, Mizushima Y, Katagiri K, Tochino Y. Breeding of a non-obese, diabetic strain of mice. *Jikken Dobutsu* (1980). *29*:1-13.

Mantovani A, Bonecchi R, Locati M. Tuning inflammation and immunity by chemokine sequestration: decoys and more. *Nat Rev Immunol* (2006). 6:907-918.
Mantovani A, Bonecchi R, Locati M. Tuning inflammation and immunity by chemokine sequestration: decoys and more. *Nat Rev Immunol* (2006). 6:907-918.

Many MC, Maniratunga S, Denef JF. The non-obese diabetic (NOD) mouse: an animal model for autoimmune thyroiditis. *Exp Clin Endocrinol Diabetes* (1996). 104:17–20.

Mathieu C, Waer M, Laureys J, Rutgeerts O, Bouillon R. Prevention of autoimmune diabetes in NOD mice by 1,25 dihydroxyvitamin D_3. *Diabetologia* (1994). 37:552–558.

Mellanby RJ, Thomas D, Phillips JM, Cooke A. Diabetes in non-obese diabetic mice is not associated with quantitative changes in CD4+ CD25+ Foxp3+ regulatory T cells. *Immunology* (2007). 121:15-28.

Menard L, Saadoun D, Isnardi I, Ng YS, Meyers G, Massad C, Price C, Abraham C, Motaghedi R, Buckner JH, Gregersen PK, Meffre E. The PTPN22 allele encoding an R620W variant interferes with the removal of developing autoreactive B cells in humans. *J Clin Invest* (2011).121:3635-3644.

Montane J, Bischoff L, Soukhatcheva G, Dai DL, Hardenberg G, Levings MK, Orban PC, Kieffer TJ, Tan R, Verchere CB. Prevention of murine autoimmune diabetes by CCL22-mediated Treg recruitment to the pancreatic islets. *J Clin Invest* (2011). 121:3024-3028.

Morimoto J, Yoneyama H, Shimada A, Shigihara T, Yamada S, Oikawa Y, Matsushima K, Saruta T, Narumi S. CXC chemokine ligand 10 neutralization suppresses the occurrence of diabetes in nonobese diabetic mice through enhanced β cell proliferation without affecting insulitis. *J Immunol* (2004).173:7017-7024.

Muto A, Tashiro S, Nakajima O, Hoshino H, Takahashi S, Sakoda E, Ikebe D, Yamamoto M, Igarashi K. The transcriptional programme of antibody class switching involves the repressor Bach2. *Nature* (2004). 429:566-571.

Nejentsev S, Howson JM, Walker NM, Szeszko J, Field SF, Stevens HE, Reynolds P, Hardy M, King E, Masters J, Hulme J, Maier LM, Smyth D, Bailey R, Cooper JD, Ribas G, Campbell RD, Clayton DG, Todd JA, Wellcome Trust Case Control Consortium. Localization of type 1 diabetes susceptibility to the MHC class I genes HLA-B and HLA-A. *Nature* (2007). 450:887–892.

Nichols J, Jones K, Phillips JM, Newland SA, Roode M, Mansfield W, Smith A, Cooke A. Validated germline-competent embryonic stem cell lines from nonobese diabetic mice. *Nat Med* (2009). 15:814-818.

Nistico L, Buzzetti R, Pritchard LE, Van der Auwera B, Giovannini C, Bosi E, Larrad MT, Rios MS, Chow CC, Cockram CS, Jacobs K, Mijovic C, Bain SC, Barnett AH, Vandewalle CL, Schuit F, Gorus FK, Tosi R, Pozzilli P, Todd JA. The CTLA-4 gene region of chromosome 2q33 is linked to, and associated with, type 1 diabetes. *Hum Mol Genet* (1996). 5:1075–1080.

Nithiyananthan R, Heward JM, Allahabadia A, Franklyn JA, Gough SCL. Polymorphism of the CTLA-4 gene is associated with autoimmune hypothyroidism in the United Kingdom. *Thyroid* (2002). 12: 3-6.

Oaks MK, Hallett KM, Penwell RT, Stauber EC, Warren SJ, Tector AJ. A native soluble form of CTLA-4. *Cell Immunol* (2000). 201:144-153.

Oestreich KJ, Mohn SE, Weinmann AS. Molecular mechanisms that control the expression and activity of Bcl-6 in TH1 cells to regulate flexibility with a TFH-like gene profile. *Nat Immunol* (2012). 13:405-11.

Ogasawara K, Hamerman JA, Ehrlich LR, Bour-Jordan H, Santamaria P, Bluestone JA, Lanier LL. NKG2D blockade prevents autoimmune diabetes in NOD mice. *Immunity* (2004). 20:757–767.

Onengut-Gumuscu S, Ewens KG, Spielman RS, Concannon P. A functional polymorphism (1858C/T) in the PTPN22 gene is linked and associated with type I diabetes in multiplex families. *Genes Immun* (2004). 5:678-680.

Orozco G, Sanchez E, Gonzalez-Gay MA, Lopez-Nevot MA, Torres B, Caliz R, Ortego-Centeno N, Jimenez-Alonso J et al. Association of a functional single-nucleotide polymorphism of PTPN22, encoding lymphoid protein phosphatase, with rheumatoid arthritis and systemic lupus erythematosus. *Arthritis Rheum* (2005). 52:219-224.

Ostrov DA, Shi W, Schwartz JC, Almo SC, Nathenson SG. Structure of murine CTLA-4 and its role in modulating T cell responsiveness. *Science* (2000). 290:816-819.

Owerbach D, Gabbay KH. Localization of a type I diabetes susceptibility locus to the variable tandem repeat region flanking the insulin gene. *Diabetes* (1993). 42: 1708-1714.

Owerbach D, Nerup J. Restriction fragment length polymorphism of the insulin gene in diabetes mellitus. *Diabetes* (1982). 31: 275-277.

Palmer JP. Insulin autoantibodies: their role in the pathogenesis of IDDM. *Diabetes Metab Rev* (1987). 3:1005-1015.

Pecot CV, Calin GA, Coleman RL, Lopez-Berestein G, Sood AK. RNA interference in the clinic: challenges and future directions. *Nat Rev Cancer* (2011). 11:59-67.

Penaranda C , Bluestone JA. Is Antigen Specificity of Autoreactive T Cells the Key to Islet Entry? *Immunity* (2009). 31: 534-536.

Peng Y, Laouar Y, Li MO, Green EA, Flavell RA. TGF-β regulates in vivo expansion of Foxp3-expressing $CD4^{+}CD25^{+}$ regulatory T cells responsible for protection against diabetes. *Proc Natl Acad Sci USA* (2004). 101:4572–4577.

Pernod G, Fish R, Liu JW, Kruithof EK. Increasing lentiviral vector titer using inhibitors of protein kinase R. *BioTechniques* (2004). 36(4):576-8, 580.

Pescovitz MD, Greenbaum CJ, Krause-Steinrauf H, Becker DJ, Gitelman SE, Goland R et al. Rituximab, B-lymphocyte depletion, and preservation of beta-cell function. *N Engl J Med* (2009). 361:2143-2152.

Prochazka M, Serreze DV, Frankel WN, Leiter EH. NOR/Lt mice: MHC matched diabetes-resistant control strain for NOD mice. *Diabetes* (1992). 41:98-106.

Pugliese A, Zeller M, Fernandez A, Zalcberg LJ, Bartlett RJ, Ricordi C, Pietropaolo M, Eisenbarth GS, Bennett ST, Patel DD. The insulin gene is transcribed in the human thymus and transcription levels correlate with allelic variation at the *INS*

VNTR-IDDM2 susceptibility locus for type-1 diabetes. *Nat Genet* (1997). 15: 293-297.

Qu HQ, Grant SF, Bradfield JP, Kim C, Frackelton E, Hakonarson H, Polychronakos C. Association of RASGRP1 with type 1 diabetes is revealed by combined follow-up of two genome-wide studies. *J Med Genet* (2009). 46(8):553-554.

Rhode A, Pauza ME , Barral AM, Rodrigo E, Oldstone MBA, von Herrath MG, Christen U. Islet-Specific Expression of CXCL10 Causes Spontaneous Islet Infiltration and Accelerates Diabetes Development. *J Immunol* (2005). 175:3516-3524.

Rieck M, Arechiga A, Onengut-Gumuscu S, Greenbaum C, Concannon P, Buckner JH. Genetic Variation in PTPN22 Corresponds to Altered Function of T and B Lymphocytes. *J Immunol* (2007). 179: 4704-4710.

Rivas MA, Beaudoin M, Gardet A, Stevens C, Sharma Y, Zhang CK, Boucher G, Ripke S, Ellinghaus D, Burtt N, Fennell T, Kirby A, Latiano A, Goyette P, Green T, Halfvarson J, Haritunians T, Korn JM, Kuruvilla F, Lagacé C, Neale B, Lo KS, Schumm P, Törkvist L; National Institute of Diabetes and Digestive Kidney Diseases Inflammatory Bowel Disease Genetics Consortium (NIDDK IBDGC); United Kingdom Inflammatory Bowel Disease Genetics Consortium; International Inflammatory Bowel Disease Genetics Consortium, Dubinsky MC, Brant SR, Silverberg MS, Duerr RH, Altshuler D, Gabriel S, Lettre G, Franke A, D'Amato M, McGovern DP, Cho JH, Rioux JD, Xavier RJ, Daly MJ. Deep resequencing of GWAS loci identifies independent rare variants associated with inflammatory bowel disease. *Nat Genet* (2011). 43:1066-1073.

Rotwein P, Yokoyama S, Didier DK, Chirgwin JM. Genetic analysis of the hypervariable region flanking the human insulin gene. *Am J Hum Genet* (1986). 39: 291-299.

Salomon B, Lenschow DJ, Rhee L, Ashourian N, Singh B, Sharp A, Bluestone JA. B7/CD28 costimulation is essential for the homeostasis of the $CD4^{+}CD25^{+}$

immunoregulatory T cells that control autoimmune diabetes. *Immunity* (2000). 12:431–440.

Salomon B, Rhee L, Bour-Jordan H, Hsin H, Montag A, Soliven B, Arcella J, Girvin AM, Padilla J, Miller SD, Bluestone JA. Development of spontaneous autoimmune peripheral polyneuropathy in B7-2- deficient NOD mice. *J Exp Med* (2001). 194:677–684.

Santamaria P. The long and winding road to understanding and conquering type 1 diabetes. *Immunity* (2010). 32:437-445.

Sawcer S, Jones HB, Feakes R, Gray J, Smaldon N, Chataway J, Robertson N, Clayton D, Goodfellow PN, Compston A. A genome screen in multiple sclerosis reveals susceptibility loci on chromosome 6p21 and 17q22. *Nat Genet* (1996). 13:464-468.

Scollay RG, Butcher EC, Weissman IL. Thymus cell migration. Quantitative aspects of migration. cellular traffic from the thymus to the periphery in mice. *Eur J Immunol* (1980). 10(3):210-8.

Semana G, Gausling R, Jackson RA, Hafler DA. T cell autoreactivity to proinsulin epitopes in diabetic patients and healthy subjects. *J Autoimmun* (1999). 12:259–267.

Serreze DV, Chapman HD, Varnum DS, Hanson MS, Reifsnyder PC, Richard SD, Fleming SA, Leiter EH, Shultz LD. B lymphocytes are essential for the initiation of T cell-mediated autoimmune diabetes: analysis of a new "speed congenic" stock of NOD.Ig mu null mice. *J Exp Med* (1996). 184:2049-2053.

Serreze DV, Leiter EH, Christianson GJ, Greiner D, Roopenian DC. Major histocompatibility complex class I-deficient NOD-B2mnull mice are diabetes and insulitis resistant. *Diabetes* (1994). 43:505-509.

Serreze DV, Leiter EH. Genes and cellular requirements for autoimmune diabetes susceptibility in nonobese diabetic mice. *Curr Dir Autoimmun* (2001). 4:31 –67.

Shen Y, Lyons P, Cooley M, Davidson D, Veillette A, Salgia R, Griffin JD, Schaller MD. The noncatalytic domain of protein-tyrosine phosphatase-PEST targets paxillin for dephosphorylation in vivo. *J Biol Chem* (2000). 275: 1405-1413.

Shevach EM. Mechanisms of foxp3+ T regulatory cell-mediated suppression. *Immunity* (2009). 30(5):636-45.

Shizuru JA, Taylor-Edwards C, Banks BA, Gregory AK, Fathman CG. Immunotherapy of the nonobese diabetic mouse: treatment with an antibody to T-helper lymphocytes. *Science* (1988). 240:659–662.

Silveira PA, Baxter AG. The NOD mouse as a model of SLE. *Autoimmunity* (2001). 34:53–64.

Singer O, Verma IM. Applications of lentiviral vectors for shRNA delivery and transgenesis. *Curr Gene Ther* (2008). 8:483-8.

Smyth D, Cooper JD, Collins JE, Heward JM, Franklyn JA, Howson JM et al. Replication of an association between the lymphoid tyrosine phosphatase locus (LYP/PTPN22) with type 1 diabetes, and evidence for its role as a general autoimmunity locus. *Diabetes* (2004). 53:3020-3023.

Smyth DJ, Plagnol V, Walker NM, Cooper JD, Downes K, Yang JH, Howson JM, Stevens H, McManus R, Wijmenga C, Heap GA, Dubois PC, Clayton DG, Hunt KA, van Heel DA, Todd JA. Shared and distinct genetic variants in type 1 diabetes and celiac disease. *N Engl J Med*. 2008 Dec 25;359(26):2767-77.

Smyth DJ, Cooper JD, Bailey R, Field S, Burren O, Smink LJ, Guja C, Ionescu-Tirgoviste C, Widmer B, Dunger DB, Savage DA, Walker NM, Clayton DG, Todd JA. A genome-wide association study of nonsynonymous SNPs identifies a type 1 diabetes locus in the interferon-induced helicase (IFIH1) region. *Nat Genet* (2006). 38:617–619.

Soderstrom I, Bergman ML, Colucci, F, Lejon K, Bergqvist I, Holmberg D.

Establishment and characterization of RAG-2 deficient non-obese diabetic mice. *Scand J Immunol* (1996). 43:525-530.

Sojka DK, Hughson A, Sukiennicki TL, Fowell DJ. Early kinetic window of target T cell susceptibility to $CD25^+$ regulatory T cell activity. *J Immunol* (2005). 175: 7274 - 7280.

Stanford SM, Krishnamurthy D, Falk MD, Messina R, Debnath B, Li S, Liu T, Kazemi R, Dahl R, He Y, Yu X, Chan AC, Zhang ZY, Barrios AM, Woods VL Jr, Neamati N, Bottini N. Discovery of a novel series of inhibitors of lymphoid tyrosine phosphatase with activity in human T cells. *J Med Chem* (2011). 54:1640-1654.

Stephens A, Mason D. CD25 is a marker for $CD4^+$ thymocytes that prevent autoimmune diabetes in rats, but peripheral T cells with this function are found in both $CD25^+$ and $CD25^-$ subpopulations. *J Immunol* (2000). 165:3105–3110.

Szanya V, Ermann J, Taylor C, Holness C, Fathman CG. The subpopulation of $CD4^+CD25^+$ splenocytes that delays adoptive transfer of diabetes expresses L-selectin and high levels of CCR7. *J Immunol* (2002). 169:2461–2465.

Tang QZ, Henriksen KJ, Bi MY, Finger EB, Szot G, Ye J, Masteller EL, McDevitt H, Bonyhadi M, Bluestone JA. In vitro-expanded antigen-specific regulatory T cells suppress autoimmune diabetes. *J Exp Med* (2004). 199:1455–1465.

Tarbell KV, Yamazaki S, Olson K, Toy P, Steinman RM. $CD25^+$ $CD4^+$ T cells, expanded with dendritic cells presenting a single autoantigenic peptide, suppress autoimmune diabetes. *J Exp Med* (2004). 199: 1467 – 1477.

Thornton AM, Korty PE, Tran DQ, Wohlfert EA, Murray PE, Belkaid Y, Shevach EM. Expression of Helios, an Ikaros transcription factor family member, differentiates thymic-derived from peripherally induced $Foxp3^+$ T regulatorycells. *J Immunol* (2010). 184(7):3433-41.

Tisch R, McDevitt H. Insulin-dependent diabetes mellitus. *Cell* (1996). 85:291–297.

Tivol EA, Borriello F, Schweitzer AN, Lynch WP, Bluestone JA, Sharpe AH. Loss of CTLA-4 leads to massive lymphoproliferation and fatal multiorgan tissue destruction, revealing a critical negative regulatory role of CTLA-4. *Immunity* (1995). 3:541-547.

Todd JA, Walker NM, Cooper JD, Smyth DJ, Downes K, Plagnol V, Bailey R, Nejentsev S, Field SF et al. Robust associations of four new chromosome regions from genome-wide analyses of type 1 diabetes. *Nat Genet* (2007). 39:857–864.

Todd JA, Wicker LS. Genetic protection from the inflammatory disease type 1 diabetes in humans and animal models. *Immunity* (2001). 15:387–395.

Ueda H, Howson JM, Esposito L, Heward J, Snook H, Chamberlain G, Rainbow DB, Hunter KM, Smith AN, Di Genova G, Herr MH, Dahlman I, Payne F, Smyth D, Lowe C, Twells RC et al. Association of the T-cell regulatory gene CTLA4 with susceptibility to autoimmune disease. *Nature* (2003). 423:506-511.

Undlien DE, Bennett ST, Todd JA, Akselsen HE, Ikäheimo I, Reijonen H, Knip M, Thorsby E, Rønningen KS. Insulin gene region-encoded susceptibility to IDDM maps upstream of the insulin gene. *Diabetes* (1995). 44: 620-625.

Vafiadis P, Bennett S, Todd JA, Nadeau J, Grabs R, Goodyer CG, Wickramasinghe S, Colle E, Polychronakos C. Insulin expression in human thymus is modulated by *INS* VNTR. *Nat Genet* (1997). 15: 289-292.

Vafiadis P, Ounissi-Benkalha H, Palumbo M, Grabs R, Rousseau M, Goodyer CG, Polychronakos C. Class III alleles of the variable number of tandem repeat insulin polymorphism associated with silencing of thymic insulin predispose to type 1 diabetes. *J Clin Endocrinol Metab* (2001). 86: 3705-3710.

van Oene M, Wintle RF, Liu X, Yazdanpanah M, Gu X, Newman B, Kwan A, Johnson B, Owen J, Greer W et al. Association of the lymphoid tyrosine phosphatase R620W variant with rheumatoid arthritis, but not Crohn's disease, in Canadian populations. *Arthritis Rheum* (2005). 52:1993-1998.

Vang T, Congia M, Macis MD, Musumeci L, Orru V, Zavattari P, Nika K, Tautz L, Taskén K, Cucca F, Mustelin T, Bottini T. Autoimmune-associated lymphoid tyrosine

phosphatase is a gain-of-function variant. *Nat Genet* (2005). 37:1317–1319.

Vang T, Miletic AV, Arimura Y, Tautz L, Rickert RC, Mustelin T. Protein tyrosine phosphatases in autoimmunity. *Annu Rev Immunol* (2008). 26:29–55.

Velaga MR, Wilson V, Jennings CE, Owen CJ, Herington S, Donaldson PT, Ball SG, James RA, Quinton R, Perros P, Pearce SH. The codon 620 tryptophan allele of the lymphoid tyrosine phosphatase (LYP) gene is a major determinant of Graves' disease. *J Clin Endocrinol Metab* (2004). 89:5862-5865.

Vijayakrishnan L, Slavik JM, Illes Z, Greenwald RJ, Rainbow D, Greve B, Peterson LB, Hafler DA, Freeman GJ, Shape AH, Wicker LS, Kuchroo VK. An autoimmune disease-associated CTLA-4 splice variant lacking the B7 binding domain signals negatively in T cells. *Immunity* (2004). 20:563–575.

Viola A, Gupta N. Tether and trap: regulation of membrane-raft dynamics by actin-binding proteins. *Nat Rev Immunol* (2007). 7:889-896.

Wallace C, Smyth DJ, Maisuria-Armer M, Walker NM, Todd JA, Clayton DG. The imprinted DLK1-MEG3 gene region on chromosome 14q32.2 alters susceptibility to type 1 diabetes. *Nat Genet* (2010). 42(1):68-71.

Wang B, Gonzalez A, Benoist C, Mathis D. The role of $CD8^+$ T cells in the initiation of insulin-dependent diabetes mellitus. *Eur J Immunol* (1996). 26:1762–1769.

Wang B, Lemay S, Tsai S, Veillette A. SH2 domain-mediated interaction of inhibitory protein tyrosine kinase Csk with protein tyrosine phosphatae-HSCF. *Mol Cell Biol* (2001). 21:1077–1088.

Wang ET, Sandberg R, Luo S, Khrebtukova I, Zhang L, Mayr C, Kingsmore SF, Schroth GP, Burge CB. Alternative isoform regulation in human tissue transcriptomes. *Nature* (2008). 456: 470-476.

Wang S, Dong H, Han J, Ho WT, Fu X, Zhao ZJ. Identification of a variant form of tyrosine phosphatase LYP. *BMC Mol Biol* (2010). 11:78.

Wang Y, Pontesilli O, Gill RG, La Rosa FG, Lafferty KJ. The role of $CD4^+$ and $CD8^+$ T cells in the destruction of islet grafts by spontaneously diabetic mice. *Proc Natl Acad Sci USA* (1991). 88:527-531.

Waterhouse P, Penninger JM, Timms E, Wakeham A, Shahinian A, Lee KP, Thompson CB, Griesser H, Mak TW. Lymphoproliferative disorders with early lethality in mice deficient in Ctla-4. *Science* (1995). 270:985-988.

Waterman M, Xu W, Stempak JM, Milgrom R, Bernstein CN, Griffiths AM, Greenberg GR, Steinhart AH, Silverberg MS. Distinct and overlapping genetic loci in Crohn's disease and ulcerative colitis: correlations with pathogenesis. *Inflamm Bowel Dis* (2011). 17(9):1936-42.

Weiss-Haljiti C, Pasquali C, Ji H, Gillieron C, Chabert C, Curchod ML, Hirsch E, Ridley AJ, Hooft van Huijsduijnen R, Camps M, Rommel C. Involvement of phosphoinostide 3-kinase gamma, Rac, and PAK signaling in chemokine-induced macrophage migration. *J Biol Chem* (2004). 279:43273-43284.

Wen L, Ley RE, Volchkov PY, Stranges PB, Avanesyan L. Innate immunity and intestinal microbiota in the development of Type 1 diabetes. *Nature* (2008). 455: 1109–1113.

Wesoly J, van der Helm-van Mil AH, Toes RE, Chokkalingam AP, Carlton VE, Begovich AB, Huizinga TW. Association of the PTPN22 C1858T single-nucleotide polymorphism with rheumatoid arthritis phenotypes in an inception cohort. *Arthritis Rheum* (2005). 52:2948-2950.

Wicker LS, Leiter EH, Todd JA, Renjilian RJ, Peterson E, Fischer PA, Podolin PL, Zijlstra M, Jaenisch R, Peterson LB. Beta 2-microglobulin-deficient NOD mice do not develop insulitis or diabetes. *Diabetes* (1994). 43:500-504.

Wicker LS, Todd JA, Peterson LB. Genetic control of autoimmune diabetes in the NOD mouse. *Annu Rev Immunol* (1995).13:179–200.

Wiegard C, Frenzel C, Herkel J, Kallen KJ, Schmitt E, Lohse AW. Murine Liver antigen presenting cells control suppressor activity of $CD4^+CD25^+$ regulatory T cells. *Hepatology* (2005). 42:193-199.

Wing K, Onishi Y, Prieto-Martin P, Yamaguchi T, Miyara M, Fehervari Z, Nomura T, Sakaguchi S. CTLA-4 control over FoxP3+ regulatory T cell function. *Science* (2008). 322:271-275.

Wong FS, Visintin I, Wen L, Flavell RA, JanewayCA. CD8 T cell clones from young nonobese diabetic (NOD) islets can transfer rapid onset of diabetes in NOD mice in the absence of CD4 cells. *J Exp Med* (1996). 183:67–76.

Wu AJ, Hua J, Munson SH, McDevitt HO. Tumor necrosis factor-alpha regulation of CD4+CD25+ T cell levels in NOD mice. *Proc Natl Acad Sci USA* (2002). 99:12287-12292.

Wu J, Katrekar A, Honigberg LA, Smith AM, Conn MT, Tang J, Jeffery D, Mortara K, Sampang J, Williams SR, Buggy J, Clark JM. Identification of substrates of human protein-tyrosine phosphatase PTPN22. *J Biol Chem* (2006). 281:11002-11010.

Yagi H, Nomura T, Nakamura K, Yamazaki S, Kitawaki T, Hori S, Maeda M, Onodera M, Uchiyama T, Fujii S, Sakaguchi S. Crucial role of FOXP3 in the development and function of human CD25+CD4+ regulatory T cells. *Int Immunol* 2005; 16: 1643–56.

Yang SH, Cheng PH, Sullivan RT, Thomas JW, Chan AW. Lentiviral integration preferences in transgenic mice. *Genesis* (2008). 46(12): 711-718.

Yoon JW, Onodera T, Notkins AL. Virus-induced diabetes mellitus. XV. Beta cell damage and insulin-dependent hyperglycemia in mice infected with coxsackie virus B4. *J Exp Med* (1978). 148: 1068–1080.

Zhang J, Zahir N, Jiang Q, Miliotis H, Heyraud S, Meng X, Dong B, Xie G, Qiu F, Hao Z, McCulloch CA, Keystone EC, Peterson AC, Siminovitch KA. The autoimmune disease-associated PTPN22 variant promotes calpain-mediated Lyp/Pep

degradation associated with lymphocyte and dendritic cell hyperresponsiveness. *Nat Genet* (2011). 43:902-907.

Zikherman J, Hermiston M, Steiner D, Hasegawa K, Chan A, Weiss A. *PTPN22* deficiency cooperates with the CD45 E613R allele to break tolerance on a non-autoimmune background. *J Immunol* (2009). 182: 4093-4106.

Publications

1. *Ptpn22* silencing in the NOD model indicates type 1 diabetes-associated allele is a gain-of-function variant. Zheng P, Kissler S. (1st author, submitted to *Diabetes*)

2. The soluble CTLA-4 splice variant protects from type 1 diabetes and potentiates regulatory T-cell function. Gerold KD, Zheng P, Rainbow DB, Zernecke A, Wicker LS, Kissler S. Diabetes. 2011 Jul;60(7):1955-63.

3. A novel type III crustin (CrusEs2) identified from Chinese mitten crab *Eriocheir sinensis*. Mu C, Zheng P, Zhao J, Wang L, Qiu L, Zhang H, Gai Y, Song L. Fish Shellfish Immunol. 2011 Jul;31(1):142-7.

4. Molecular characterization and expression of a crustin-like gene from Chinese mitten crab, *Eriocheir sinensis*. Mu C, Zheng P, Zhao J, Wang L, Zhang H, Qiu L, Gai Y, Song L. Dev Comp Immunol. 2010 Jul;34(7):734-40.

5. The immune responses in Chinese mitten crab *Eriocheir sinensis* challenged with double-stranded RNA. Dong C, Zhao J, Song L, Wang L, Qiu L, Zheng P, Li L, Gai Y, Yang G. Fish Shellfish Immunol. 2009 Mar;26(3):438-42.

6. A cyclophilin A inducible expressed in gonad of zhikong scallop Chlamys farreri. Song X, Wang L, Song L, Zhao J, Zhang H, Zheng P, Qiu L, Liu X, Wu L. Mol Biol Rep. 2009 Jul;36(6):1637-45.

7. cDNA cloning, characterization and mRNA expression of a pacifastin light chain gene from the Chinese mitten crab *Eriocheir sinensis*. Gai Y, Wang L, Song L, Zhao J, Qiu L, Wang B, Mu C, Zheng P, Zhang Y, Li L, Xing K. Fish Shellfish Immunol. 2008 Nov;25(5):657-63.

8. Molecular cloning and expression of a novel Kazal-type serine proteinase inhibitor gene from Zhikong scallop *Chlamys farreri*, and the inhibitory activity of its recombinant domain. Wang B, Zhao J, Song L, Zhang H, Wang L, Li C, Zheng P, Zhu L, Qiu L, Xing K. Fish Shellfish Immunol. 2008 May;24(5):629-37.

9. A lectin (CfLec-2) aggregating Staphylococcus haemolyticus from scallop *Chlamys farreri*. Zheng P, Wang H, Zhao J, Song L, Qiu L, Dong C, Wang B, Gai Y, Mu C, Li C, Ni D, Xing K. Fish Shellfish Immunol. 2008 Mar;24(3):286-93.

10. A prophenoloxidase from the Chinese mitten crab *Eriocheir sinensis*: gene cloning, expression and activity analysis. Gai Y, Zhao J, Song L, Li C, Zheng P, Qiu L, Ni D. Fish Shellfish Immunol. 2008 Feb;24(2):156-67.

Affidavit

I hereby confirm that my thesis entitled "*Ptpn22* silencing in the NOD model of type 1 diabetes indicates the human susceptibility allele of *PTPN22* is a gain-of-function variant" is the results of my own work. I did not receive any help or support from commercial consultants. All sources and/or materials applied are listed and specified in the thesis.

Furthermore, I confirm that this thesis has not been submitted as part of another examination process neither in identical nor in similar form.

Würzburg, July 15th, 2012 _____

Place, Date Signature (Peilin Zheng)